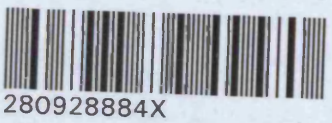

UNIVERSITY OF LONDON THESIS

Degree PhD Year 2006 Name of Author MARTIN
Yella

COPYRIGHT

This is a thesis accepted for a Higher Degree of the University of London. It is an unpublished typescript and the copyright is held by the author. All persons consulting the thesis must read and abide by the Copyright Declaration below.

COPYRIGHT DECLARATION

I recognise that the copyright of the above-described thesis rests with the author and that no quotation from it or information derived from it may be published without the prior written consent of the author.

LOAN

Theses may not be lent to individuals, but the University Library may lend a copy to approved libraries within the United Kingdom, for consultation solely on the premises of those libraries. Application should be made to: The Theses Section, University of London Library, Senate House, Malet Street, London WC1E 7HU.

REPRODUCTION

University of London theses may not be reproduced without explicit written permission from the University of London Library. Enquiries should be addressed to the Theses Section of the Library. Regulations concerning reproduction vary according to the date of acceptance of the thesis and are listed below as guidelines.

A. Before 1962. Permission granted only upon the prior written consent of the author. (The University Library will provide addresses where possible).

B. 1962 - 1974. In many cases the author has agreed to permit copying upon completion of a Copyright Declaration.

C. 1975 - 1988. Most theses may be copied upon completion of a Copyright Declaration.

D. 1989 onwards. Most theses may be copied.

This thesis comes within category D.

☐ This copy has been deposited in the Library of UCL

☐ This copy has been deposited in the University of London Library, Senate House, Malet Street, London WC1E 7HU.

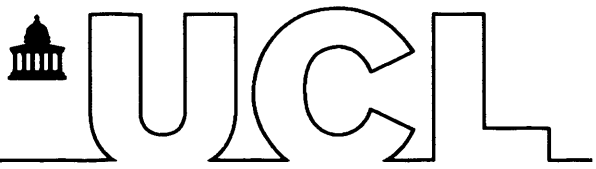

Investigation of the Batten disease protein CLN6

Yella Martin

A thesis submitted for the degree of Doctor of Philosophy in the University of London

October 2006

General and Adolescent Paediatric Unit
Centre of Human Molecular Genetics
Institute of Child Health
University College London

Supervisors:
Dr. Sara E. Mole
Professor Daniel F. Cutler

ProQuest LLC
789 East Eisenhower Parkway
P.O. Box 1346
Ann Arbor, MI 48106-1346

Declaration

I, Yella Martin, confirm that the work presented in this thesis is my own. Where information has been derived from other sources, I confirm that this has been indicated in the thesis.

Abstract

The neuronal ceroid lipofuscinoses (NCLs, Batten Disease) are a group of lysosomal storage disorders caused by mutations in known and unknown proteins with different cellular locations. Mutations in the *CLN6* gene cause a type of variant late infantile NCL (vLINCL). The CLN6 protein is located in the ER and how mutations in CLN6 cause accumulation of storage material in the lysosome is unclear. The aims of this thesis were to establish the tools and techniques necessary to analyse the CLN6 protein and to utilise these to investigate its subcellular location, to identify proteins that interact with CLN6 and to elucidate the early cellular responses to loss of functional vLINCL proteins, CLN5, CLN6 and CLN8. It was shown that CLN6 can be detected by Western blotting, indirect immunofluorescence and immunoprecipitation. A construct of CLN6 fused to horseradish peroxidase was cloned for localisation studies by indirect immunofluorescence and electron microscopy. CLN6 protein and mRNA levels could be depleted using RNA interference and this depletion assessed by Western blotting, indirect immunofluorescence and Q-PCR. It was not possible to establish whether CLN6 is located within a sub-domain of the ER using indirect immunofluorescence or electron microscopy. There was no effect on the localisation or stabilisation of wild-type or mutant CLN6 when proteasomal or lysosomal inhibitors were used, indicating that CLN6 does not traffic to the lysosome and that wild-type and mutant CLN6 were not degraded by ER-associated degradation. Endogenous CLN6 was identified in co-immunoprecipitation experiments, confirming that it may bind to itself. No other proteins were identified that bind to CLN6. Depletion of CLN5, CLN6 and CLN8 resulted in an increase in the size and a redistribution to perinuclear areas of late endosomes and lysosomes. An increase in long *cis*-Golgi structures was also observed in response to siRNA against CLN6 and CLN8 but not CLN5.

Table of Contents

Text

Figures

Tables

Abbreviations

ABCA1 – ATP-binding cassette transporter A1

Acetate – sodium acetate

AMF-R – autocrine motility factor receptor

AP – adaptor complex

APS – ammonium persulphate

ASA – arylsulphatase A

ATP – adenosine triphosphate

Azide – sodium azide

BFA – brefeldin A

BLOC – biogenesis of lysosomal-related organelle complex

BME – beta-mercaptoethanol

bp – basepair

BSA – bovine serum albumin

Cacodylate – sodium cacodylate

C. elegans – *Caenorhabditis elegans*

CFTR – cystic fibrosis transmembrane conductance regulator

CHR – chromogen

CL – curvilinear profile

cm – centimeter

CNS – central nervous system

COP – coatomer protein

CsCl – caesium chloride

CTSD – cathepsin D

DAB – diamino benzedene

DDSA – dodecenyl succinic anhydride

DMP-30 – 2,4,6 tri(dimethylamenomethyl) phenol

DMSO – dimethyl sulphoxide

DNA – deoxyribonucleic acid

ds – double-stranded

dNTP – deoxyribonucleotide triphosphate

EDTA – ethylene diamine tetraacetic acid

EGTA – ethylene glycol tetraacetic acid

eIF – translation initiation factor

EMPR – progressive epilepsy with mental retardation

ER – endoplasmic reticulum

ERAD – ER associated degradation

ERES – ER exit site

ERGIC – ER-Golgi intermediate compartment

f – final bleed

FCS – foetal calf serum

FGE – FGly-generating enzyme

FGly - formylglycine

FP – fingerprint body

GFP – green fluorescent protein

GROD – granular osmiophilic deposit

H_2O – distilled water

HCl – hydrochloric acid

HDL-C – high density lipoprotein cholesterol

hNMP – human nuclear matrix protein

HRP – horseradish peroxidase

HSC – heat shock cognate protein

HSP – heat shock protein

IF – indirect immunofluorescence

INCL – infantile NCL

IP – immunoprecipiation

JNCL – juvenile NCL

kDa - kilodalton

L – ligation

LINCL – late infantile NCL

LSD – lysosomal storage disorder

MAM – mitochondrial associated membranes of the ER

min – minute(s)

mM – millimolar

mm - millimeter

MNA – methylnadic anhydride

MnSOD – manganese superoxide dismutase

MRC-LMCB – Medical Research Council Laboratory for Molecular Cell Biology

mRNA – messenger RNA

MSD – multiple sulphatase deficiency

mtHSP – mitochondrial heat shock protein

MTOC – microtubule organising centre

NCL – neuronal ceroid lipofuscinosis

NDLB – non-denaturing lysis buffer

NE – nuclear envelope

nm – nanometer

nt – nucleotide

OSER – organised smooth ER

p – purified antibody

PBS – phosphate buffered saline

PCR – polymerase chain reaction

PDI – protein disulphide isomerase

PFA – paraformaldehyde

PPR – pentatricopeptide repeat

PPT1- palmitoyl thioesterase 1

QC – quality control

QuIF – quantitative immunofluorescence

Q-PCR – quantitative reverse transcription polymerase chain reaction

RAP – receptor associated protein

RER – rough ER

RL – rectilinear body

RNA – ribonucleic acid

RNAi – RNA interference

RT – room temperature

S. cerevisiae – *Saccharomyces cerevisiae*

SDS – sodium dodecyl sulphate

SER – smooth ER

siRNA – small interfering RNA

S. pombe – Schizosaccharomyces pombe

SRP – signal recognition particle

SUMF-1 – sulphatase modifying factor-1

tER – transitional ER

TGN – *trans*-Golgi network

TLC – Tram, Lag, CLN8

TMD – transmembrane domain

TPPI – tripeptidyl peptidase I

TSA – tyramide signal amplification

U – units

UCL – University College London

vLINCL – variant late infantile NCL

WB – Western blotting

μl – microliter

1. Introduction

1.1 Overview

The neuronal ceroid lipofuscinoses (NCLs, Batten Disease) are a group of lysosomal storage disorders caused by mutations in known and unknown proteins with different cellular locations such as endoplasmic reticulum (ER), ER-Golgi intermediate compartment (ERGIC), lysosomes and elsewhere. They are the most common neurodegenerative disorder in children and most display autosomal recessive Mendelian inheritance. Mutations in the *CLN6* gene cause a type of variant late infantile NCL (vLINCL). The CLN6 protein is located in the ER and it is unclear how mutations in CLN6 cause accumulation of storage material in the lysosome.

The introduction is divided into two sections. The first includes a brief introduction to lysosomal storage disorders, the endoplasmic reticulum and its functions and the lysosome. The second section focuses on the NCLs and introduces the different proteins involved, with a particular focus on the CLN6 protein. This is followed by a description of the aims of this project.

1.2 Lysosomal storage disorders

Lysosomal storage disorders (LSDs) share the common phenomenon of accumulation of storage material in the lysosome accompanied by cellular pathology. Over 40 different LSDs have been described to date with different components of storage material and different affected cell types (Vellodi, 2005). They tend to be progressive, although the rate of progression is variable, and show almost exclusively recessive autosomal inheritance. Most LSDs result from a defect in a lysosomal hydrolase, leading to incomplete degradation of macromolecules and subsequent accumulation of these products (Futerman and van Meer, 2004; Winchester et al., 2000).

To date only three LSDs have been shown to be caused by a long-range effect between the endoplasmic reticulum and the lysosome. One of these is multiple sulphatase deficiency (MSD), a rare autosomal recessive LSD characterised by decreased activity of all known sulphatases. This family of proteins is comprised of eight enzymes, seven lysosomal and one microsomal, which hydrolyse sulphate esters (Schmidt et al., 1995). The sulphatases are post-translationally modified in the ER by the FGly-generating enzyme (FGE), which converts a cysteine residue to formylglycine (FGly). This modification is essential for the catalytic activity of sulphatases. A deficiency in FGE, caused by mutations in the *sulphatase modifying factor-1 (SUMF-1)* gene, results in unmodified, inactive sulphatases. This leads to impaired lysosomal catabolism of sulphated glycolipids and glycosaminoglycans (Dierks et al., 2003; Landgrebe et al., 2003; Schmidt et al., 1995). The other two LSDs caused by mutations in proteins located in the ER are variant late infantile NCL (vLINCL) caused by mutations in the genes *CLN6* and *CLN8*. These will be discussed in detail below.

1.3 Endoplasmic reticulum

The CLN6 protein has been shown to be located in the membrane of the endoplasmic reticulum (Heine et al., 2004; Mole et al., 2004), although its function in this organelle is currently unknown.

The endoplasmic reticulum (ER) is a continuous organelle, which extends through all parts of the cytoplasm and fulfils a number of functions. It consists of an interconnected membrane system with distinct sub-domains: the nuclear envelope (NE) and the peripheral ER, consisting of the rough ER (RER) and the smooth ER (SER). The NE surrounds the nucleus with two sheets of membrane, which connect at nuclear pores (Holmer and Worman, 2001). The peripheral ER is a network of sheets and tubules that are found dispersed throughout the cytoplasm (Voeltz et al., 2002). The simplest way of distinguishing between the RER and the SER is that the RER is covered with ribosomes and arranged in flat sheets, which have a granular appearance, while the SER lacks ribosomes and appears as more convoluted tubules (Shibata et al., 2006; Voeltz et al., 2006). The ribosomes that cover the RER associate with channels that allow entry of newly synthesised proteins into the ER by co-translational translocation. The function of the SER includes export into the exocytic pathway via transitional ER as well as sequestration of proteins and some cell-type specific processes. For example, in liver cells the SER is involved in detoxification of hydrophobic substances whereas in steroid producing cells a number of steps in steroid synthesis occur here (Voeltz et al., 2002). SER that is organised into stacks (organised smooth ER) has also been implicated as the site of aggregated misfolded protein in some pathological conditions (Dickson et al., 2002; Hewett et al., 2000).

The main functions of the ER are translocation of nascent proteins, folding and post-translational modification, export into the exocytic pathway, recycling, ER-associated degradation, calcium storage, autophagy and lipid synthesis and transport. Proteins located in the ER can be involved in one or more of these processes.

1.3.1 Translocation

As proteins are translated from messenger RNA (mRNA) on ribosomes in the cytoplasm, a proportion of these proteins are destined for the ER. Such proteins are synthesised with a signal sequence that is recognised by the signal recognition particle (SRP). SRP binds the signal sequence and targets the ribosome with the nascent polypeptide chain to the ER membrane (Walter and Blobel, 1980; Walter and Blobel, 1981a; Walter and Blobel, 1981b; Walter et al., 1981). The emerging protein is inserted into the translocation channel, the Sec61 complex, and further synthesised directly into the lumen of the ER (Kleizen and Braakman, 2004). This process is referred to as co-translational translocation. Another method of translocation was identified in yeast, although it has not yet been shown to exist in higher eukaryotes. This is referred to as post-translational translocation. Proteins that use this method are translated in the cytoplasm where they bind to the Sec62/63 complex in their unfolded state. This is then targeted to the Sec61 channel and the unfolded protein translocated with the help of the ER chaperone BiP (Matlack et al., 1999; Osborne et al., 2005).

1.3.2 Folding and post-translational modifications

The environment inside the ER is optimised to assist protein folding by its extracytosolic milieu, the presence of chaperone complexes and the opportunity for a number of post-translational modifications to occur. Folding takes place while a protein is being translocated into the ER. The quality control system (QC) recognises correctly folded proteins and regulates ER export to the Golgi. Chaperones are part of the primary QC and act as folding sensors by binding to misfolded proteins and retaining them in the ER. Some chaperones such as BiP assist in the folding of all proteins while others act on specific groups of proteins, such as calnexin and calreticulin that promote the folding of glycoproteins (Helenius et al., 1997). Chaperones can also assist in folding and perform post-translational modifications simultaneously. Protein disulphide isomerase (PDI) catalyses the oxidation, isomerisation and reduction of disulphide bonds while

retaining incorrectly folded proteins in the ER (Ellgaard and Helenius, 2003). A very important type of post-translational modification that occurs in the ER is the addition of N-linked core oligosaccharides to nascent proteins by the oligosaccharyltransferase complex. These basic glycans are further modified in the ER and in the Golgi (Helenius and Aebi, 2001). More recently it has been suggested that palmitoylation events can also occur in the ER and that this modification is necessary for ER export of some transmembrane proteins such as the nicotinic acetylcholine receptor (Drisdel et al., 2004; Lam et al., 2006).

1.3.3 ER export

Proteins that are folded correctly and have signal sequences targeting them to other organelles leave the ER and traffic to the Golgi apparatus. Exit from the ER occurs through a subdomain of the smooth, ribosome-free ER called transitional (t) ER or ER exit sites (ERES) (Bannykh et al., 1996; Palade, 1975; Stephens, 2003). Here, coatomer protein (COP) II coated vesicles are generated through interactions between Sec12, Sar1, the Sec23/24 complex and the Sec13/31 complex (Antonny and Schekman, 2001; Barlowe et al., 1994). Proteins exit the ER either by bulk flow or through interactions with transport receptors or accessory proteins (Lee et al., 2004). Several proteins are involved in recruiting cargo proteins into COPII vesicles. These proteins are called secondary QC proteins and are usually specific to the family of proteins they sort. An example of this is the ER-Golgi intermediate compartment (ERGIC)–53 protein, which acts as a transport receptor for glycoproteins (Appenzeller et al., 1999). Another example is the receptor associated protein (RAP) which escorts members of the low density lipoprotein receptor family to the Golgi and prevents premature ligand binding (Herrmann et al., 1999). Once proteins arrive at the Golgi they can be further post-translationally modified and sorted for trafficking to other destinations in the cell (Ellgaard and Helenius, 2003).

1.3.4 Recycling

As the ER is continuously exporting components to the ERGIC and the Golgi via COPII coated vesicles, it is necessary to recycle ER-resident proteins back to the ER. This occurs via vesicles coated with the COPI complex of proteins in a mechanism termed retrograde transport. Proteins traffic from the Golgi through the ERGIC and then back to the ER (Lee et al., 2004; Martinez-Menarguez et al., 1999; Orci et al., 1993). ER residents have specific retention signals to facilitate their recognition and transport. The best-known is the KDEL sequence which is present on the carboxy terminus of many soluble ER proteins (Munro and Pelham, 1987). This signal binds to a KDEL specific receptor which can directly interact with the COPI coat proteins and thereby facilitate retrieval to the ER (Ellgaard and Helenius, 2003; Lewis and Pelham, 1990). CLN8 is an example of a protein recycled from the ERGIC to the ER (Lonka et al., 2000).

1.3.5 ERAD

Proteins that are unable to fold properly in the ER are eventually targeted for ER-associated degradation (ERAD). Firstly, substrates are recognised by chaperones as misfolded and targeted for retro-translocation into the cytoplasm. Retro-translocation has been reported to occur via the translocon channel Sec61 (Tsai et al., 2002). However other complexes have also been implicated in this mechanism, such as the Derlin-1/VIMP complex which has been shown to be involved in retro-translocation of proteins with misfolded luminal domains (Ye et al., 2004). While substrates are retro-translocated they become poly-ubiquitinated on the cytosolic side of the ER. This acts as the signal for degradation by the proteasome complex and release of the degraded components into the cytoplasm (Hiller et al., 1996; Romisch, 2005).

1.3.6 Calcium storage

Calcium plays an important role in signalling and many other cellular processes, such as chaperone-mediated protein folding in the ER, ER overload and the unfolded protein response (Paschen, 2001). The ER is the main calcium storage compartment of the cell (Meldolesi and Pozzan, 1998). Disturbances in homeostasis of calcium levels are sufficient to trigger cellular damage and have been implicated in neuronal injury and death most likely by apoptosis and necrosis (Lehotsky et al., 2003).

1.3.7 Autophagy

The major degradative pathways in the cell are lysosomal degradation, cytosolic degradation by the proteasome and autophagy. The latter is a process involved in the turnover of cellular constituents such as organelles (Klionsky and Emr, 2000). In this process, intracellular organelles such as mitochondria are first sequestered away from the remaining cytosol by a double membrane. The resulting autophagosome structure then fuses with the lysosome to form an autolysosome, inside which the constituents are degraded by acid hydrolases (Dunn, 1990). The origin of the sequestering membrane remains controversial. Some research suggests that it contains markers of the rough ER (Dunn, 1990). Others have found evidence of Golgi or post-Golgi markers (Locke and Sykes, 1975; Yamamoto et al., 1990), while others have shown that it arises from crescent-shaped membranes in the cytoplasm, termed autophagosome precursors (Mizushima et al., 2001). The extent to which the ER is involved in autophagy remains unclear. It was recently reported that autophagy can be triggered by ER stress (Yorimitsu et al., 2006). Furthermore, recent data has shown that one of the proteins required for autophagy mammalian (m) Atg9 is a transmembrane protein that recycles between the trans-Golgi network (TGN) and late endosomes (Young et al., 2006). As transmembrane proteins are folded in the lumen of the ER and then transported to the Golgi, the ER certainly has a function in ensuring the availability of this and other proteins involved in autophagy.

1.3.8 Lipid synthesis and transport

The ER is one of the sites of *de novo* lipid synthesis. Lipids are synthesised on the luminal side of the ER after which they traffic to other sites in the cell. The vLINCL protein CLN8 has been proposed to be have a lipid-sensing domain and to be involved in the activation of lipid synthesis and the synthesis of ceramide moieties (Winter and Ponting, 2002). Since lipids lack the conventional trafficking signals observed on proteins, they must have a specific sorting mechanism (Holthuis and Levine, 2005). Sorting along the endocytic and exocytic pathways has been observed for certain lipids; however, it has yet to be fully elucidated how this is achieved. Other modes of lipid transfer from the ER have been investigated more successfully. The ER comes in close contact with other organelles such as mitochondria, the plasma membrane, the *trans*-Golgi network, endosomes and lysosomes. Evidence has accumulated for lipid traffic across these so-called membrane contact sites (Holthuis and Levine, 2005).

1.4 Lysosome

Lysosomes are membrane-bound organelles of 0.5 μm diameter and are the major site of cellular degradation (de Duve, 2005; de Duve et al., 1955). Molecules can traffic to the lysosome from the plasma membrane via the endocytic pathway, from the ER and the Golgi apparatus via the biosynthetic pathway and through the autophagic pathway (Luzio et al., 2003; Mullins and Bonifacino, 2001). Lysosomes have a pH of approximately 5, which is maintained by the vacuolar ATPase proton pump. The pH is lower than in other organelles and this provides optimum conditions for lysosomal hydrolases, as these are less active in higher pH environments (Eskelinen et al., 2003). Lysosomal hydrolases metabolise macromolecules into low molecular mass components which pass through the lysosomal membrane into the cytoplasm where they are reused by the cell (Winchester et al., 2000). Lysosomes also carry a number of highly glycosylated integral membrane proteins in their limiting membrane, named lamps, limps and lgps, but they lack the mannose 6-phosphate

receptor, which distinguishes them from endosomes (Eskelinen et al., 2003; Kornfeld and Mellman, 1989; Mullins and Bonifacino, 2001). Lysosomes are found dispersed throughout the cytoplasm and clustered in the perinuclear region near the microtubule organising centre (MTOC). This distribution is microtubule-dependent and becomes altered in response to mutations in BLOC-3 (biogenesis of lysosomal-related organelles complex 3) and changes in cytoplasmic pH (Falcon-Perez et al., 2005; Heuser, 1989; Matteoni and Kreis, 1987). In many LSDs there is a defect in the delivery or function of acid hydrolases, which leads to a disruption of lysosomal function and accumulation of undegraded material.

1.5 Neuronal Ceroid Lipofuscinosis

The NCLs were first described almost 200 years ago by Stengel (Stengel, 1826; Stengel, 1982). However, it was only in 1969 that Zeman and Dyken introduced the name NCL to distinguish them from the gangliosidoses (Goebel, 1999; Zeman and Dyken, 1969). The common characteristic of the NCLs is the presence of autofluorescent storage material resembling ceroid and lipofuscin lipopigments that also accumulate during the normal ageing process. This storage material is observed in many tissues and cell types, but the pathological effect of the disease is most prominent in the central nervous system (CNS) and the eyes. There are several subtypes of NCL, each of which is associated with a distinct gene and differs according to age of onset, disease progression and severity and the morphological appearance of the storage material (Goebel, 1999; Wisniewski et al., 2001).

Age of onset was originally used to classify the NCLs into infantile, late infantile, juvenile, and the rare adult onset types. Genes assigned to the respective subtypes were *CLN1, CLN2, CLN3* and *CLN4*. This classification has been adapted over the years as more genes involved in causing NCL phenotypes were identified. It now includes a group of variant late infantile NCL (vLINCL) with a similar disease phenotype, caused by mutations in the genes *CLN5, CLN6, CLN7* or *CLN8*, and the most recent addition to the NCL classification *Cathepsin D* (*CTSD*), mutations in which cause congenital NCL. The genes for *CLN4* and *CLN7* have not yet been identified. Other mutations in mice genes have also been reported but not yet identified in humans.

Common pathological characteristics of NCL disease progression include progressive visual deterioration leading to blindness, epilepsy, intellectual and motor decline. Eventually all affected individuals die prematurely due to death of cortical neurons (Goebel, 1999).

The appearance of the storage material is characteristic for each type of NCL and has long been used as a diagnostic tool (Goebel, 1999). There are four main

types of storage with some additional variant forms: granular osmiophilic deposits (GRODs), curvilinear profiles (CL), rectilinear bodies (RL) and fingerprint bodies (FP).

Changes in lysosomal pH have been reported as a result of mutations in NCL genes (Holopainen et al., 2001), although it has not been elucidated to date how this affects lysosomal function in NCL patients. Fibroblast cell lines from patients with mutations in *CLN1, CLN3, CLN5, CLN6* and *CLN8* showed increased lysosomal pH, with *CLN6* and *CLN1* being the most affected. A slight reduction in lysosomal pH was observed in fibroblast cells from patients with mutations in *CLN2*.

Below is a brief overview of the different forms of NCL, where the gene has been identified, with particular focus on the group of variant late infantile NCLs. CLN6 will be introduced separately in section 1.6.

1.5.1 CLN1

Mutations in *CLN1* cause infantile (I)NCL (Goebel, 1999; Santavuori et al., 1974). Mutations in *CLN1* causing NCLs with later onset have also been reported (Bonsignore et al., 2006; Goebel, 1999; van Diggelen et al., 2001)(Mole, et al., 2006, *in press*).

INCL is distinct from the other NCL types, except for congenital NCL caused by mutations in *CTSD*, in the appearance of the storage material as granular osmiophilic deposits (GRODs), which has been used as a diagnostic marker. The protein component of the storage material mainly contains saposins A and D (Haltia et al., 1973; Tyynela et al., 1993).

The *CLN1* gene encodes the enzyme palmitoyl protein thioesterase 1 (PPT1), which removes palmitate groups from S-acylated proteins (Camp and Hofmann, 1993). It is located in lysosomes in non-neuronal cells and in axons,

synaptosomes and synaptic vesicles in neuronal cells (Ahtiainen et al., 2003; Hellsten et al., 1996; Lehtovirta et al., 2001; Verkruyse and Hofmann, 1996). Its *in vivo* substrates remain unknown.

Two mouse models have been generated to date. The Ppt1 knockout mouse (Gupta et al., 2001) shows disease progression similar to INCL and was used to show a reduction in the pool of synaptic vesicles in cortical neurons (Virmani et al., 2005). The *Ppt1Δex4* mouse (Jalanko et al., 2005) also shows disease progression similar to INCL. Recently a *Drosophila melanogaster* model with Ppt1-deficiency was generated, which has accumulation of abnormal, non-GROD storage material and a reduced lifespan without evidence of neurodegeneration (Hickey et al., 2006).

1.5.2 Cathepsin D

Congenital NCL was first observed in White Swedish Landrace sheep and was found to be caused by a mutation in ovine *cathepsin D* (Jarplid and Haltia, 1993; Tyynela et al., 2000). Recently, mutations in *CTSD* have been shown to cause congenital NCL in humans as well and the storage material described as GRODs (Siintola et al., 2006b). This is thought to be the most aggressive form of NCL with the earliest age of onset (Siintola et al., 2006a). Mutations resulting in residual cathepsin D activity have been reported to cause NCL with onset in late infancy (Steinfeld et al., 2006).

Cathepsin D is an aspartic proteinase, which is localised in lysosomes. It has also been reported to be involved in a number of other cellular processes, such as apoptosis, autophagy and different types of cancer (Garcia et al., 1990; Kagedal et al., 2001; Liaudet-Coopman et al., 2006; Uchiyama, 2001; Vigneswaran et al., 2000).

A cathepsin D-deficient *Drosophila* model was reported to have storage material resembling GRODs and to show modest age-dependent neurodegeneration (Myllykangas et al., 2005). A mouse model was originally generated to study the

function of cathepsin D (Saftig et al., 1995) and later shown to have storage material resembling GRODs and fingerprint profiles (Koike et al., 2000). A naturally occurring mutation in cathepsin D has also been reported in American Bulldogs. It has residual enzymatic activity which explains the onset of disease in young adulthood (Awano et al., 2006b).

1.5.3 CLN2

The *CLN2* gene encodes the lysosomal tripeptidyl-peptidase I (TPP-I) enzyme and mutations in TPP-I have been described to cause classic late infantile NCL (LINCL) (Sharp et al., 1997; Sleat et al., 1997). Some mutations of *CLN2* can also cause NCL with delayed onset and slower disease progression (Sleat et al., 1999).

The storage material appears as curvilinear profiles and the protein component contains mainly subunit c of the mitochondrial ATP synthase complex (Lake and Hall, 1993); but other components have been reported such as saposins A and D (Tyynela et al., 1995) and β-amyloid precursor protein (Wisniewski et al., 1990).

Fibroblast cells from INCL patients were shown to be deficient in TPP-I (Sohar et al., 1999; Vines and Warburton, 1999). TPP-I is a lysosomal serine-carboxyl peptidase that removes tripeptides from the N-terminus of small peptides but not large proteins (Vines and Warburton, 1999; Warburton and Bernardini, 2000). It is synthesised as a 67 kDa precursor form which is processed into a 46 kDa mature N-glycosylated protein (Ezaki et al., 1999; Golabek et al., 2003; Lin et al., 2001; Sleat et al., 1997). Mutants affecting conserved regions of the protein have been shown to remain in the ER, indicating that the mutant proteins are most likely misfolded (Steinfeld et al., 2004). However, a mutation in one of the N-glycosylation sites results in a protein that traffics normally to the lysosome but remains catalytically inactive. This mutation is associated with a more severe disease phenotype (Tsiakas et al., 2004).

The *in vivo* substrates of TPP-I remain unknown, although the protein has been implicated in initiating the lysosomal degradation of subunit c of the mitochondrial ATP synthase (Ezaki et al., 2000; Ezaki et al., 1999; Ezaki et al., 1995; Kida et al., 2001). It has furthermore been shown to be involved in the degradation of the neuropeptide neuromedin B, indicating that it might have a special function in neurons (Kopan et al., 2004). CLN2 has been reported to interact with CLN5 (Vesa et al., 2002).

A mouse model of Cln2 was generated, which has no detectable enzymatic activity and displays similar clinical features to human patients (Sleat et al., 2004). A naturally occurring model exists in Dachshund dogs resulting from a mutation in the canine *TPP1* gene (Awano et al., 2006a).

1.5.4 CLN3

Mutations in *CLN3* cause the most common form of NCL with juvenile onset (JNCL). The storage material in patients resembles fingerprint profiles (Goebel, 1999) and CLN3 patients are the only NCL patients with vacuolated lymphocytes (Anderson et al., 2005; Derwort and Detering, 1959). The protein is highly conserved and homologues have been described in mouse, rabbit, dog, sheep, *C. elegans*, *S. cerevisiae* and *S. pombe* suggesting that it has an essential function in eukaryotic cells (Goebel, 1999).

The CLN3 protein was predicted to be a transmembrane protein spanning the membrane either five (Mao et al., 2003a) or six times (Janes et al., 1996). In the six transmembrane model, the N- and C-termini of CLN3 have been shown to protrude into the cytoplasm (Kyttala et al., 2004a). The protein was shown to be glycosylated and different isoforms were detected in a range of 45 – 66 kDa depending on the glycosylation state (Ezaki et al., 2003).

Controversy still exists about the intracellular localisation of CLN3. It has been shown to localise to the membranes of lysosomes and late endosomes (Ezaki et al., 2003) and also to synaptosomes (Luiro et al., 2001) and early endosomes

(Kyttala et al., 2004a) in neurons. CLN3 has also been shown to traffic via the plasma membrane (Mao et al., 2003b; Persaud-Sawin et al., 2004). Other groups have reported that CLN3 is localised in the Golgi apparatus, recycling endosomes and lipid rafts on the plasma membrane (Kremmidiotis et al., 1999; Persaud-Sawin et al., 2004; Rakheja et al., 2004).

Lysosomal targeting of CLN3 has been shown to be mediated by either one or two motifs, a dileucine motif in the second cytosolic loop (Kyttala et al., 2004a; Storch et al., 2004) and an unconventional motif in the C-terminal tail (Kyttala et al., 2004a). Conflicting data exists about the mechanism by which CLN3 traffics intracellularly. Trafficking has been proposed to be dependent on both of the adaptor complexes (AP-) 1 and AP-3 (Kyttala et al., 2004b; Mao et al., 2003b) or independent of them (Storch et al., 2004).

The function of CLN3 remains unknown, although it has been implicated in many cellular mechanisms. CLN3 has been reported to bind to the microtububule binding protein Hook1 (Luiro et al., 2004) and also to CLN5 (Vesa et al., 2002). Receptor mediated endocytosis has been shown to be reduced in fibroblast cell lines from CLN3 patients (Luiro et al., 2004). It was also reported that the levels of lysosomal glycoproteins containing mannose-6-phosphate modifications, including TPP-I, were highly increased in brain samples from JNCL patients. This was accompanied by an increase in enzymatic activity of TPP-I, however this increase was not to the same extent as the increase in protein levels, indicating that there may be an accumulation of enzymatically inactive TPP-I in neurons of JNCL patients (Sleat et al., 1998).

The most common mutation (85% of disease chromosomes) in *CLN3* is a 1 kb deletion that encodes a truncated protein that is retained in the ER (Jarvela et al., 1999). It has recently been suggested that this mutant is partially functional, reclassifying JNCL from a loss of function to a mutation specific disease (C. Kitzmuller, R. Haines, S. Mole, personal communication).

Several mouse models for CLN3 exist, the Cln3 knock-out mouse (Cln3 -/-), which is missing exons one to six (Greene et al., 1999), and the Cln3 knock-in mouse, which is missing exons seven and eight (Cotman et al., 2002). Both models display neurodegeneration similar to JNCL. Microarray studies on brains from the Cln3 knock-out mouse implicated Cln3 in diverse functions such as mitochondrial glucose metabolism, cytoskeleton and synaptosome (Luiro et al., 2006). Mitochondrial abnormalities and changes in lysosomal size and distribution as well as a decrease in endocytosis were observed in the Cln3 knock-in mouse (Fossale et al., 2004), and it was further shown that there was a disruption in the maturation of autophagic vacuoles (Cao et al., 2006). In the yeast model *S. pombe* the CLN3 homologue Btn1p has been shown to involved in regulating vacuole homeostasis (Gachet et al., 2005). In the *S. cerevisiae* model deleted for Btn1p, the protein has been implicated in vacuole pH homeostasis and arginine transport (Kim et al., 2003; Pearce et al., 1999; Pearce and Sherman, 1998). There is also a *C. elegans* model of CLN3, which is mutated in all three homologues of *CLN3* and which displays a mild phenotype (de Voer et al., 2005).

1.5.5 CLN5

A rare form of vLINCL caused by mutations in *CLN5* is found predominantly in Finland. The storage material in vLINCL patients resembles fingerprint and curvilinear profiles with some non-classical condensed fingerprint profiles and lamellar inclusions (Mole et al., 2005). CLN5 was predicted to be a transmembrane protein (Savukoski et al., 1998) and has been shown to be glycosylated and to localise to lysosomes (Isosomppi et al., 2002; Vesa et al., 2002). CLN5 has four methionies, each of which can act as a start codon for translation. Conflicting data exists about the molecular weight of CLN5, whether it is a soluble or transmembrane protein and about the intracellular trafficking of CLN5 constructs modelling the most common naturally occurring mutants.

It has been reported that four isoforms of CLN5 can exist. The longest one has been shown to be a membrane protein and the three shorter forms soluble (Vesa

et al., 2002), while it was shown in parallel that CLN5 only exists as a soluble protein (Isosomppi et al., 2002). Furthermore, has been shown that murine Cln5 is a soluble protein which localises to lysosome in non-neuronal cells and to lysosomes and additional non-lysosomal compartments in neurons (Holmberg et al., 2004). However, more recently it has been reported that CLN5 exists as four integral membrane isoforms (Bessa et al., 2006). The molecular weight of the protein has been reported in the range of 45 to 60 kDa (Bessa et al., 2006; Isosomppi et al., 2002; Vesa et al., 2002). The most common disease-modelling mutants have been reported to localise to the lysosome but one also to the Golgi (Isosomppi et al., 2002; Vesa et al., 2002).

CLN5 has been reported to interact with both CLN2 and CLN3. Interaction between CLN5 and CLN2 was abolished with four of the most common disease mutants, while the interaction with CLN3 was retained (Vesa et al., 2002). It has also been reported that mRNA levels of CLN3 are reduced in fibroblast cell lines from CLN5 patients (Bessa et al., 2006).

A mouse model of CLN5 was developed (Cln5-/-) which mimics the progressive neurodegeneration seen in patients (Kopra et al., 2004). Naturally occurring models of CLN5 exist in Border collie dogs (Melville et al., 2005) and Devon cattle (Houweling et al., 2006a).

1.5.6 CLN8

This form of vLINCL is very varied phenotypically, ranging from a disease similar to vLINCL caused by mutations in *CLN5* and *CLN6* to what was originally called Northern epilepsy or progressive epilepsy with mental retardation (EPMR). The EPMR phenotype is to date confined to a remote geographic area in North-Eastern Finland and is caused by a mild mutation in *CLN8* (Ranta et al., 1999), although it has been suggested that EPMR may occur in other populations as well (Hirvasniemi et al., 1994). Other variants caused by mutations in the *CLN8* gene are Turkish vLINCL, which was originally thought to be linked to mutations in *CLN7* (Mitchell et al., 2001; Ranta et al., 2004), and

Italian vLINCL, which suggests that mutations in *CLN8* are more widespread than previously thought (Cannelli et al., 2006). The storage material in CLN8 patients varies according to the mutation and severity of the disease. Data on this subject is still very limited, however fingerprint profiles and mixed fingerprint and curvilinear profiles have been reported (Mole et al., 2005).

CLN8 was predicted to be a transmembrane protein (Ranta et al., 1999) and later shown to be primarily resident in the ER but also recycling between the ER and the ERGIC (Lonka et al., 2000). It has also been reported to have an additional location in neurons (Lonka et al., 2004). CLN8 is a 33 kDa protein which does not undergo proteolytic processing and which contains an ER-retrieval signal (KKRP) (Lonka et al., 2000). CLN8 can form homodimers (Heine et al., 2006, *in press*).

CLN8 is part of the TLC family of proteins, whose function has been proposed to be involved in the synthesis of ceramide moieties and the activation of lipid synthesis. Other members of this family are TRAM which is involved in polypeptide translocation into the ER and the *S. cerevisiae* Lag1 which facilitates ER to Golgi transport of GPI-anchored proteins (Winter and Ponting, 2002). Mass spectrometric analysis of cerebral samples from two CLN8 patients revealed changes in sphingo- and phospholipid profiles, which was proposed to affect membrane stability, lipid peroxidation, vesicular trafficking and neurotransmission (Hermansson et al., 2005).

A naturally occurring mouse model called *mnd* exists, carrying a 1-bp insertion in *Cln8*, which is predicted to result in a truncated protein (Bronson et al., 1993; Ranta et al., 1999). Using this model it was shown that Cln8 may be involved in maturation, differentiation and survival of different neuronal populations with the expression of Cln8 mRNA in postnatal brains being the highest in the cortex and the hippocampus (Lonka et al., 2005). It was also shown that in *mnd* mice, mitochondrial associated membranes of the ER (MAM) were aberrant and a reduction in phospholipid biosynthetic enzyme activity was observed (Vance et

al., 1997). Another naturally occurring model of CLN8 has been identified in English Setter dogs, which contain a missense mutation (Katz et al., 2005).

1.6 CLN6

Ultra-structurally vLINCL patients with mutations in *CLN6* show a mixed pattern of variant rectilinear (RL) and fingerprint (FP) complexes accumulating as storage material in the brain. Pure FPs can be seen in intestinal neurons and curvilinear (CL), FP and RL complexes in visceral storage. Lymphocytes are not vacuolated as observed in CLN3 (Goebel and Wisniewski, 2004). Subunit c storage can be observed in brain but not in liver, adrenals and endocrine pancreas (Elleder et al., 1997). Lysosomal pH in fibroblast cell lines from patients is increased (Holopainen et al., 2001).

Age of onset in CLN6 can be very varied, ranging from as early as 18 months to as late as 8 years, but more commonly occurs around age 4. Patients usually present with visual failure or seizures. Progressive visual deterioration, loss of speech and intellectual decline, motor delay, ataxia, epilepsy, disarthria and irritability are among the most common symptoms. Loss of all motor skills occurs between the ages of 4 and 10 years. Patients usually die prematurely in the second or third decade of life (Goebel, 1999; Mole et al., 2005).

CLN6 was originally mapped to a region on human chromosome 15q22-23 by homozygosity mapping in two consanguineous families of Indian origin (Sharp et al., 1999) and the gene identified in 2002 in parallel by two groups using conserved haplotype markers in a Costa Rican subset of families (Gao et al., 2002) and fine mapping and mutational analysis of candidate genes (Wheeler et al., 2002). Twenty-five mutations have been reported to date in families from different countries (Sharp et al., 2003; Siintola et al., 2005; Teixeira et al., 2003)(www.ucl.ac.uk/ncl).

When work for this thesis was started, very limited information was available about CLN6. The protein was predicted to be a 311 amino acid novel protein conserved among vertebrates and bearing no known functional or sequence homology to other known proteins. The protein has seven predicted transmembrane domains (TMD) with mutations found both in TMDs and intraorganellar loops (Gao et al., 2002; Wheeler et al., 2002). It has been shown in fibroblast cells and brain extracts from CLN6 patients and the OCL6 sheep model that there was an increase in the expression and protein levels of the mitochondrial reactive oxygen species stress response protein manganese superoxide-dismutase (MnSOD), suggesting a response to oxidative stress and inflammation (Heine et al., 2003).

In recent years, a number of key publications have advanced knowledge about CLN6. Heine, et al. first showed that overexpressed CLN6 was a resident of the ER, as detected by co-localisation with the rough ER marker PDI, that this protein had a molecular weight of 27 kDa and could form homodimers (Heine et al., 2004). In the same publication it was shown that in fibroblast cells from CLN6 patients, the OCL6 sheep and the *nclf* mouse, the sorting and processing of the lysosomal hydrolase cathepsin D was normal. Further, the activities of two other lysosomal enzymes, beta-hexosaminidase and arylsulphatase A (ASA) were normal (Heine et al., 2004) and it had previously been reported that TPP-I activity was also normal in fibroblasts from CLN6 patients (Sohar et al., 1999). This indicated that trafficking from the ER to the lysosome was not affected by mutant CLN6, at least with respect to the proteins tested. However, it was shown that endocytosis of ASA from the plasma membrane to the lysosome was increased and yet its lysosomal degradation decreased, suggesting an impairment of lysosomal function (Heine et al., 2004).

It was then confirmed that endogenous CLN6 was also located in the ER, as shown by partial overlap with the rough ER marker PDI, although the molecular weight of the protein was reported to be slightly higher at 30 kDa (Mole et al., 2004). In samples from two CLN6 patients, no protein could be detected by Western blotting. Constructs tagged with green fluorescencent protein (GFP)

modelling some of the mutations observed in CLN6 patients as well as wild-type CLN6 were overexpressed. All of these constructs localised to the ER, which indicated that the CLN6 phenotype was not caused by mislocalisation of the mutant proteins, but rather by non-functional proteins. It was further suggested that the mutant proteins may be degraded more rapidly, however no data has been published about the turn-over times of CLN6 mutants to date.

Very recently, the topology, ER retention and oligomerisation of CLN6 were investigated further (Heine et al., 2006, *in press*). It was reported that the N-terminus of CLN6 is in the cytoplasm, the protein has an odd number of transmembrane domains and the C-terminus protrudes into the lumen of the ER, confirming the orientation of the suggested topological model (Wheeler et al., 2002). The potential ER retention motifs in CLN6 were mutated, and it was shown that none of them played a role in CLN6 retention. However, the N-terminal 49 amino acids as well as the two most distal transmembrane domains were implicated in ER retention, although the residues involved in this were not identified. Similar results were also shown when CLN6 was overexpressed in primary hippocampal mouse neurons. Furthermore, in neuronal cell bodies CLN6 located to structures positive for the ER marker PDI. However, in neuronal extensions, this co-localisation was only partial, and CLN6 could also be detected in tubular structures negative for PDI. This is similar to the co-localisation of endogenous CLN6 and PDI in HEK293 cells where overlap was only partial (Mole et al., 2004). CLN6 may therefore be located within regions of the ER other than PDI-positive rough ER, or in an additional location in neuronal cells. Furthermore, it was shown that CLN6 does not heterodimerise with the vLINCL ER-resident protein CLN8 and that the homodimerisation of CLN6 is mediated by regions in both the N- and C-termini. The same regions could be involved in interactions of CLN6 with other proteins.

Microarray studies of fibroblast cells lines from CLN6 patients have recently been reported (Teixeira et al., 2006). Twelve genes were identified and confirmed to be upregulated. These were grouped into the following cellular processes: extracellular matrix remodelling, signalling, apoptosis and

immuno/inflammatory response. Alterations in cholesterol homeostasis and proteoglycan metabolism were further implicated in this data. Indeed it was shown in fibroblast cell lines from CLN6 patients that cholesterol and ganglioside GM2 accumulated in lysosomes and that urinary glycosaminoglycans showed a different profile in CLN6 patients compared to normal control individuals.

A naturally occurring mouse model of CLN6, *nclf,* exists which carries a 1-bp insertion in the murine orthologous *Cln6* gene on mouse chromosome 9 (Bronson et al., 1998; Wheeler et al., 2002). There are also two naturally occurring sheep models, the South Hampshire model, OCL6, and the Merino model, which both carry mutations in the ovine *CLN6* gene (Broom et al., 1998; Broom et al., 1999; Cook et al., 2002; Houweling et al., 2006b; Tammen et al., 2001). Mutations in the Merino sheep model were recently identified while mutations in the South Hampshire model, which was reported to have decreased levels of CLN6 mRNA, remain to date unknown (Tammen et al., 2006). The South Hampshire sheep model was originally used to show that two thirds of storage material in NCL was of protein origin and to identify subunit c of the mitochondrial ATP synthase as a major component of the storage material (Palmer et al., 1986a; Palmer et al., 1989; Palmer et al., 1986b). Recently it was shown that neurodegeneration can be detected in distinct regions of the brain of South Hampshire sheep before the onset of symptoms (Oswald et al., 2005). This was observed in the form of glial activation and did not correlate with the distribution of the storage material, indicating that neurodegeneration and storage material could be independent processes.

In summary, CLN6 is an ER-resident protein of unknown function and mutant forms of CLN6 cause the lysosomal storage and neurodegeneration observed in vLINCL. The link between the ER and the lysosome in vLINCL and the relationship of the vLINCL proteins to each other remain to date unknown.

1.6.1 Possible functions of CLN6

As CLN6 is located in the ER, it is likely that it has a specific function in this organelle. It could be postulated that this function is not essential, otherwise mutations in *CLN6* would lead to embryonic lethality, but instead would be highly specialised. The following hypotheses were proposed:

- CLN6 could be located in a sub-domain of the ER that interacts with mitochondria, as the storage material is in part of mitochondrial origin.
- CLN6 could be located in a sub-domain of the ER that interacts with the lysosome and could in this way contribute directly to a disruption in lysosomal homeostasis.
- CLN6 may interact with ER or other NCL proteins. CLN6 has been reported to interact with itself, but not with CLN8. The identification of an interaction partner would aid in the elucidation of its function. It may interact with known ER proteins, which would implicate it in one of the various function of the ER. It could also interact with other NCL proteins, in particular the other vLINCL protein CLN5 and play a role in its transition through the ER.
- The functions of CLN5, CLN6 and CLN8 may be functionally linked as they all cause the vLINCL disease phenotype. Although they are not located in the same organelle, they could play important roles in the same cellular pathway.

1.7 Project aims

The aims of this project were to establish the tools and techniques necessary to analyse the CLN6 protein and to utilise these to investigate in further detail its subcellular location, to identify proteins that interact with CLN6 and to elucidate the early cellular responses to loss of functional vLINCL proteins, CLN5, CLN6 and CLN8. This would provide insight into the function of the CLN6 protein, the disease mechanism of vLINCL at the cellular level and the relationship between the vLINCL proteins.

2. Materials and Methods

2.1 List of reagents

Listed here are frequently used reagents, including information about the manufacturer they were purchased from and whether they were stored as a stock solution.

Acrylamide (30% acrylamide/0.8% bisacrylamide): Sigma
Agar: Sigma
Agarose: Sigma
Ammonium chloride: Sigma
Ammonium sulphate: Fisons
Ampicillin: Sigma
Antifade Gold reagent with DAPI: Molecular probes
APS (ammonium persulphate, Sigma): 10% stock solution.

Beta-mercaptoethanol (BME): Sigma
Butanol: Sigma
Bromophenol blue: BDH
BS^3: Pierce
BSA aqueous (Sigma): stock solution of 2 mg/ml.
BSA powder: Sigma

CsCl (Caesium chloride): Sigma
Colloidal coomassie (Sigma): 20% stock solution
Coomassie G250: Sigma

DAB (TAAB): 3% stock in 0.05 M Tris-HCl, pH 7.6.
DDSA: TAAB
Dextran blue: Molecular Probes
D-MEM high glucose: Gibco

DMP-30: TAAB

DMSO: Sigma

DNA marker: 1 kb ladder (Promega)

DSP: Pierce

DSS: Pierce

Dynabeads: Dynal biotech (Sheep anti rabbit beads)

EDTA: Sigma

EGTA: Sigma

Ethanol: BDH

Ethanolamine: Sigma

Ethidium bromide: Sigma

FCS: Biowest

Formaldehyde-37: Sigma

Gelatin (fish, Sigma): 20% stock

Gentamycin: Gibco

Glacial acetic acid (acetic acid): BDH

Glucose: Sigma

Gluteraldehyde: TAAB

Glycerol: Sigma

Glycine: Sigma

HEPES: Sigma

Hydrogen peroxide: Sigma

Hydrochloric acid (HCl): BDH

Isopropanol: BDH

LB: Sigma

Leupeptin (Merk Biosciences): stock solution of 100 mg/ml in H_2O.

Magnesium chloride ($MgCl_2$): Sigma

Magnesium sulphate ($MgSO_4$): Sigma

MEM-α with glutamax: Gibco

Methanol: BDH

MG-132 (Merk Biosciences): stock solution of 50 mg/ml in DMSO.

MNA: TAAB

Mowiol: Calbiochem

NP-40 (Igepal): Sigma

NZ amine: Sigma

Osmium: BDH

PBS: Sigma

Pepstatin (Merk Biosciences): stock solution of 100 mg/ml in H_2O.

PFA (Paraformaldehyde): Polysciences

Ponceau S: Sigma

Potassium acetate: Sigma

Potassium dihydrogen phosphate (KH_2PO_4): BDH

Potassium ferricyanide: Sigma

Propylene oxide: Fisher

Protease inhibitor mix: Sigma

Protein markers: Standard markers molecular weights 30-200 kDa (Sigma), Rainbow marker high and low molecular weights (Amersham)

Saponin (Sigma): 20% stock.

SDS (Sigma): 10% stock solution

Silver nitrate: Sigma

SOC media: Invitrogen

Sodium acetate (acetate): Sigma

Sodium azide (azide): Sigma

Sodium cacodylate: TAAB

Sodium carbonate: Fisons

Sodium bicarbonate ($NaHCO_3$): Sigma

Sodium chloride (NaCl): Sigma

Sodium hydrogen phosphate (Na_2HPO_4): Sigma

Sodium hydroxide (NaOH): Sigma

Sodium sulphate: BDH

Sodium thiosulphate: BDH

SYBR green: Finnzymes

TAAB resin: TAAB

Tannic acid: TAAB

TEMED: Sigma

Tris Base: Sigma

Triton-X: Sigma

Trypsin: Sigma

Tryptone: Sigma

TSA-kit (reagent and amplification reagent): Perkin Elmer

Tween-20: Sigma

Yeast extract: Sigma

2.2 Antibodies

2.2.1 Antibody production

Polyclonal antibodies were raised against human CLN6. Peptide synthesis and immunisation were performed by Eurogentec (Seraing, Belgium). Peptides were chosen according to the following criteria:

- Approximately 20 amino acids long
- Containing as many antigenic amino acids as possible (H, K, A, L, N, R)
- Located at hydrophilic regions in the protein
- Determined by BLAST not to be present in other proteins
- Located in regions less conserved across species

Peptides were EP01293-MEATRRRQHLGATGG (residues 1-15) for 1746/1747 and EP01294-ARHGSVSADDEAAR (residues 28-39) for 1748/1749 coupled to KLH. A cysteine residue was added to force coupling to the C-terminal side of peptide EP01293 since this corresponds to the amino terminus of CLN6. First injection was in complete Freunds Adjuvant, subsequent injections (at day 14, 28 and 58) with incomplete Freunds Adjuvant. Final bleed antisera were taken after three months.

2.2.2 Antibody purification

Peptides were coupled to NHS-activated sepharose in HiTrap affinity columns (Amersham Biosciences). Peptides were dissolved at 4 mg/ml in coupling buffer (0.2 M $NaHCO_3$, 0.5 M NaCl, pH 8.3). Columns were washed in ice-cold 1 mM HCl using a Gilson Minipuls 3 pump. The peptide solution was injected onto the column and coupled for 2 hours at RT (room temperature). The columns were then washed with Buffer A (0.5 M ethanolamine, 0.5 M NaCl, pH 8.3) and Buffer B (0.1 M acetate, 0.5 M NaCl, pH 4) a number of times. Columns were stored in 10 mM Tris, pH 7.5 with 0.1% azide at 4°C.

To purify the antibodies, columns were washed in Start buffer (0.5 M NaCl, 10 mM Tris, pH 7.5, cold) and Elution buffer (100 mM glycine, pH 2.5, cold) and equilibrated in Start buffer. 8 ml aliquots of antisera were purified at a time. Samples were spun to pellet debris for 5 min at 1,000 rpm in a Sorval TC centrifuge (rotor H400). Samples were then applied onto the columns and pumped on a circular loop for 4 hours on ice. Columns were then washed with 10 mM Tris, pH 7.5 followed by Start buffer until the effluent was clear. Six 1 ml fractions of eluted antibody in Elution buffer were collected. 100 µl 1 M Tris, pH 8 was added to each to neutralise the Elution buffer. Samples were run on SDS-Page gels and stained with colloidal comassie to ascertain which fractions contained the purified antibody. These fractions (usually fractions 2 and 3) were pooled and aliquots of 50 µl were stored at –20°C.

The columns were washed and stored in 10 mM Tris, pH 7.5 with 0.1% azide at 4°C.

2.2.3 List of antibodies used

Name	Description	Application	Dilution	Source
1746p	Human CLN6, rabbit polyclonal	IF, WB, IP	IF 1:1,000; WB 1:500, IP 3 µl Ab / 2 ml lysate	(Mole et al., 2004)
1747p	Human CLN6, rabbit polyclonal	IF, WB, IP	IF 1:1,000; WB 1:500, IP 3 µl Ab / 2 ml lysate	(Mole et al., 2004)
1748p	Human CLN6, rabbit polyclonal			(Mole et al., 2004)
1749p	Human CLN6, rabbit polyclonal			(Mole et al., 2004)
Actin	Rabbit monoclonal	IF	1:500	Sigma
Calreticulin	Rabbit polyclonal	IF	1:50	ABR
IB5	CD 63, mouse monoclonal	IF	1:300	(Fraile-Ramos et al., 2001)
H4A3	Lamp-1, mouse monoclonal	IF	1:100	Hybridoma bank
EEA-1	Mouse monoclonal	IF	1:100	BD Transduction Laboratories
GFP	Sheep polyclonal	IF	1:100	Biogenesis
PDI (RL90)	Mouse monoclonal	IF	1:50	AbCam
GM130	Mouse monoclonal	IF	1:100	BD Transduction Laboratories
Gamma-actin	Sheep polyclonal	WB	1:500	Chemicon
Beta-tubulin	Mouse monoclonal	WB	1:500	Sigma
eIF4AIII (hNMP65)	Mouse monoclonal	WB	1:300	(Tange et al., 2005)
mtHSP70	Mouse monoclonal	WB	1:1000	(Bhattacharyya et al., 1995)

Table 2.2.3.1: Primary antibodies

WB: Western blotting, IF: Indirect immunofluorescence, IP: immunoprecipitation

Name	Tag	Application	Dilution	Source
Goat anti rabbit	HRP	WB	1:4,000	Jackson
Goat anti mouse	HRP	WB	1:4,000	Jackson
Donkey anti sheep	FITC	IF	1:100	Jackson
Donkey anti rabbit	Cye 5	IF	1: 200	Jackson
Goat anti rabbit	Alexa 488	IF	1:400	Invitrogen
Goat anti rabbit	Alexa 588	IF	1:400	Invitrogen
Goat anti mouse	Alexa 488	IF	1:400	Invitrogen
Goat anti mouse	Alexa 588	IF	1:400	Invitrogen
Goat anti mouse	IR Dye 800	QuIF	1:1,000	Li-Cor
Goat anti rabbit	IR Dye 800	QuIF	1:1,000	Li-Cor

Table 2.2.3.2: Secondary antibodies

WB: Western blotting, IF: indirect immunofluorescence, QuIF: quantitative immunofluorescence

2.3 Cloning and Molecular Biology

2.3.1 Restriction digest

The following template reaction set-up was used for all restriction digests:

Buffer	2 µl
DNA	1-3 µl
BSA	0.2 µl
Restriction enzyme	1 µl
H_2O	
Final volume:	20 µl

Buffers, BSA and enzymes were supplied by Promega, enzymes were at 10 U/µl. Incubation time was 1 hr (2 hr if 2 enzymes were used and the buffer system in combination was less than 100% efficient for one of the enzymes) at 37°C.

2.3.2 Ligation

A series of ligations (L) were set up for cloning inserts into vectors. Different ratios were used to optimise ligation of insert into vector as shown in figure 2.3.2. Ligations were performed at 4°C overnight.

(µl)	L 1	L 2	L 3	L 4	L 5	L 6
Vector	1	1	1	1	1	1
Insert	1	0.5	1.4	0	3	6
H_2O	6	6.5	5.6	7	4	0
Ligase	1	1	1	1	1	1
Buffer	1	1	1	1	1	1

Table: 2.3.2: Ligations

2.3.3 Site directed mutagenesis (with all primers)

Reagents were from the Quickchange II XL kit (Stratagen).
Reactions were set up according to the following template:

10x Reaction buffer	5 µl
10 ng/µl DNA	1 µl
10 ng/µl Forward Primer	12.5 µl
10 ng/µl Reverse Primer	12.5 µl
dNTPs	1 µl
Quicksolution	3 µl
H_20	15 µl
Total volume	50 µl

1 µl Pfu Ultra HF DNA polymerase (2.5 U/µl) was added to the reaction and samples run in a MJ Research PTC-200 Peltier Thermal Cycler PCR machine on the following program:

95°C 1 min

18 cycles of:

95°C	50 sec
60°C	50 sec
68°C	1 min
followed by:	
68°C	7 min

1 µl Dpn (10 U/µl) was added and the restriction digest performed for 1 hr at 37°C. Samples were stored at 4°C.

2.3.4 Transformation

Competent cells (DH 5 alpha or XL-10 Gold from Quickchange II XL kit for site-directed mutagenesis) were thawed on ice and aliquoted into 45 µl per transformation under sterile conditions. 2 µl BME (Quickchange II XL kit) was added for 10 min. 10 µl ligation products or 2 µl site-directed mutagenesis products were added for 30 min on ice. Samples were heat shocked at 42°C for 30 sec. After 2 min on ice, cells were rescued in 500 µl of either SOC media or NZY+ broth (1 g NZ amine, 0.5 g yeast extract, 0.5 g NaCl, at pH 7, add 1.25 ml 1 M $MgCl_2$, 1 ml 1 M $MgSO_4$, 2 ml 20% glucose, 1 l final volume) for 1 hour at 37°C with 250 rpm in an Eppendorf Thermomixer Compact. Samples were then plated on Agar plates (15 g/l agar in LB, autoclaved), containing relevant antibiotics such as ampicillin, and left to grow overnight at 37°C or over the weekend at RT.

2.3.5 DNA and RNA preparations

2.3.5.1 Mini, Midi and Maxi DNA Preparations

DNA preparations were done with Qiagen Kits according to the manufacturer's instructions. DNA was eluted in H_20 and stored at -20°C.

2.3.5.2 Caesium chloride preparations

400 ml of LB (10 g tryptone, 5 g yeast extract, 10 g NaCl in 1 l H_20, pH 7, autoclaved) was inoculated with a starter culture and incubated overnight in a Kuehner ISF-1-W shaking incubator. Samples were centrifuged for 20 min at 6,000 rpm in a Beckman HLA-1624 rotor. Pellets were resuspended in buffer P1 (50 mM glucose, 25 mM Tris, pH 8, 10 mM EDTA, pH 8, autoclaved and stored at 4°C). Buffer P2 (0.2 M NaOH, 1% SDS, made fresh) was added for 10 min. Buffer P3 (3 M potassium acetate, stored at 4°C) was added and the samples centrifuged for 15 min at 9,000 rpm in the same rotor. Supernatants were poured through a tea strainer into ice-cold isopropanol. This was centrifuged for 15 min at 9,000 rpm. The supernatant was discarded and the pellet dissolved in 5.5 ml TE (10 mM Tris, pH 7.5, 1 mM EDTA). To this 550 µl of 5 mg/ml ethidium bromide was added followed by 6 g of CsCl. Samples were spun for 5 min at 4,000 rpm in a Sorvall H400 rotor to pellet debris and the optical density measured and adjusted to 1.55-1.56 with 1.1 g CsCl/ml TE if necessary. Cleared solutions were loaded into Beckman Quick-Seal centrifuge tubes and sealed. Tubes were spun at 100,000 rpm overnight in a Beckman ultracentrifuge in a TLN100 rotor at 20°C. Plasmid bands were removed from the tubes and the ethidium bromide extracted with water-saturated butanol until the solutions appeared clear. Two volumes of water were added and to this two total volumes of ethanol. Extra ethanol was added if necessary until a DNA precipitate was visible. Samples were spun at 9,000 rpm in JLA-16.250 rotor for 15 min at 4°C in glass tubes. Pellets were washed in 70 % ethanol and air-dried. Pellets were resuspended in H_2O and the concentration measured in a GeneQuant Pro spectrophotometer. DNA was stored at -20°C.

2.3.5.3 RNA preparations

RNA preparations were done with Qiagen Kits according to the manufacturer's instructions. Cells were lysed and passed through a QiaShredder and RNA extracted using an RNeasy mini kit. RNA was eluted in RNase free H_20 and stored at -20°C.

2.3.6 DNA sequencing

DNA sequencing was provided by the MRC Geneservice. Innoculated starter cultures were grown overnight in a shaking incubator in a total volume of 2 ml LB. 1 ml of sample was sent to the MRC Geneservice for sequencing. Sequences were analysed using programs DNA Star and DNA Strider.

2.3.7 Agarose gels

Gels contained 1% agarose in TAE (4.84 g Tris, 1 ml glacial acetic acid, 2 ml 0.5 M EDTA, pH 8, total volume 1 l) and 4% ethidium bromide. Gels were run at 100 mV for 30 min. DNA 1 kb ladder was used as a loading control.

2.3.8 List of constructs used

Construct	Source
CLN6-HRP	Yella Martin, Claudia Kitzmüller
Sec24-GFP	(Stephens et al., 2000)
GFP-cytochrome b(5)	(Pedrazzini et al., 2000)

Table 2.3.8: Constructs used

2.3.9 Q-PCR

RNA was reverse transcribed into (complementary) cDNA in a Techne Genius PCR machine, according to the following protocol (all reagents were from Invitrogen):

total RNA	8 µl
random hexamers	1 µ
10 mM dNTP mix	1µl

65°C for 5 min, 4°C for at least 1 min. The following were then added:

10x RT buffer	2 µl
25 mM $MgCl_2$	4 µl
0.1 M DTT	2 µl
RNase OUT (40 U/µl)	1 µl
SuperScript III RT (200 U/µl)	1 µl

25°C for 10 min, 50 °C for 50 minutes, 85°C for 5 min, 4°C. 1 µl RNase H was added at 37°C for 20 min. Samples were either used immediately or stored at -20°C.

Q-PCR was performed in an MJ Research DNA Engine Opticon 2 with the following reaction mixture for each sample. Samples were done in duplicates or triplicates.

SYBR Green	12.5 µl
DNA at 100 ng/µl	6.25 µl
Primer mix at 1.2 pM	6.25 µl

Conditions were:

95°C	10 min
40 cycles of:	
95°C	10 sec
54°C	15 sec
72°C	15 sec
plate read	
77°C	1 sec
plate read	
followed by:	
72°C	10 min

melting curve 65 – 95°C, read every 0.5°C, hold 1 sec

72°C	8 min

Samples were analysed using Opticon Monitor 2 program and Microsoft Excel.

2.3.10 Primers and siRNA

Primers:

CLN5	For GCC CCT TTC TGG TGT AAT CAA G
	Rev TCC CAT TTT CCT TCC AGT GAA (Bessa et al., 2006)
CLN6	For CCC ATT GCC ATG CTG GTA TTC CC
	Rev GGC GGT GGT TGA CAG AGT CAC CC
CLN8	Qiagen Quantitect validated primers Hs_CLN8_1_SG and
	For CCA CCT GTC CAA CTT GAT CTT CCG G
	Rev CGG ACC AGC CCG CCT TAA GAG CAT CC
GAPDH	For CAG CCT CAA GAT CAT CAG C
	Rev GTC TTC TGG GTG GCA GTG AT
Actin	For GCG AGA AGA TGA CCC AGA T
	Rev TGG TGG TGA AGC TGT AGC C

For: forward primer, Rev: reverse primer

siRNAs were designed and chosen according to the guidelines on the Qiagen website (www.qiagen.com) and verified by BLAST sequence alignment:

CLN5-1	GGACAGGTCAGTTCATAAA
CLN5-2	AACTGCTGTCTGGTAAAAACA
CLN6-1	CCGGTCTCTTCCTCGGAAA
CLN6-2	CCAGAGACCGAGAGCATGA
CLN8-1	CAAGGTGTATAGTAACCTA
CLN8-2	CGCTAATCATTAATCCATA
Control	ACGUGACACGUUCGGAGAA

2.4 Cell culture

2.4.1 List of cell types/lines used

Cell line name	Species	Transformed/Primary	Source
HEK293	Human	Transformed	Culter lab
HeLa	Human	Transformed	Culter lab
Human fibroblasts	Human	Primary	Mole lab and others

Table 2.4.1: Cell types/lines used

2.4.2 List of fibroblast cells lines used

Name	Type	Mutation	Protein	Source
Hs68	Healthy control			CRUK
BR3	Healthy control			Peter Clingen, UCL
48BR	Healthy control			Peter Clingen, UCL
HF364Pa	CLN6	I154del/c.829-832delGTCG; c.837delG	p.[Ile154del]+[Val277fs]	Kohlschutter, Braulke
HF423Pa	CLN6	c.316insC/c.316insC	p.[Arg106fs]+[Arg106fs]	GOS
HF471Pa	CLN6	E72X/E72X	p.[Glu72X]+[Glu72X]	Boustany
HF476Pa	CLN6	R5W; D83H		Freehauf/ Boustany

Table 2.4.2: Fibroblast cell lines used

2.4.3 Culture conditions

HEK293 and HeLa cells were cultured in MEM-α with glutamax. Fibroblasts derived from skin biopsies were cultured in D-MEM high glucose. All culture media was supplemented with 10% FCS and 1% gentamycin. Cells were grown

at 37°C with 5% CO_2 in Galaxy R CO_2 incubators and split using trypsin/EDTA. Cell culture dishes were 3.5, 6, 9 or 14 cm (NUNC).

2.4.4 Transfection

Amaxa nucleofector and nucleofection kits were used for transient transfections. Subconfluent cells were trypsinised and counted in a Coulter Z2 cell counter. 0.5 to 2 x 10^7 cells were used per nucleofection with kits as follows:

Cell line	Kit	Program
HEK293	Cell line V	A-23
HeLa	Cell line R	I-13

Table 2.4.4: Transfections

Cells were mixed with 100 µl nucleofector solution per nucleofection and 1-5 µg DNA or 4-10 µl siRNA and nucleofected in the supplied vials. Cells were rescued immediately after nucleofection in normal growth medium, seeded in 6 or 9 cm dishes and cultured for times indicated.

2.4.5 Microinjection

All microinjections were performed by Dr. Claudia Kitzmüller, UCL. DNA or siRNA was diluted to 0.1 µg/µl in H_20. Cells were co-microinjected with Dextran Blue at 5 µg/µl to identify microinjected cells. Borosilicate glass capillaries (Harvard Apparatus) were pulled into needles using a Flaming/Brown Micropipette Puller (Sutter Instruments), settings were: heat = 447, pull = 35, velocity = 55, time = 250. Cells were grown to subconflucency on glass coverslips and the coverslips scored using a diamond scorer to ease identification of injected cells. Cells in the vicinity of the scored cross were injected using an Eppendorf Micromanipulator 5171.

2.5 Protein work

2.5.1 Cell extracts

For immunoprecipitations, media was aspirated from culture dishes and cells placed on ice, washed x2 in cold PBS (137 mM NaCl, 2.7 mM Kcl, 10 mM KH_2PO_4, 2 mM Na_2HPO_4, in 1 l H_20, pH 7.4, sterile), then lysed in either non-denaturing lysis buffer (NDLB, 500 mM Tris-HCl, pH 7, 200 mM NaCl, 7.5 mM EDTA, 7.5 mM EGTA, 0.5% Triton-X, 0.25% NP-40, protease inhibitors) or NET lysis buffer (200 mM NaCl, 75 mM Tris-HCl, pH 7, 7.5 mM EDTA, 1% Triton X-100, protease inhibitors) as indicated. Lysates were scraped off the dishes using a rubber policeman and transferred into Eppendorf tubes and incubated on ice for 10 min. Lysates were centrifuged at 12,000 rpm for 10 min at 4°C in a Beckman Avanti 30 Centrifuge with a F2402H rotor. Supernatants were transferred to fresh tubes and total lysates immunoprecipitated as described below.

For Western Blotting, cells were trypsinised and washed x2 in PBS. Pellets were resuspended in NET buffer for 10 min on ice. Lysates were then centrifuged as described. To determine total protein content, Bio-Rad protein assay reagent was used according to protocol. Either 2 µl total lysates were diluted 1:10 or used neat. Of this between 1 and 10 µl were diluted in H_2O (total volume 800 µl) and added to 200 µl protein assay reagent. A freshly prepared dilution series of bovine serum albumin (BSA) was used as a standard. Absorbance at 600 nm was measured using GeneQuant Pro and samples adjusted to a total concentration of 1µg/µl in 3x non-reducing SDS-PAGE sample buffer (150 nM Tris-HCl, pH 6.8, 2% SDS, 0.1% bromophenol blue, 10% glycerol).

2.5.2 Immunoprecipitation and crosslinking

For crosslinking experiment, crosslinkers DSS, DSP and BS^3 were weighted using a AND HM-200 balancing scale and made up to a stock solution of 25 mM in either desiccated DMSO or HEPES lysis buffer:

Crosslinker	Cell-permeable	Cleavable	Buffer
DSS	Yes	No	DMSO
DSP	Yes	Yes	DMSO
BS^3	No	No	HEPES lysis buffer

Table: 2.5.2: Cross-linkers

For cell-permeable crosslinkers, cells grown to confluency on 9 cm dishes were washed 3x in cold PBS and incubated with crosslinker in PBS (final concentration 25 μM) at room temperature for 30 min and quenched with Tris, pH 7.2, to a final concentration of 200 mM, for 15 min. Total lysates were obtained in NET buffer as described above.

For non-permeable crosslinkers, total cell extracts were obtained as described above, however HEPES lysis buffer (50 mM HEPES, pH 7.6, 200 mM NaCl, 1% Triton-X, protease inhibitors) was used as the presence of Tris quenches crosslinking activity. Cell lysates were incubated with crosslinker (final concentration 25 μM) for 30 min at room temperature and the reaction quenched by the addition of Tris, pH 7.2, to a final concentration of 200 mM, for 15 min.

For immunoprecipitation, lysates were either pre-cleared or incubated with primary antibody for 30 min at 4°C with rotation. For pre-clearing steps, sheep anti rabbit magnetic dynabeads were washed x2 in PBS with 0.1% BSA, x1 in PBS, x1 in lysis buffer. The beads were added to the lysates and incubated for 1 hr at 4°C with rotation. Lysates were then transferred from the beads into fresh tubes and incubated with primary antibody as described. After incubation, washed beads were added to the lysate with primary antibody for 2 hr or overnight at 4°C with rotation. Beads were then washed x5 in NDLB or NET

wash buffer (50 mM NaCl, 75 mM Tris-HCl, pH 7, 7.5 mM EDTA, 1% Triton-X) as indicated and resuspended in 30-50 µl 1-3x non-reducing SDS-PAGE sample buffer. Samples were either stored at -20°C or immediately run on SDS-PAGE gels as described below.

2.5.3 SDS-PAGE

10% SDS-PAGE gels with 6% stacking gels were used in all experiments unless indicated otherwise. For a 0.75 mm separating gel: 1.5 ml H_2O, 0.95 ml 1.5 M Tris-HCl, pH 8.8, 1.3 ml acrylamide, 37.5 µl 10% SDS, 37.5 µl 10% APS, 3.8 µl TEMED with a 6% stacking gel: 1.06 ml H_2O, 0.5 ml 0.5 M Tris-HCl, pH 6.8, 0.4 ml acrylamide, 20 µl SDS, 20 µl APS, 2 µl TEMED. Samples were stored at -20°C and reduced when indicated by addition of 3% beta-mercaptoethanol. Reduced and non-reduced samples were boiled for 5 min. Small gels were run using the Bio-Rad Mini-Protean 3 system (200 mV for 45 min) and large gels using the Bio-Rad Protean II xi Cell system (7-10 mA overnight at 4°C).

2.5.4 Coomassie staining 1 and 2

Gels were fixed for 1 hr in 2% acetic acid, 50% methanol. Colloidal coomassie reagent was diluted 1:5 in water and this stock solution stored in the dark. The stock solution was diluted 1:1 with methanol and gels stained in this for at least 1 hr to overnight. Gels were rinsed briefly in 5% acetic acid, 25% methanol and then fully destained for no more than 1 hr in 25% methanol. Following this, gels were placed in water and photographed in a Bio-Rad GS800 calibrated densitomer scanner. Gels were subsequently dried onto 3 MM paper for storage.

For subsequent analysis by mass spec, gels were fixed for at least 20 min in 45% methanol, 1% acetic acid and 54% water. Gels were then stained for 12-18 hours in 17% ammonium sulphate, 34% methanol, 0.5% acetic acid, 0.1% Coomassie

G250 and destained in water until the desired contrast was achieved. Bands were excised immediately (see Mass Spectrometry, chapter 2.5.7).

2.5.5 Silver staining

Gels were fixed in 50% methanol, 12% acetic acid for 2 hr to overnight followed by 3 x 20 min washes in 50% ethanol. Gels where then washed with 0.02% sodium thiosulphate for 1 min and washed 3 x 20 sec in water. Gels were then impregnated with 0.1% silver nitrate for 20 min and rinsed 2 x 20 sec in water. Gels were developed in 3% sodium carbonate, 0.0002% sodium thiosulphate, 0.0093% formaldehyde-37 until the desired contrast was achieved. Gels were then washed 2 x 2 min in water and the staining stopped in 50% methanol, 12% acetic acid for 10 min. Following this, gels were washed with 50% methanol for 20 min and finally rinsed and stored in 1% acetic acid. Gels were photographed in a Bio-Rad GS800 calibrated densitometer scanner and dried down onto 3 MM filter paper or bands cut out for analysis by mass spectromety (see 2.5.7).

2.5.6 Western blotting

Protein was transferred using the Bio-Rad Transblot SD Semi-dry Transfer Cell at 10 mV for 35 min onto BioScience Protran Nitrocellulose Transfer Membrane in Semi-dry transfer buffer (2.93 g glycine, 5.81 g Tris, 0.375 g SDS, 200ml methanol, final volume 1 l). Membranes were protein assayed with 0.2% Ponceau S and blocked for 1 hr or overnight at 4°C in 5% Marvel dry-milk powder in TBS-Tween (TBS (Tris-buffered saline, 61 g Tris, 87 g NaCl, final volum 1 l, pH 7.4) with 0.1% Tween-20). Primary antibody was diluted in TBS-Tween with 3% BSA and membranes incubated in this for 1 hr with shaking. Membranes were subsequently washed 3 x 5 min in TBS-Tween and incubated in secondary antibody diluted in TBS-Tween with 3% BSA for 1 hr. This was followed by washes for 30 - 45 min in TBS-Tween. Membranes were incubated with SuperSignal West Pico Chemiluminescent Substrate (Pierce) for 1 min and

exposed to Hyperfilm ECL (Amersham Bioscience) or Biomax MR (Kodak) film and developed in a XOGraph Imaging Systems Compact X4 developer.

Films were scanned using a Bio-Rad GS800 calibrated densitometer scanner when indicated and the optical density of bands measured using Quantity One software.

2.5.7 Mass spectrometry

Cutting bands:
Bands were cut in a laminar flow hood to avoid contamination. A fresh scalpel blade was used and dipped in methanol in between cutting individual bands. Bands were cut from the gel and placed in Eppendorf tubes, which had been washed with methanol and twice with water. The bands were subsequently washed twice with water and stored at -20°C until sample processing.

Maldi-Tof mass spectroscopy sequencing was performed by either Dr. Oliver Kleiner, UCL and Eisai or by Dr. Catherine Lilley, Cambridge.

2.5.8 Indirect immunofluorescence and quantitative immunofluorescence (QuIF)

Subconfluent cells grown on coverslips were fixed in 3% paraformaldehyde (PFA) for 15 min, washed x1 in PBS with 50 mM ammonium chloride and 0.2% saponin and permeabilised in the same solution for 15 min. Coverslips were stored in PGAS (PBS with 0.2% gelatin, 0.02% azide, 0.02% saponin) for at least 5 min or overnight at 4°C. Antibodies were diluted in PGAS, coverslips were incubated in primary antibody for 1 hr, washed x3 in PGAS and incubated in secondary antibody in the dark for 30 min. This was followed by x3 washes in PGAS, x2 in PBS, x2 in H_2O. Coverslips were mounted using Antifade Gold Reagent with DAPI or in Mowiol (for QuIF). Confocal pictures were taken using

the 60x objective on a Biorad (Hercules) MRC 1024 confocal microscope and imported into Image J or Adobe Photoshop for visualisation without further modifications. Quantitative Immunofluorescence images were taken on the Li-Cor Odyssey imager and analysed using the supplied software and Microsoft Excel.

2.5.9 TSA staining of HRP containing cells

Coverslips of cell transfected with HRP chimeric constructs were fixed in PBS with 3% paraformaldehyde for 15 min, washed once and quenched for 15 min in PBS with 50 mM ammonium chloride. Coverslips were washed x2 with PBS and incubated 4 min in 1:50 TSA reagent in amplification reagent. The reaction was quenched for at least 30 sec in 0.2% azide in PBS. Coverslips were washed x2 in PBS and either mounted onto glass slides with Antifade Gold reagent or permeabilised with saponin as described above for further indirect immunofluorescence.

2.6 Electron microscopy

2.6.1 DAB reaction for HRP chimeras

Coverslips were fixed for 15 min in 2% paraformaldehyde /1.5% glutaraldehyde in 0.1 M sodium cacodylate (cacodylate). Cells were rinsed x2 in cacodylate followed by 3 x 5 min washes in 0.05 M Tris-HCl, pH 7.6 (Tris buffer). 250 µl DAB stock (3% stock in Tris buffer, stored at -20°C) was diluted in 10 ml Tris buffer and 7 µl hydrogen peroxide was added. Coverslips were incubated in DAB reaction mix for 30 min at room temperature in the dark. Coverslips were then washed 3 x 5 min in Tris buffer and rinsed x2 in cacodylate. This was followed by osmication and embedding as described below.

2.6.2 Embedding

Coverslips were fixed for 15 min in 2% paraformaldehyde /1.5% glutaraldehyde in 0.1 M sodium cacodylate (cacodylate). Coverslips were washed x2 in cacodylate. This was followed by osmication in 1% osmium, 1.5% potassium ferricyanide for 1 hour at 4°C. After 3 washes in cacodylate, samples were stored at 4°C overnight. Coverslips were incubated for 45 min in 1% tannic acid in 0.05 M sodium cacodylate followed by 5 min incubation in 1% sodium sulphate in 0.05 M sodium cacodylate. Coverslips were rinsed with water and washed for 3 min. This was followed by stepwise dehydration of the cells in increasing concentrations of ethanol: 2 x 5 min washes each in 70% ethanol, 90% ethanol and 100% ethanol. Epon was prepared according to the following recipe or multiples of it: 7.2 ml TAAB resin, 2.85 ml DDSA (Dodecenyl succinic anhydride), 4.95 ml MNA (Methylnadic anhydride), 0.3 ml DMP-30 (2,4,6 Tri(Dimethylamenomethyl) phenol). Coverslips were transferred into a 50:50 mix of propylene oxide and epon in aluminium dishes for 1 hour. The mix was replaced by neat epon for 2 x 2 hours. Coverslips were inverted onto capsules of polymerised epon and allowed to polymerise overnight in a Scientific Laboratory Supplies oven at 60°C. Coverslips were removed from the epon sticks by plunging into liquid nitrogen.

Ultrathin (60 nm) sections were cut, stained, an images taken on a Phillips EM420 electron microscope by Dr. Lucy Collinson, MRC LMCB.

Results

Chapter 3 – Setting up the Tools and Techniques

This chapter describes the tools and techniques developed to investigate the CLN6 protein. In order to answer the questions set out in the aims of this project, certain tools and techniques were required, most of which were not already available. The following questions were addressed in this context:

Can CLN6 be detected in Western blotting and indirect immunofluorescence?

Can CLN6 be immunoprecipiated?

Is it possible to generate a chimeric construct of CLN6 and horseradish peroxidase for detection by indirect immunofluorescence and electron microscopy?

Can CLN6 protein levels be reduced using RNA interference?

3.1 Western analysis

Four polyclonal antibodies to human CLN6 were previously raised in the laboratory. One of these, 1747p, was reported to detect endogenous CLN6 as a band of 30 kDa in Western blotting (Mole et al., 2004). All available CLN6 antibodies were tested for use in Western blotting.

The antibodies had been raised against peptides specific to CLN6 as described in Materials and Methods, chapter 2.2.1. Briefly, peptide sequences shown in table 3.1 were chosen for their antigenic properties and their non-conserved amino acids. Both are directed against regions in the N-terminus of CLN6 as shown in figure 3.1.1.

Peptide name	Peptide sequence	Residues
EP01293	MEATRRRQHLGATGG	1-15
EP01294	ARHGSVSADDEAAR	28-39

Table 3.1: Antibody peptides

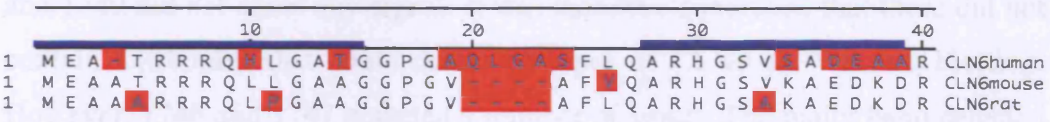

Figure 3.1.1: Sequence alignment of human, rat and mouse CLN6
Non-conserved sequences are indicated in red and antibody peptide coverage indicated in blue (sequence alignment DNA Star).

Peptides were injected into rabbits according to the scheme set out in figure 3.1.2 below. Final bleed plasma samples were collected and used in subsequent experiments as unpurified antisera, denoted by the letter f for final bleed. Antisera were further affinity purified against the original peptides to produce purified antibodies, denoted by the letter p for purified.

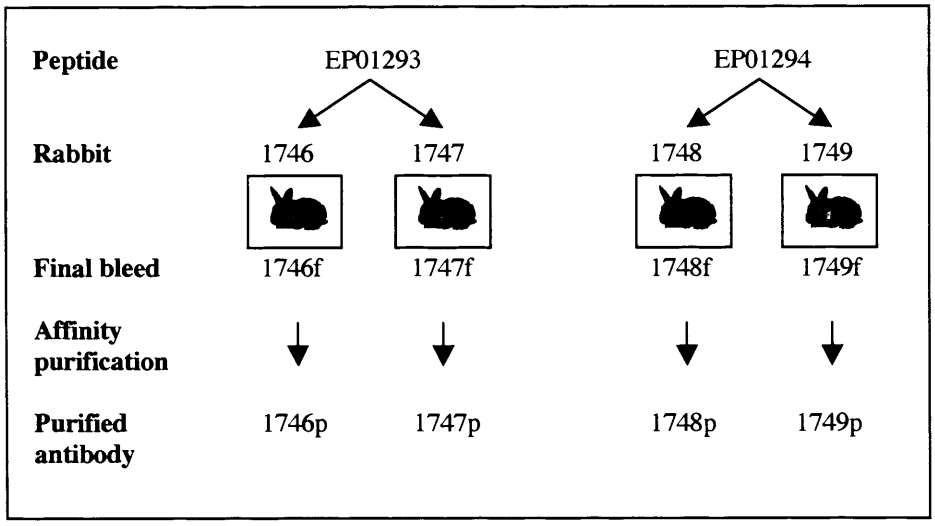

Figure 3.1.2: Schematic overview of production of CLN6 antibodies

Unpurified antisera and purified antibodies were tested in Western blotting on HEK293 cell total lysate. The dilution used for unpurified antisera was 1:100, for purified antibodies 1:500. The results of this are shown in figure 3.1.3 panel A. Overall, the unpurified antisera showed more background staining and a larger number of bands. This was expected as final bleed plasma may contain a number of endogenous antibodies. Unpurified antisera and purified antibodies for 1748 and 1749 did not show any signal. It was therefore concluded that these did not contain antibodies that could detect epitopes of CLN6 by Western blotting. However, 1746 and 1747 detected a number of bands. The major band detected by both 1746f and 1746p was at 25 kDa with a minor band at 28 kDa. The latter corresponded to the major band detected by 1747f and 1747p. There was also a minor band at 34 kDa in 1747f and 1747p. To find out which bands were specific for CLN6, the purified antibodies were further tested in different cell types, including fibroblast cells from the CLN6 patient HF476Pa. This cell line has a mutation at amino acid position 5 (R5W), which is within the region covered by the peptide that 1746p and 1747p were raised against. It was therefore expected that these two antibodies at least should not be able to detect CLN6 in this sample, as any CLN6 protein produced would likely have an altered tertiary structure in this region.

Panels B and C in figure 3.1.3 show Western blots of cell extracts from HEK293 cells, HeLa cells, the healthy control fibroblast cell line BR3 and the CLN6 patient fibroblast cell line HF476Pa. An antibody against tubulin was used as a control to detect tubulin by Western blotting, indicating the presence of cell extract and validating the Western blot procedure. The same amount of total protein was loaded in each lane, but differences in tubulin band intensity were observed between the different cell types. As expected, antibodies 1748p and 1749p did not detect any bands. 1746p showed a major band at 25 kDa, which was present in all samples including cells from the CLN6 patient, and a minor band at 28 kDa, which was faint but absent in cells from the CLN6 patient. 1747p detected a minor band at 34 kDa in all samples. There was also an additional minor band at 30 kDa, which was present in all samples and which ran as a doublet just above the major band. The major band at 28 kDa was absent in cells from the CLN6 patient, as marked in panel B in figure 3.1.3 by the star. Therefore, the band at 28 kDa corresponded to endogenous CLN6, consistent with published results.

1747p was chosen for use in subsequent Western blots as it detected CLN6 as its major band as well as showing less background signal than 1746p. It was further noted that different cell types contained different amounts of CLN6 as demonstrated by the intensity of the band detected by Western blotting. More CLN6 was detected in HEK293 cells than in HeLa cells and in turn more than in fibroblast cells. This information was used to subsequently choose cell lines most suited for different types of experiments.

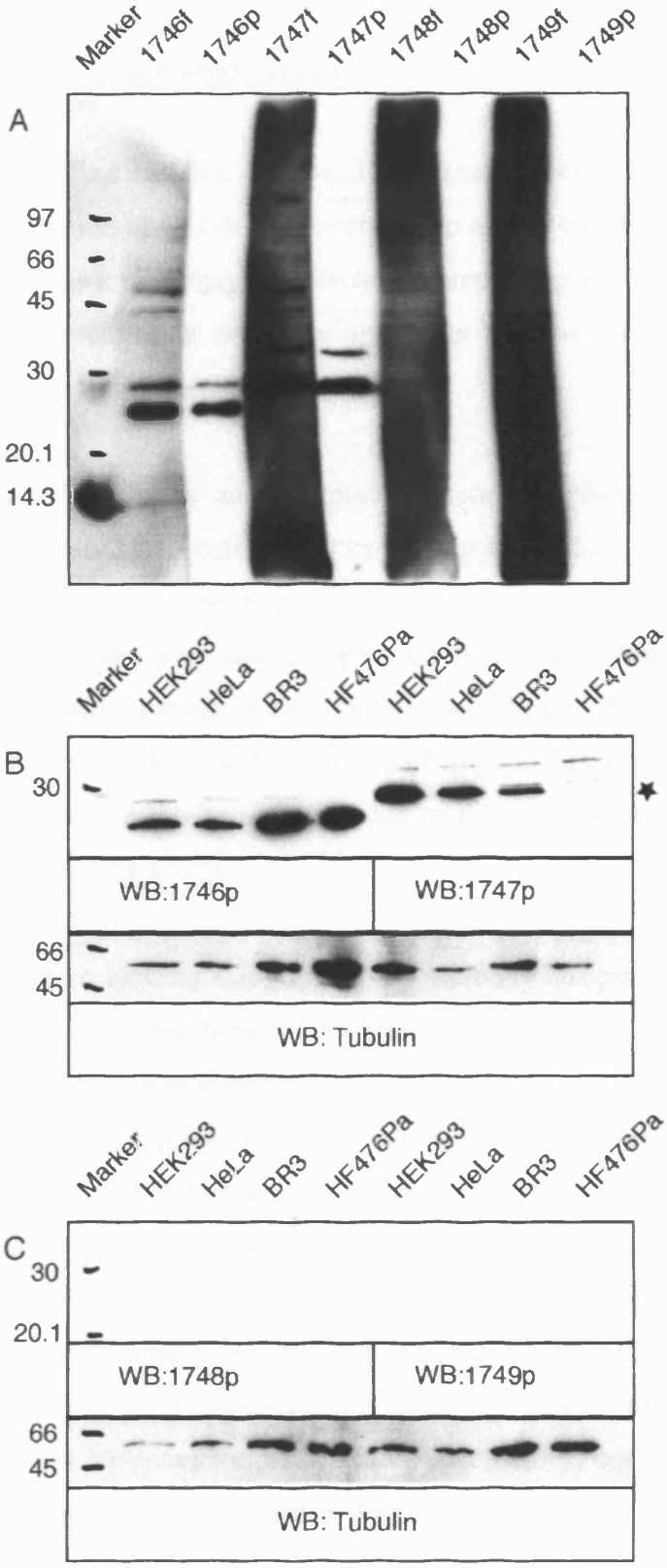

Figure 3.1.3: CLN6 Western blotting

(A) Final bleed antisera (f, dilution 1:100) and purified CLN6 antibodies (p, dilution 1:500) were tested in Western blotting in HEK293 cells. Purified antibodies (B) 1746p, 1747p, (C) 1748p and 1749p were further tested in HEK293, HeLa and fibroblast cells from healthy control (BR3) and CLN6 patient (HF476Pa). The band corresponding to CLN6 is denoted by the star.

3.2 CLN6 Immunoprecipitation

The four purified CLN6 antibodies were tested for efficiency of immunoprecipitation of CLN6. Although 1748p and 1749p did not give a signal by Western blotting, they may be able to immunoprecipiate CLN6 as it is often the case that an antibody might recognise an epitope on a protein by one technique but not by another.

Figure 3.2 panel A shows an attempted immunoprecipitation of endogenous CLN6 from HEK293 total cell lysates by all four antibodies. 1747p was used to detect CLN6 by Western blotting. No CLN6 was detected using 1747p when either 1748p or 1749p were used to immunoprecipitate. 1746p and 1747p both immunoprecipitated a protein of 28 kDa, corresponding to the CLN6 band in the total cell lysate. Therefore, both 1746p and 1747p were able to immunopreciptiate endogenous CLN6 that could subsequently be detected by Western blotting using 1747p.

However, Western blotting using the 1746p antibody has previously shown the detection of an additional band at 25 kDa that was present in a patient with a mutation in CLN6. It was tested whether 1746p would also immunoprecipitate this band. Figure 3.2 panel B shows an immunoprecipitation using 1746p detected by Western blotting using both 1746p and 1747p. In both the total lysate before and after immunoprecipitation, 1746p detected a major band around 25 kDa and a minor band at 28 kDa, the latter one being CLN6. However, in the immunoprecipitated sample, only the band corresponding to CLN6 was detected. This was confirmed by Western blotting using 1747p. This experiment showed that 1746p could immunoprecipitate CLN6 specifically, but not the additional protein of 25 kDa, which it detected in Western blotting.

It was decided to use 1747p as the preferred tool for immunoprecipitation of CLN6 as it was more specific in Western blotting than 1746p. A further experiment was conducted to ensure that CLN6 was binding specifically to the antibody and not non-specifically to the magnetic beads that the antibody was

bound to. Figure 3.2 panel C shows an immunoprecipitation with and without 1747p. The CLN6 band was only detected when the 1747p antibody was present. From this experiment, it was concluded that immunoprecipitation of CLN6 by the 1747p antibody is specific.

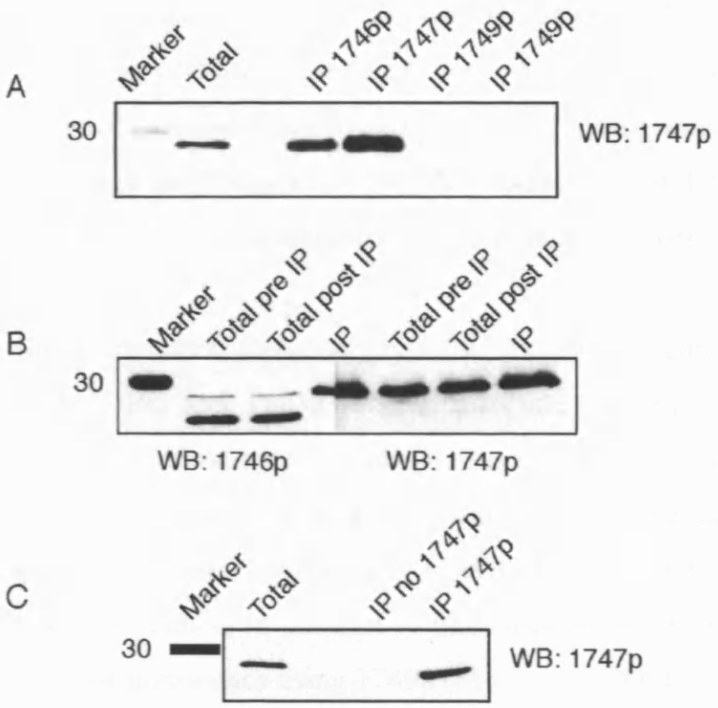

Figure 3.2: CLN6 Immunoprecipitation

(A) CLN6 was immunoprecipitated from HEK293 total cell lysate using the four purified polyclonal CLN6 antibodies. (B) CLN6 was immunoprecipitated using the 1746p antibody and detected by Western blotting using 1746p and 1747p antibodies. (C) CLN6 was immunoprecipitated with and without addition of the 1747p antibody.

3.3 Indirect immunofluorescence

CLN6 has been reported to localise to the ER (Heine et al., 2004; Mole et al., 2004). The four polyclonal antibodies were tested for use in indirect immunofluorescence (immunofluorescence) followed by detection by confocal microscopy. Although the 1748p and 1749p antibodies did not detect any signal in Western blotting, they were tested for use in immunofluorescence.

Figure 3.3.1 shows immunofluorescence in HEK293 cells using the four purified antibodies. Both 1746p and 1747p showed punctate staining throughout the cytosol as well as discontinous staining around the nucleus. This staining pattern is reminiscent of ER, consistent with published results (Heine et al., 2004; Mole et al., 2004). Antibodies 1748p and 1749p did not detect CLN6 by immunofluorescence. This is in contrast to published results showing reticular staining by immunofluorescence using 1749p (Mole et al., 2004).

To confirm the localisation of CLN6 staining as ER, the 1747p antibody was used for co-localisation with protein disulphide isomerase (PDI), an ER chaperone protein, in HEK293 and HeLa cells. Figure 3.3.2 shows partial co-localisation of CLN6 with PDI in both cell types. This confirms the previously published localisation of CLN6 where co-localisation of endogenous and overexpressed CLN6 with different antibodies against PDI had also been observed (Heine et al., 2004; Mole et al., 2004).

From these experiments it was concluded that 1746p and 1747p were reliable antibodies for detection of CLN6 by immunofluorescence. It was decided to use 1747p as the preferred antibody for investigating CLN6 as it was able to detect CLN6 by Western blotting as well as immunofluorescence with less non-specific background than 1746p.

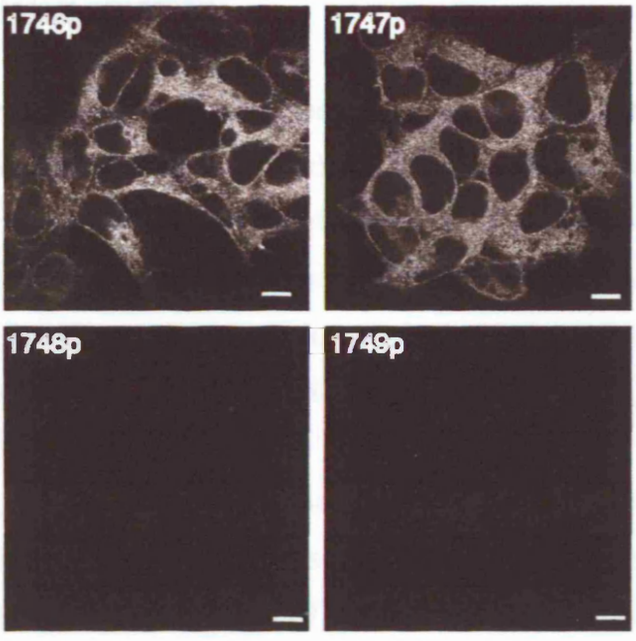

Figure 3.3.1: CLN6 Immunofluorescence
Purified CLN6 antibodies were tested for their ability to detect CLN6 in HEK293 cells. 1746p and 1747p were used at dilutions of 1:1,000, 1748p and 1749p were used at 1:100. Bar, 10 µm.

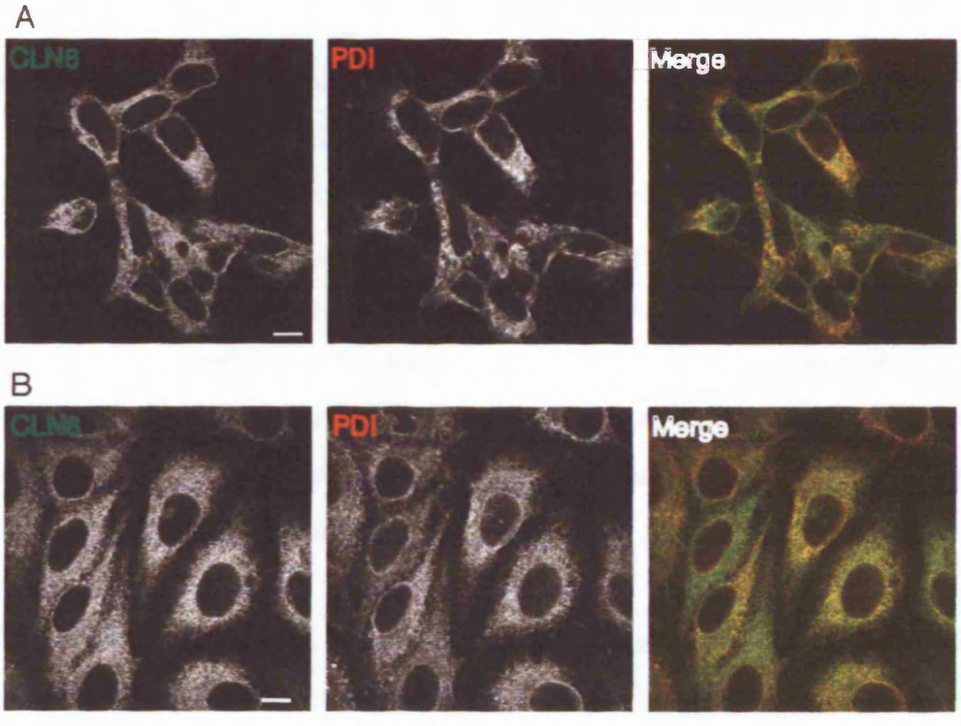

Figure 3.3.2: CLN6 shows partial co-localisation with Protein Disulphide Isomerase
CLN6 (green) was co-localised with the ER-resident protein PDI (red) in (A) HEK293 and (B) HeLa cells. Bar, 10 µm.

3.4 CLN6-HRP chimera

GFP-tagged wild-type and mutant constructs of CLN6 are very useful tools for a variety of experiments, including immunofluorescence, Western blotting and immunoprecipitation. However, for localisation studies using transmission electron microscopy, horseradish peroxidase-chimera constructs are a useful alternative. The electron dense reaction product of horseradish peroxidase can be detected without the use of antibodies.

The enzyme horseradish peroxidase (HRP) is a plant glycoprotein that can oxidise several cellular substances and form covalent cross-links between proteins (Hayat, 1993; Stahmann, 1977). HRP reacts with hydrogen peroxide in the following reaction:

$$HRP + H_2O_2 \rightarrow HRP{\cdot}H_2O_2$$
$$(HRP{\cdot}H_2O_2) + (CHR)H_2 \rightarrow HRP + 2H_20 + CHR\downarrow$$

After HRP forms a complex with hydrogen peroxide, this reacts with a chromogen (CHR) to form HRP, water and a precipiate of the chromogen (Hayat, 1993). There are a number of different chromogens that can be used to react with HRP. Diaminobenzidine (DAB) and its derivatives are used in light and electron microscopy (Graham and Karnovsky, 1966). An HRP-chimera is therefore a powerful tool for localisation studies. HRP has been shown to stay enzymatically active when fused to chimeric proteins (Hopkins, 1985) as well as after fixation. Furthermore, the DAB reaction product does not diffuse out of the compartment it was generated in (Connolly et al., 1994).

To construct the CLN6-HRP chimera, HRP was fused to the C-terminus of CLN6 as this protrudes into the lumen of the ER (Heine et al., 2004). Therefore, the DAB reaction product would be retained within the ER in the locality of the CLN6 protein.

The *CLN6* gene was excised from pcDNA3.1/NT-GFP-TOPO-CLN6 (Mole et al., 2004) using the restriction enzymes *Nhe*I and *Not*I. This gave fragments of 1019 bp and 6093 bp with the following overhangs: g/ctagc-*CLN6*-gc/ggccgc. The *Nhe*I-*Not*I fragment containing *CLN6* was then cloned into the mammalian expression vector pCI-neo (Promega), which had been pre-cut with *Nhe*I and *Not*I. This yielded the new construct CLN6-pCI-neo with the open reading frame of *CLN6* located at 1137-2073 bp. Next, the stop codon of *CLN6* was mutated and a new restriction site generated to allow cloning of the gene encoding ssHRP at the C-terminus of CLN6, resulting in the construct CLN6-pCI-neo-mut. The primers used for this are shown in figure 3.4.1 panel A.

The pSRα.ssHRP construct (Connolly et al., 1994) was digested with *Hind*III and the cohesive ends of the fragment removed with Endonuclease I. The fragment was then digested with *Eco*RI and ligated into the precleaved CLN6-pCI-neo-mut vector, resulting in the construct CLN6-HRP-pCI-neo. Following this, a stop codon was generated at the 3' end of *CLN6-HRP* and an additional guanine residue inserted at the 5'end of *HRP* to correct the reading frame. The primers used for these mutageneses are shown in figures 3.4.1 panels B and C. The sequence of the resulting construct pCLN6-HRP-pCI-neo, named CLN6-HRP, depicted in figure 3.4.2 panel A, was verified by sequencing analysis.

The CLN6-HRP construct was tested by overexpression in HeLa cells. Transfected cells were detected using TSA reagent from Perkin Elmer. This system utilises HRP to catalyse the deposition of fluorophore-labeled tyramide amplification reagent in fixed cells. The fluorophore labels are deposited adjacent to the HRP molecules (Perkin Elmer TSA Fluorescence Systems Handbook). In figure 3.4.2 panel B, partial co-localisation of TSA-detected CLN6-HRP with both the CLN6 antibody and the ER marker PDI can be seen. It was concluded that the construct was active and localised to regions within the ER. The results using this construct are described in chapter 4.2.

A

Sequence of CLN6	GTC	AGC	AGT	CGG	CAT	TAA	AAG	GGC	AAT	TCT	GCA	GAT	ATC	CAG	CAC
Translation	val	ser	ser	arg	his	Stop									
Mutagenesis primer	GTC	AGC	AGT	CGG	CAT	ATA	AAG	GGG	AAT	TCT	GCA	GAT	ATC	CAG	G
New translation	val	ser	ser	arg	his	leu	lys	gly	asn	ser	ala	asp	ile	gln	his
New restriction site								EcoRI							

B

Sequence of CLN6-HRP	AGA	GTG	GTC	AAC	TCT	AAT	CCA	GCA	CAG	TGG	CGG	CCG	CTT	CCC	TTT
Translation	arg	val	val	asn	ser	asn	pro	ala	gln	trp	arg	pro	leu	pro	phe
Mutagenesis primer		G	GTC	AAC	TCT	AAT	CCA	GCA	TAG	TGG	CGG	CCG	CTT	CCC	
New translation	arg	val	val	asn	ser	asn	pro	ala	Stop						

C

Sequence of CLN6-HRP	CGG	CAT	TTA	AAG	GGG	AAT	TCC	AGT	TAA	CGC	CGA	CTT
Translation	arg	his	leu	lys	gly	asn	ser	ser	STOP	arg	arg	leu
Mutagenesis primer	CGG	CAT	TTA	AAG	GGG	GAA	TTC	CAG	TTA	ACG		
New sequence of CLN6	CGG	CAT	TTA	AAG	GGG	GAA	TTC	CAG	TTA	ACG	CCG	ACT
New translation	arg	his	leu	lys	gly	glu	phe	gln	leu	thr	pro	thr

Figure 3.4.1: Mutagenesis primers used in CLN6-HRP cloning
(A) Removal of stop codon in CLN6 sequence of CLN6-pCI-neo:
The stop codon in the CLN6 sequence was removed and a new restriction site (*Eco*RI) generated to allow cloning of the ssHRP sequence onto the 3'end of CLN6, following a short linker sequence.
(B) Addition of stop codon to CLN6-HRP:
The 3'end of HRP was mutated to generate a stop codon.
(C) Mutation of HRP to correct reading frame:
The insertion of a guanine at position 2079 was necessary to correct the reading frame of HRP.

A

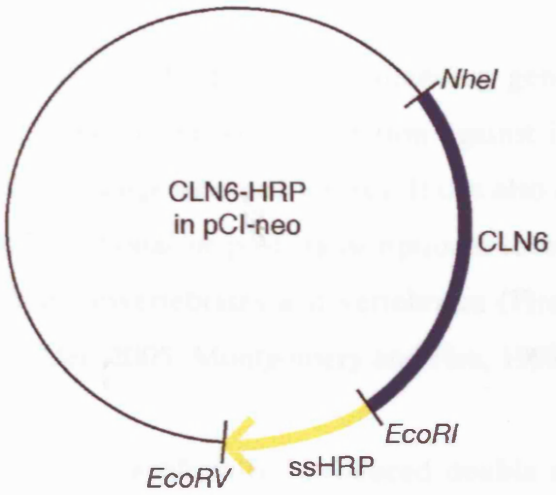

B

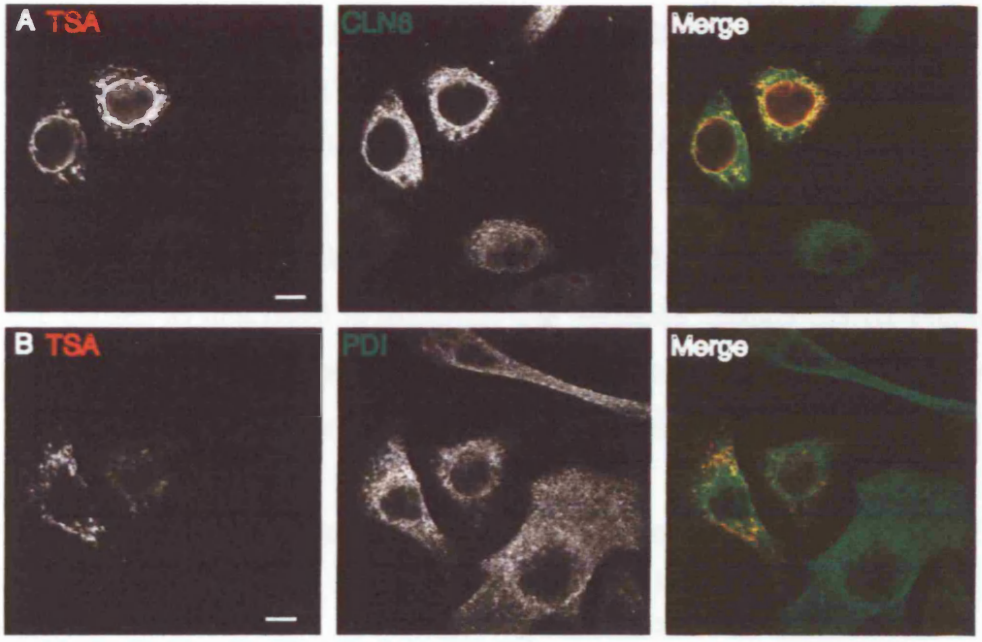

Figure 3.4.2: CLN6-HRP shows partial co-localisation with CLN6 and PDI

(A) Depiction of the CLN6-HRP construct in pcI-neo, with restriction sites used in making the construct indicated.

(B) HeLa cells were transiently transfected with CLN6-HRP. Cells were fixed 24 hours after nucleofection and stained for active HRP with TSA reagent (red) and co-localised with (A) CLN6 (green) and (B) the ER protein PDI (green). Bar, 10 µm.

3.5 CLN6 RNAi

RNA interference (RNAi) is the process of silencing gene expression. This mechanism has been shown to provide protection against invasion by mobile genetic elements such as transposons and viruses. It can also act to regulate gene expression at the transcriptional or post-transcriptional level. This process has been described in plants, invertebrates and vertebrates (Fire, 1999; Fire et al., 1998; Matzke and Birchler, 2005; Montgomery and Fire, 1998).

Endogenously occurring or artificially introduced double-stranded (ds) RNA molecules are processed into 21 – 23 nucleotide (nt) RNA fragments by proteins of the Dicer family of RNase III nucleases (Bernstein et al., 2001). These resulting short interfering (si) RNA molecules target complementary mRNAs for degradation through interaction with the RNA-induced silencing complex (RISC) (Caplen et al., 2001; Elbashir et al., 2001; Hammond et al., 2000; Nykanen et al., 2001). RNAi is a potent tool that can be used to silence genes, allowing the investigation of the resulting loss-of-function phenotype.

Two siRNAs targeting different regions of the CLN6 messenger RNA (mRNA) were chosen as described in Materials and Methods, chapter 2.3.10. Figure 3.5.1 depicts a BLAST alignment of CLN6 mRNA and the two CLN6 siRNAs. No perfect matches with other human mRNAs were found using this alignment.

```
CLN6-1 siRNA     1      CCGGTCTCTTCCTCGGAAA  19
                        ||||||||||||||||||
CLN6 mRNA        25     CCGGTCTCTTCCTCGGAAA  43

CLN6-2 siRNA     1      CCAGAGACCGAGAGCATGA  19
                        ||||||||||||||||||
CLN6 mRNA        1102   CCAGAGACCGAGAGCATGA  1120
```

Figure 3.5.1: Alignment of CLN6 mRNA (gi 1478999) and CLN6 siRNAs

The efficiency of protein depletion using these siRNAs was tested in HeLa cells. In an initial experiment, cells were transfected with each siRNA separately as

well as with a mix of both. Samples were taken at 48 hours and the remaining cells transfected in a second round of siRNA treatment. Mock samples were transfected without the addition of siRNA. Figure 3.5.2 panel A shows the results of this experiment. CLN6 protein levels were reduced by each siRNA individually as well as by a mix of the two. One and two rounds of siRNA treatment were effective at reducing CLN6 protein levels as detected by Western blotting. In a further experiment, shown in panel B, a control non-silencing siRNA (Qiagen) was used as an additional control. This confirmed that CLN6 protein levels were reduced by siRNA treatment specific to CLN6 but not by non-specific siRNA treatment. Immunofluorescence of the same experiment, figure 3.5.3, shows reduced CLN6 staining in the CLN6 depleted cells (CLN6-1, CLN6-2, CLN6-1/CLN6-2 mix) in comparison to the control siRNA treated cells. Faint background staining could still be detected in siRNA treated cells. It is unclear whether this indicates very low residual levels of CLN6 or non-specific background staining.

It is possible to use quantative reverse-transcription polymerase chain reaction (Q-PCR) to verify a reduction in the mRNA levels in siRNA-treated cells compared to mock-treated cells. The results of Q-PCR analysis of CLN6 siRNA are shown in figure 3.5.2 panel C. This shows an average reduction of CLN6 mRNA levels to 18.5% after siRNA treatment with a CLN6-1/CLN6-2 siRNA mix compared to mock treatment. The housekeeping gene *GAPDH* was used as an internal control. For subsequent experiments it was decided that use of Western blotting and immunofluorescence to show effective knock-down was preferable as this reflected protein levels as opposed to mRNA levels.

It was concluded that both siRNAs designed against CLN6 were effective in reducing CLN6 proteins levels and that optimum reduction of protein was achieved using a mix of both siRNAs. This mix was therefore used in subsequent experiments. Experiments investigating the effects of CLN6 siRNA treatment are further discussed in chapter 6.

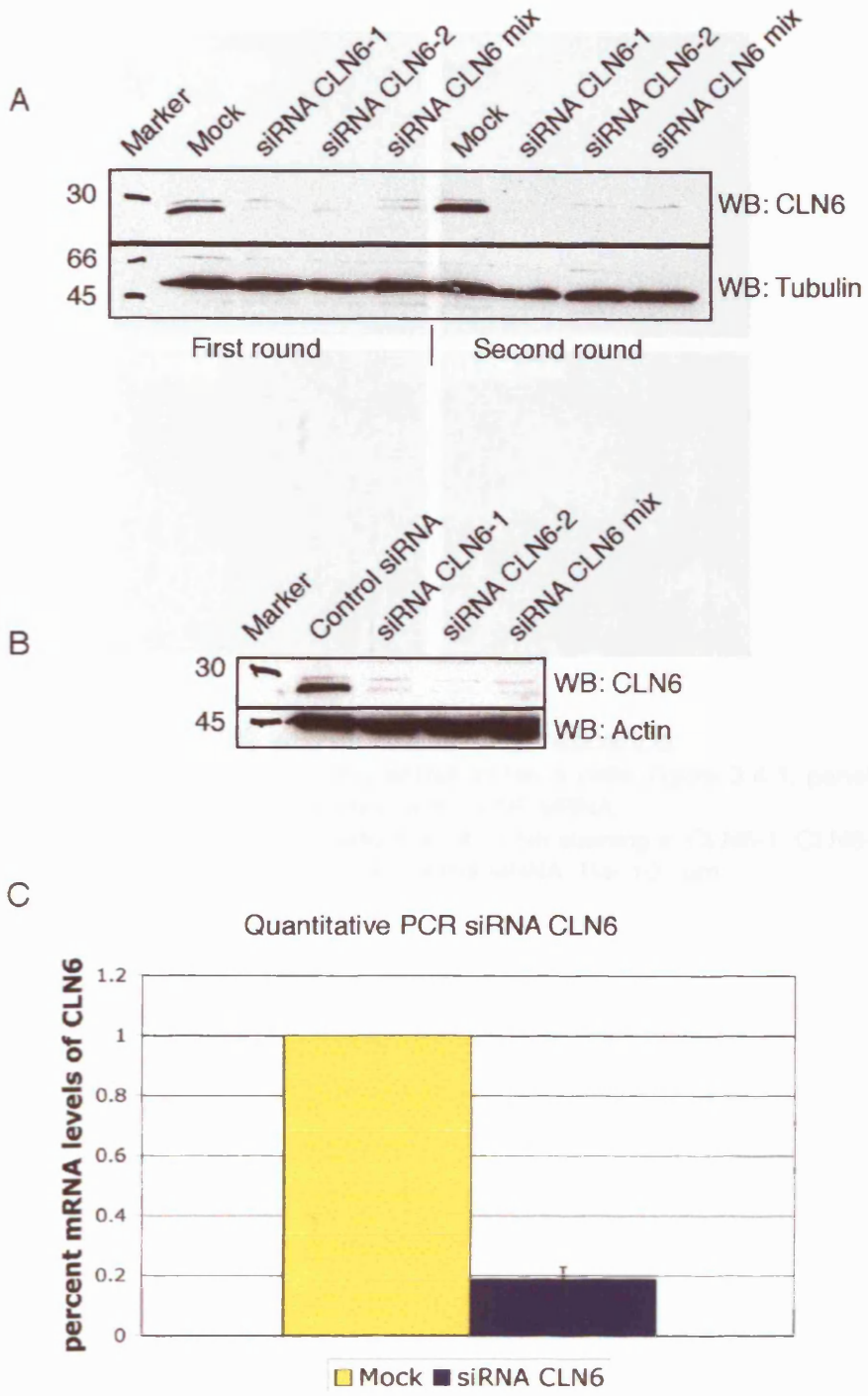

Figure 3.5.2: CLN6 siRNA

(A) CLN6 was depleted using siRNA in HeLa cells using 2 rounds of nucleofection with CLN6 siRNA constructs CLN6-1, CLN6-2 and a mix of both. Mock samples were nucleofected without siRNA. (B) CLN6 was depleted (2 rounds) in HeLa cells including a non-silencing control siRNA. (C) Quantitative PCR shows a reduction in CLN6 mRNA levels to 18.5% after siRNA treatment, n=4.

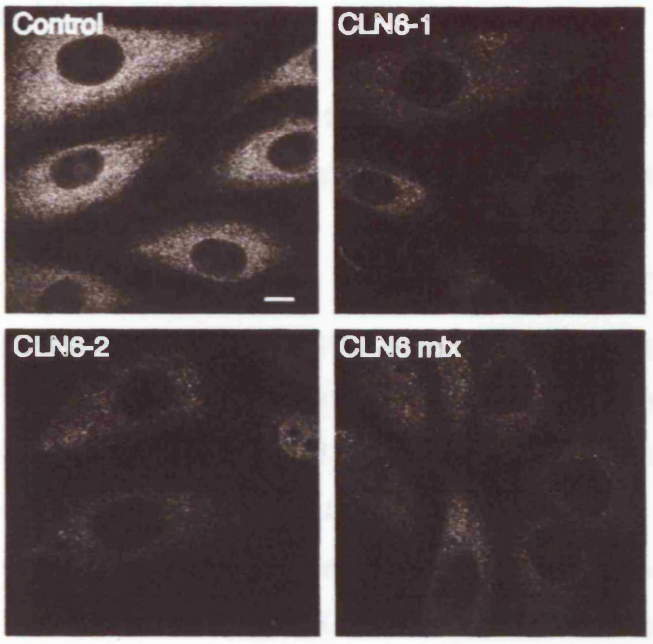

Figure 3.5.3: CLN6 siRNA Immunofluorescence

CLN6 was knocked-down using siRNA in HeLa cells (figure 3.4.1, panel B) using 2 rounds of nucleofection with CLN6 siRNA.
Immunofluorescence shows reduction of CLN6 staining in CLN6-1, CLN6-2 and mix siRNA compared to the control siRNA. Bar 10, μm.

6.3 Chapter 3 Summary

In chapter 3, the tools and methods to investigate CLN6 were established and characterised. A number of techniques were now available for future investigation:

CLN6 could be detected by Western blotting. CLN6 could be immunoprecipiated, which would allow a search for interacting proteins. It could also be detected by indirect immunofluorescence, which would allow further characterisation of its location and co-localisation with other proteins and cellular markers. The construction of the CLN6-HRP chimera made it possible to further localise CLN6 at the subcellular level using transmission electron microscopy. The effect of loss of CLN6 could be investigated using RNAi treatment and a cellular phenotype established.

Chapter 4 – CLN6 localisation

This chapter describes a detailed investigation of the subcellular location of the CLN6 protein. As the immunofluorescence pattern of endogenous CLN6 appears less tubular than classic ER marker staining and co-localisation with ER markers is only partial, it was proposed that CLN6 may be located within specific regions of the ER, which would perhaps implicate it in one of the many functions of the ER. It was also considered whether CLN6 could exit the ER and traffic to the lysosome, the site of the accumulated storage material in vLINCL, and have a specific function there. Furthermore, suggestions have been made that mutant CLN6 may be degraded faster than wild-type CLN6. Proteasomal inhibitors were used to investigate whether wild-type and/or mutant CLN6 are degraded by ER associated degradation (ERAD).

The following questions were addressed in this chapter:

Is there co-localisation between CLN6 and markers of specific functions of the endoplasmic reticulum as analysed by immunofluorescence microscopy?

Does the CLN6-HRP chimera show a distribution in a specific region of the endoplasmic reticulum at the ultra-structural level?

Is there a change in protein levels or in distribution of CLN6 in the cell upon treatment with lysosomal or proteasomal inhibitors?

4.1 CLN6 co-localisation study within the endoplasmic reticulum using immunofluorescence microscopy

The endoplasmic reticulum is a very versatile organelle and serves a multitude of purposes in the cell. Some parts of the ER are spatially segregated and have different functions, such as the smooth and rough ER, contact sites with other organelles and the transitional ER or ER exit sites. In more detail, an example of spatial segregation is the necessity for contact sites between the ER and mitochondria for the sequestration of cytosolic calcium by the mitochondria. A marker for this mitochondria-associated ER sub-domain is the autocrine motility factor receptor (AMF-R), which has been localised to a smooth sub-domain of the ER that is in direct contact with mitochondria (Wang et al., 2000).

By establishing whether CLN6 co-localises with markers of specific functions of the ER, which are spatially segregated, it may be possible to elucidate the function of CLN6.

Upon careful examination of recent literature, two proteins were identified with immunofluorescence staining patterns similar to CLN6. These were Sec24, a component of ER exit sites, and the organised smooth ER marker cytochrome b(5). Immunofluorescence images showed very punctate staining for both these proteins. Furthermore, these proteins are involved in and thus can serve as markers for distinct processes taking place in the ER.

First, it was investigated whether CLN6 co-localises with the ER exit site component Sec24. This protein is located in a complex with Sec23 and together with Sar1 and the Sec13/31 complex forms the COPII coat involved in exit from the ER to the Golgi (Antonny and Schekman, 2001; Barlowe et al., 1994). Immunofluorescence of Sec23/Sec24 in HeLa cells has been shown to be very punctate with large clusters of punctae in the perinuclear region and more dispersed punctae in the periphery of the cells (Shimoi et al., 2005). It was proposed that CLN6 was located in ER exit sites where it could have a specific function.

A Sec24-GFP construct (Stephens et al., 2000) was overexpressed in HeLa cells and cells stained with antibodies against GFP and CLN6. Figure 4.1.1 shows the results of this experiment. Sec24-GFP staining appeared as distinct and sparse punctae throughout the transfected cells as well as clustered in perinuclear regions. CLN6 staining was punctate throughout the cells. Some punctae appeared in close proximity, however no co-localisation was observed between Sec24-GFP and CLN6. From this experiment, it was concluded that CLN6 was not located in ER exit sites.

Next it was investigated whether CLN6 co-localises with the ER isoform of cytochrome b(5). Cytochrome b(5) acts as an electron transfer component in many oxidative reactions, such as anabolic metabolism of fats and steroids, catabolism of xenobiotics and the reduction of methemoglobin (reviewed in (Schenkman and Jansson, 2003)). Cytochrome b(5) is found in a membrane-bound form and a soluble form, the latter being present in red blood cells where it maintains the reduced state of haemoglobin (Hegesh et al., 1986). The membrane-bound form of cytochrome b(5) exists in two isoforms, one localised mainly in the ER and the other one in the mitochondrial outer membrane (D'Arrigo et al., 1993; Ito, 1980; Lederer et al., 1983). Overexpression of cytochrome b(5) in yeast and mammalian cells leads to a proliferation of the ER into structures called organised smooth ER (OSER) (Koning et al., 1996; Pedrazzini et al., 2000; Vergeres et al., 1993). As reported in (Snapp et al., 2003) these OSER structures are formed through low affinity interactions when several ER-resident proteins are overexpressed. It is unclear as to what the function of OSER is. Suggestions have been made that it is involved in sub-compartmentalisation of the ER, sequestration of lipophilic drugs and accumulation of misfolded membrane proteins, such as mutant peripheral myelin protein-22 in Charcot-Marie-Tooth syndrome and mutant torsin A in early onset torsion dystonia (Dickson et al., 2002; Hewett et al., 2000; Snapp et al., 2003). In (Snapp et al., 2003), the authors show that at low levels of expression of endogenous or overexpressed cytochrome b(5) the protein is located throughout the ER. The immunofluorescence pictures of low levels of GFP-cytochrome b(5) expression closely resemble the staining of CLN6. At higher levels of expression

of cytochrome b(5), bright oval structures appear near the nuclear envelope or in the periphery of the cells, which are positive for other ER markers such as PDI. Overexpression of cytochrome b(5) thus induces the sequestration of components of the peripheral ER into a newly formed, distinct sub-compartment. As the immunofluorescence patterns of cytochrome b(5) and CLN6 looked very similar in distribution, it was proposed that CLN6 could be preferentially recruited by cytochrome b(5) into the newly forming OSER structures. This would provide a clue to whether CLN6 had a function in an inducible, smooth sub-compartment of the ER or in the maintenance of ER structure.

The GFP fusion construct of cytochrome b(5) (Pedrazzini et al., 2000) was overexpressed in HeLa cells and the cells stained for CLN6. The results of this experiment are shown in figures 4.1.2 - 4.1.5. Figure 4.1.2 shows very low levels of expression of GFP-cytochrome b(5). The staining for both CLN6 and GFP-cytochrome (5) appeared very punctate. There was some degree of co-localisation, similar to that seen between PDI and CLN6 (see chapter 3.2). At slightly higher levels of overexpression, shown in figure 4.1.3, the staining for GFP-cytochrome b(5) appeared more reticular, showing a larger extent of the classic tubular structure of the ER. There was less co-localisation between GFP-cytochrome b(5) and CLN6. It appeared that both proteins were in the same compartment and the CLN6 punctae occupied regions of the tubules stained for GFP-cytochrome b(5). Very high levels of overexpression are shown in figure 4.1.4. Here, GFP-cytochrome b(5) appeared in bright, large oval OSER structures. CLN6 was partially sequestered into these structures, showing significant co-localisation, although not to the same extent as GFP-cytochrome (b), as the former remained visible to a higher degree in the periphery of the cell than the latter. The peripheral staining of CLN6 was above non-specific background levels, indicating that some protein remained in regions of the ER not incorporated in OSER. To test the possibility that CLN6 is specifically recruited to OSER, a triple labelling of highly overexpressed GFP-cytochrome b(5) with CLN6 and the ER marker PDI was performed (figure 4.1.5). Both CLN6 and PDI were partially sequestered into the OSER structures. This data suggests that there is no preferential recruitment or exclusion of CLN6 into

newly forming OSER structures. There was no indication that CLN6 has a function in this process.

The experiments described in this section showed that CLN6 is not a component of ER exit sites or implicated the conversion of ER into OSER when this is induced by overexpression of cytochrome b(5). An alternative approach to investigate whether CLN6 was located in a sub-compartment of the ER at the ultra-structural level was attempted using the CLN6-HRP construct.

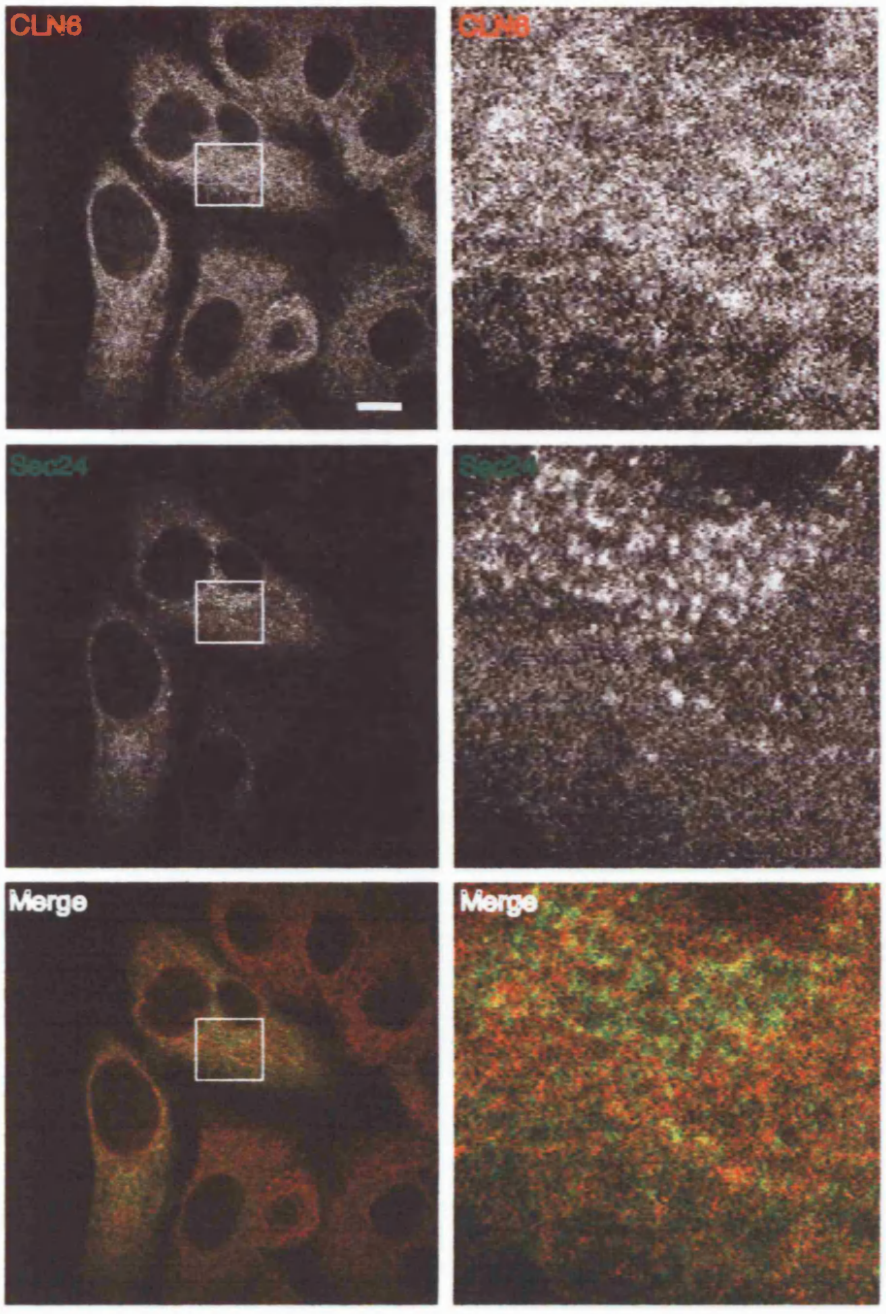

Figure 4.1.1: CLN6 shows no co-localisation with Sec24-GFP
Sec24-GFP was overexpressed in HeLa cells. Coverslips were stained with anti-GFP (green) at 1:100 and anti-CLN6 (red) at 1:1,000. Bar, 10 μm.

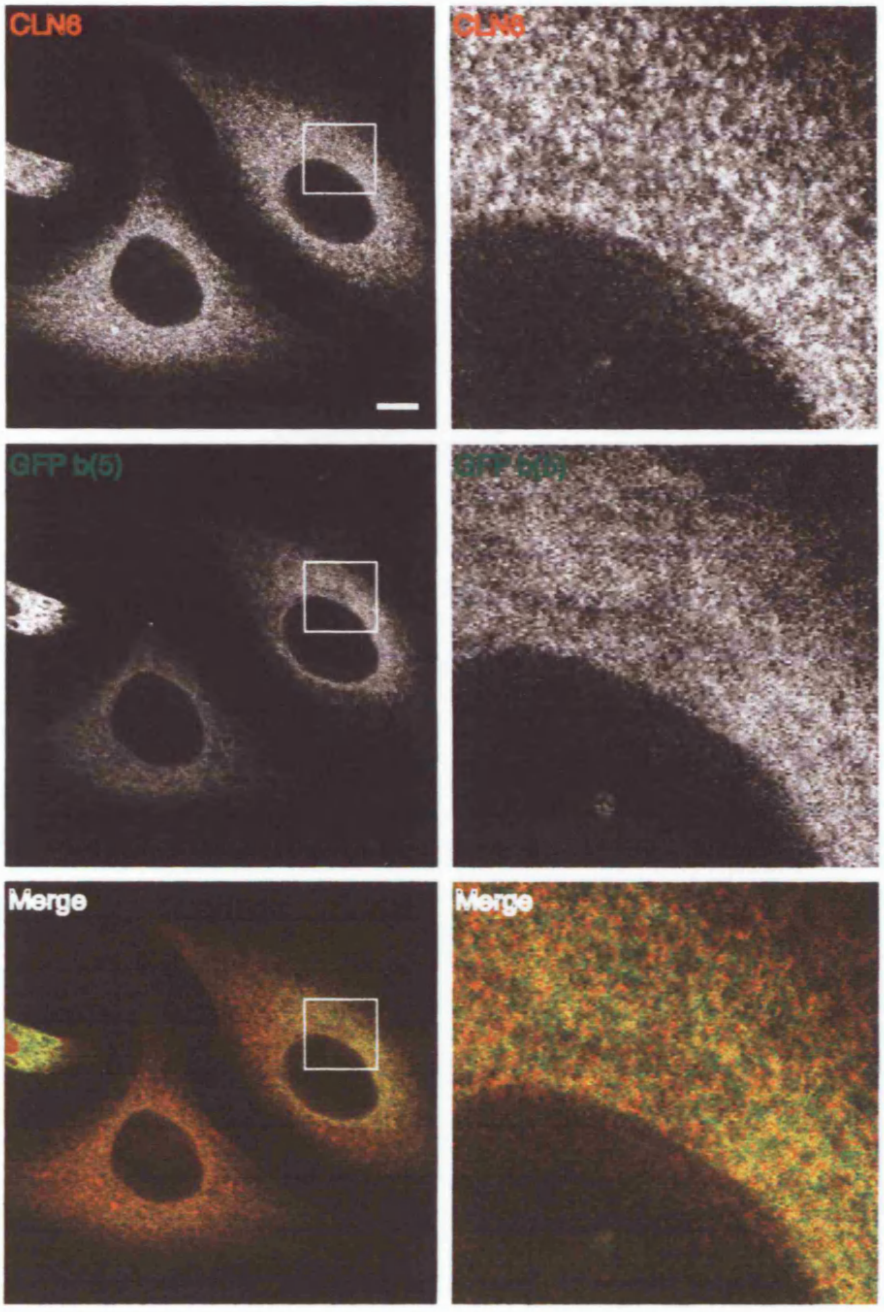

Figure 4.1.2: CLN6 shows partial co-localisation with GFP-cytochrome b(5) (low expression levels)

GFP-cytochrome b(5) (green) was overexpressed in HeLa cells. Coverslips were stained with anti-CLN6 (red) at 1:1,000. Cells shown are an example of low levels of expression of GFP-cytochrome b(5). Bar, 10 μm.

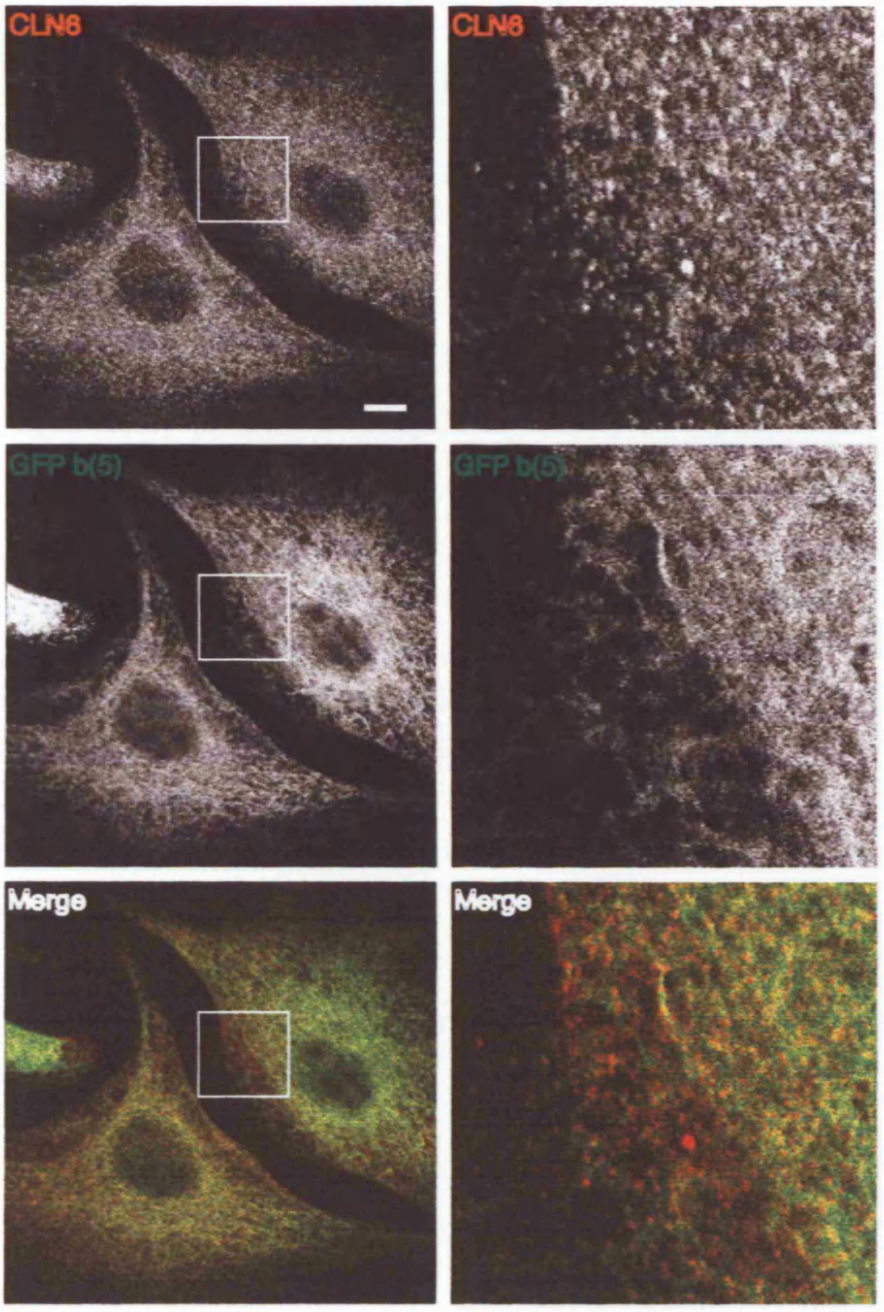

Figure 4.1.3: CLN6 shows very little co-localisation with GFP-cytochrome b(5) (low to medium expression levels)
GFP-cytochrome b(5) (green) was overexpressed in HeLa cells. Coverslips were stained with anti-CLN6 (red) at 1:1,000. Cells shown are an example of low to medium levels of expression of GFP-cytochrome b(5). Bar, 10 µm.

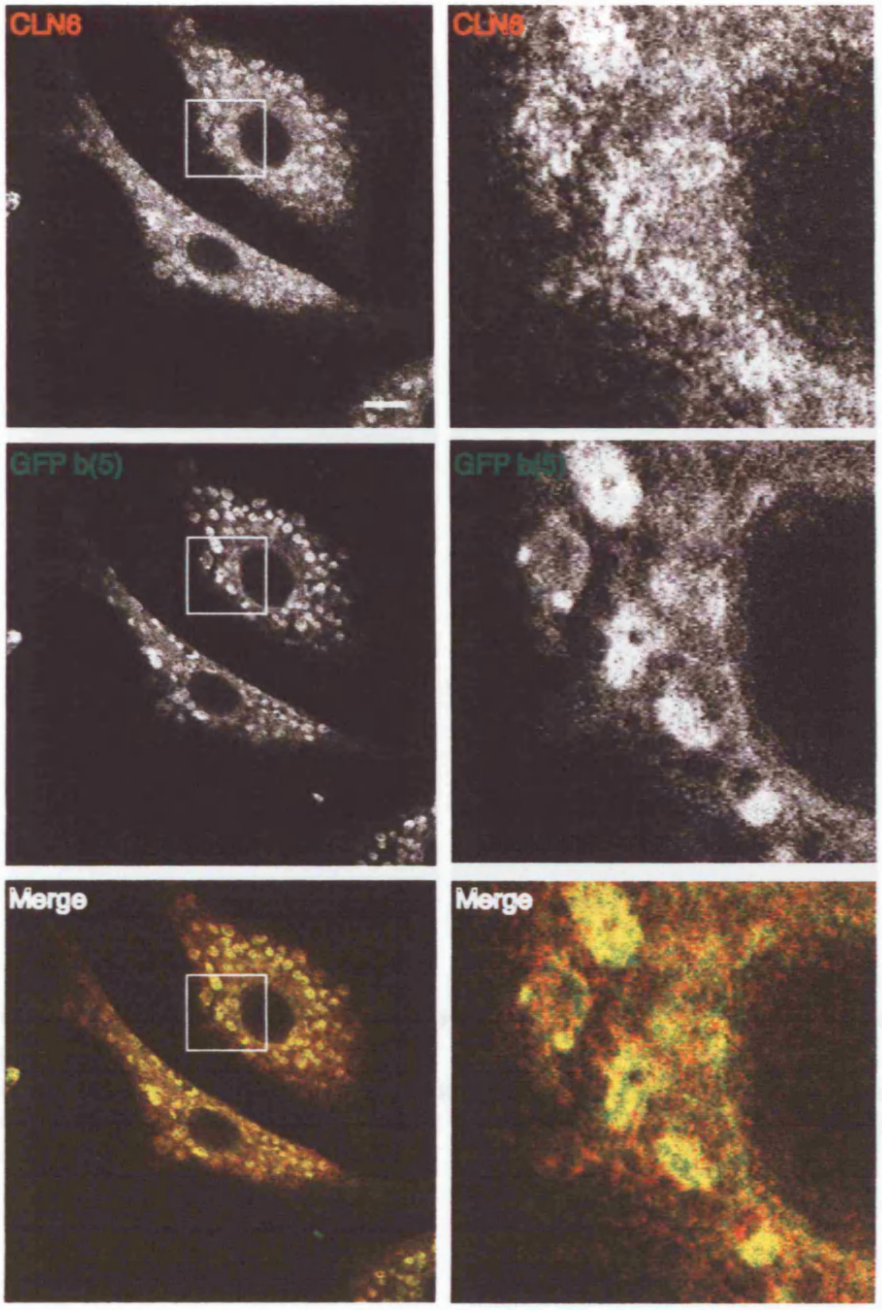

Figure 4.1.4: CLN6 shows co-localisation with GFP-cytochrome b(5) in OSER structures (high expression levels)
GFP-cytochrome b(5) (green) was overexpressed in HeLa cells. Coverslips were stained with anti-CLN6 (red) at 1:1,000. Cells shown are an example of high levels of expression of GFP-cytochrome b(5). Bar, 10 µm.

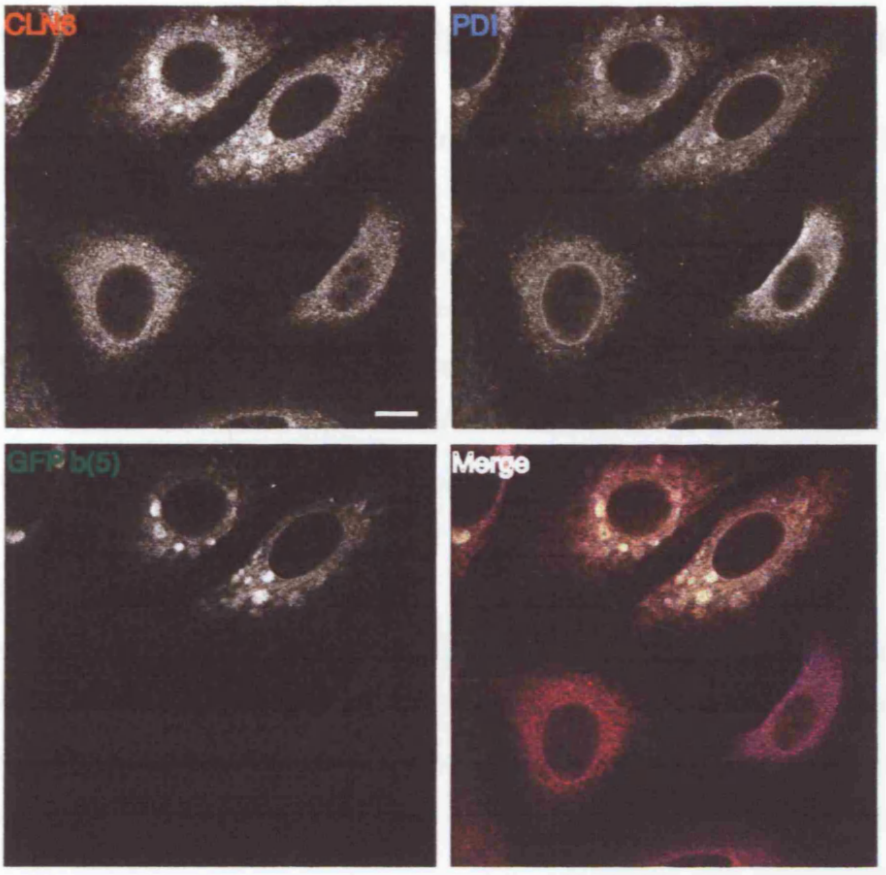

Figure 4.1.5: CLN6 and PDI co-localise with GFP-cytochrome b(5) in OSER structures

GFP-cytochrome b(5) (green) was overexpressed in HeLa cells. Coverslips were stained with anti-CLN6 (red) at 1:1,000 and anti-PDI (blue) at 1:50. Bar, 10 µm.

4.2 CLN6-HRP distribution within the endoplasmic reticulum

The design and cloning of the CLN6-HRP chimera were described in chapter 3.4, and it was further shown by using TSA reagent that the HRP was enzymatically active. While the staining in some overexpressed cells looked reticular, as expected for a protein residing in the ER, other cells showed TSA positive structures that resembled large punctae (chapter 3, figure 3.4.2). To clarify whether the CLN6-HRP construct localised to the same regions of the ER as endogenous CLN6, further co-localisation studies by immunofluorescence microscopy were conducted.

Figure 4.2.1 shows two confocal microscopy sections of a cell overexpressing CLN6-HRP, stained with TSA and an antibody against CLN6. Co-localisation in panel A was seen mainly in the perinuclear regions and around the nuclear ring. CLN6-HRP staining was continuous around the nuclear ring, whereas the antibody staining against CLN6 was non-continuous and co-localisation was therefore not complete. It has previously been observed that overexpression of CLN6 results in continuous staining of the nuclear ring, in contrast to that of endogenous CLN6 (Mole et al., 2004). This data indicates that expression levels determine the localisation of CLN6 within the ER. Less co-localisation was seen in panel B in the peripheral regions of the cell although both the TSA staining of CLN6-HRP and the antibody staining to CLN6 were visible. Figure 4.2.2 shows further co-localisation of CLN6-HRP with CLN6 antibody staining (panel A) as well as with antibody staining to the ER marker calreticulin (panel B). Co-localisation in both experiments was extensive in perinuclear regions but only partial in peripheral regions. The TSA staining of CLN6-HRP furthermore appeared aggregated in contrast to the antibody staining of endogenous CLN6, which as usual appeared punctate throughout the cell. To investigate whether this aggregated staining seen by TSA staining showed that the CLN6-HRP construct had mis-localised to a different, more spherical organelle, co-localisation with the late endosomal/lysosomal markers CD63 and Lamp-1 was performed. The results of this experiment are shown in figure 4.2.3. No co-localisation was observed between markers of late endocytic structures and the aggregated TSA

staining of CLN6-HRP. These results indicated that CLN6-HRP was in the ER, and yet its localisation was not quite the same as that of endogenous CLN6, consistent with previous results using other overexpressed CLN6 constructs (Mole et al., 2004). Furthermore, the overexpressed construct occasionally aggregated into larger punctae, which do not represent the distribution of endogenous CLN6. There was no evidence of striking organisational change of the ER when these punctae were visible.

The results of the immunofluorescence analysis of the CLN6-HRP construct confirmed that CLN6-HRP was in the ER, although not distributed exactly like endogenous CLN6. The distribution of the CLN6-HRP chimeric protein at the ultra-structural level was therefore investigated. In this initial experiment, HEK293 cells were nucleofected with CLN6-HRP and the DAB reaction performed. The samples were embedded, ultrathin sections cut and photographs taken on the Phillips EM420 electron microscope by Dr. Lucy Collinson of the MRC, LMCB. The results are shown in figures 4.2.4 and 4.2.5. The cells in both figures showed electron-dense DAB reaction material throughout the ER, particularly in and near the membranes as indicated by yellow stars. This was consistent with the localisation of endogenous CLN6 and of overexpressed CLN6-HRP as found by immunofluorescence microscopy. Figures 4.2.4 panel B and 4.2.5 panel C further show DAB reaction material throughout the nuclear envelope, which also was consistent with the results of the immunofluorescence microscopy. Interestingly, there appears to be an ER exit site cluster near the nuclear envelope, indicated in the figure 4.2.4 panel C by the label ERES. This is also positive for DAB reaction material, indicating the presence of CLN6-HRP in this region of highly specialised ER. However it was previously shown (figure 4.1.1) that there was no co-localisation between endogenous CLN6 and the ER exit site marker Sec24. This is a further indication that CLN6-HRP may not localise to the same regions of the ER as endogenous CLN6, but rather is distributed throughout the entire ER.

It was noted, that the number of cells positive for electron-dense DAB reaction material was much lower than had been predicted by the transfection efficiency

observed by immunofluorescence (30%). It is unclear why this occurred as the detection of DAB reaction material by electron microscopy is more sensitive than the detection by TSA staining. Furthermore, the cells that were transfected developed large vacuoles, especially apparent in the cell depicted in figure 4.2.5. It is possible that in order to detect the CLN6-HRP construct by DAB reaction, a significant overexpression is necessary, which may be lethal for the cells.

In conclusion, it was not possible to determine whether CLN6 is located in a sub-compartment of the ER using CLN6-HRP. It may be that the enzymatic activity of HRP is not optimal for this particular construct, and further work will be necessary if this construct is to be used for localisation studies. Future work to optimise the use of this construct might involved the use of different size linkers between the protein and the HRP domain, as the linker used in this construct is very short. It may also be possible to move the HRP domain to a different region within the CLN6 protein, although this may prevent correct folding. However, it must protrude into the lumen of the ER to ensure the DAB reaction product does not diffuse into the cytoplasm.

Furthermore, since the construct was made, it was reported that regions within the C-terminal domain are implicated in CLN6 homodimerisation (Heine, et al. 2006, *in press*). Although there is no evidence that dimerisation is required for the localisation or the function of the protein, it is possible that the addition of the HRP domain at the C-terminus of the protein may prevent it from localising correctly.

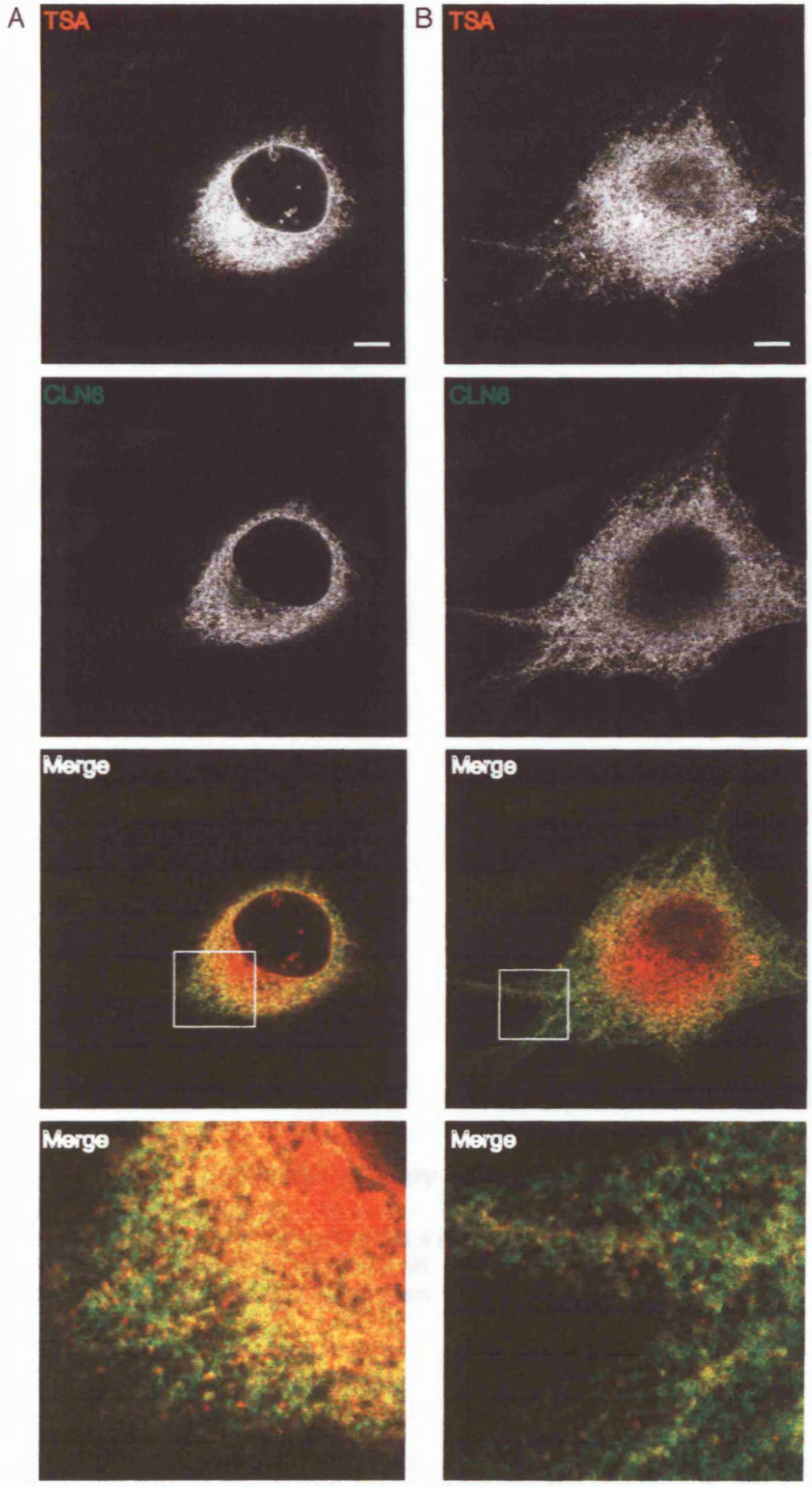

Figure 4.2.1: CLN6-HRP and CLN6 are both located in the ER
CLN6-HRP was overexpressed in HeLa cells. Coverslips were stained with TSA (red) at 1:50 and anti-CLN6 (green) at 1:1,000. (A) and (B) are confocal sections of the same cell. Bar, 10 μm.

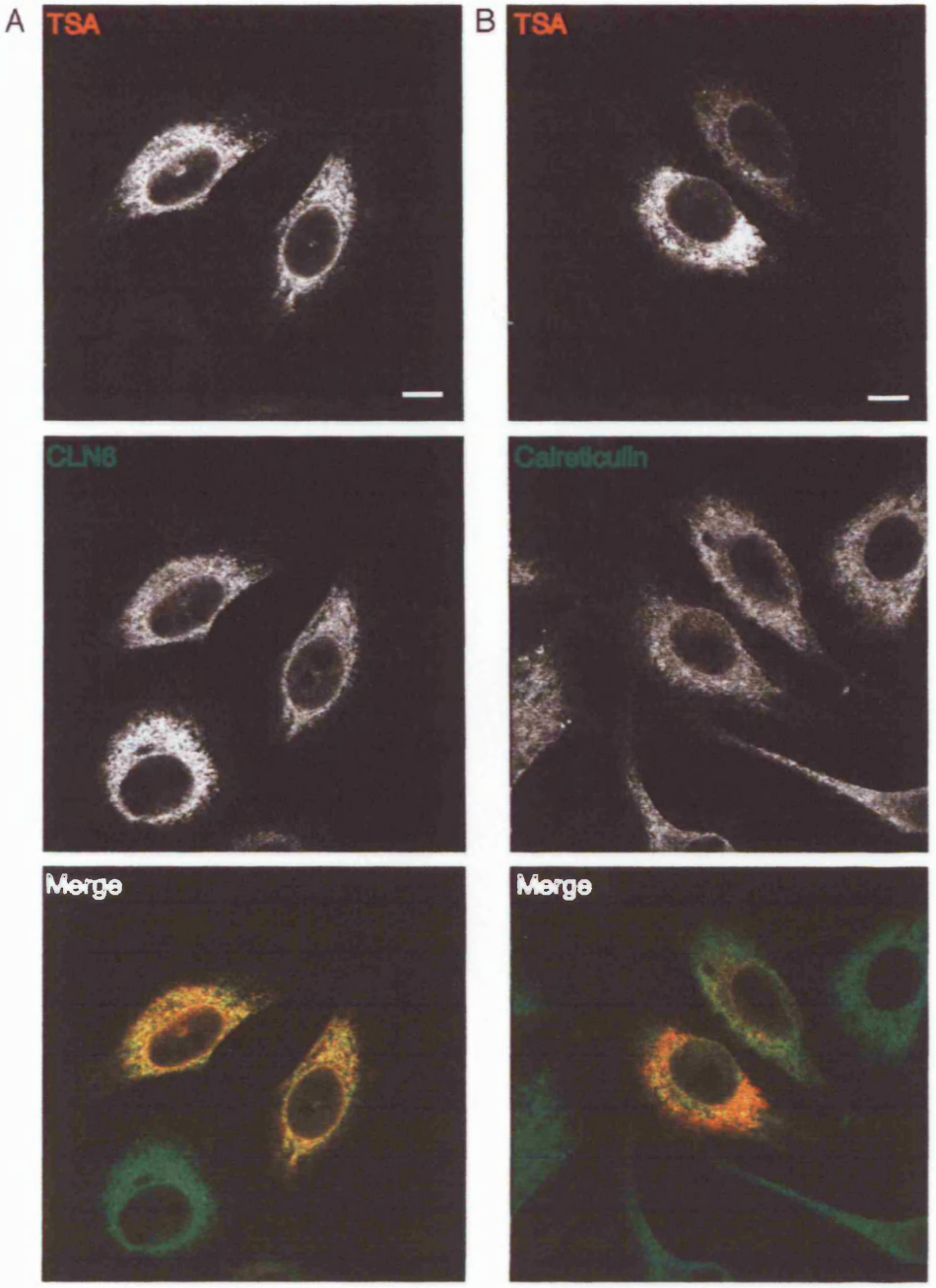

Figure 4.2.2: CLN6-HRP partially co-localises with CLN6 and Calreticulin

CLN6-HRP was overexpressed in HeLa cells. Coverslips were stained with TSA (red) at 1:50 and (A) anti-CLN6 (green) at 1:1,000 and (B) anti-Calreticulin (green) at 1:100. Bar, 10 μm.

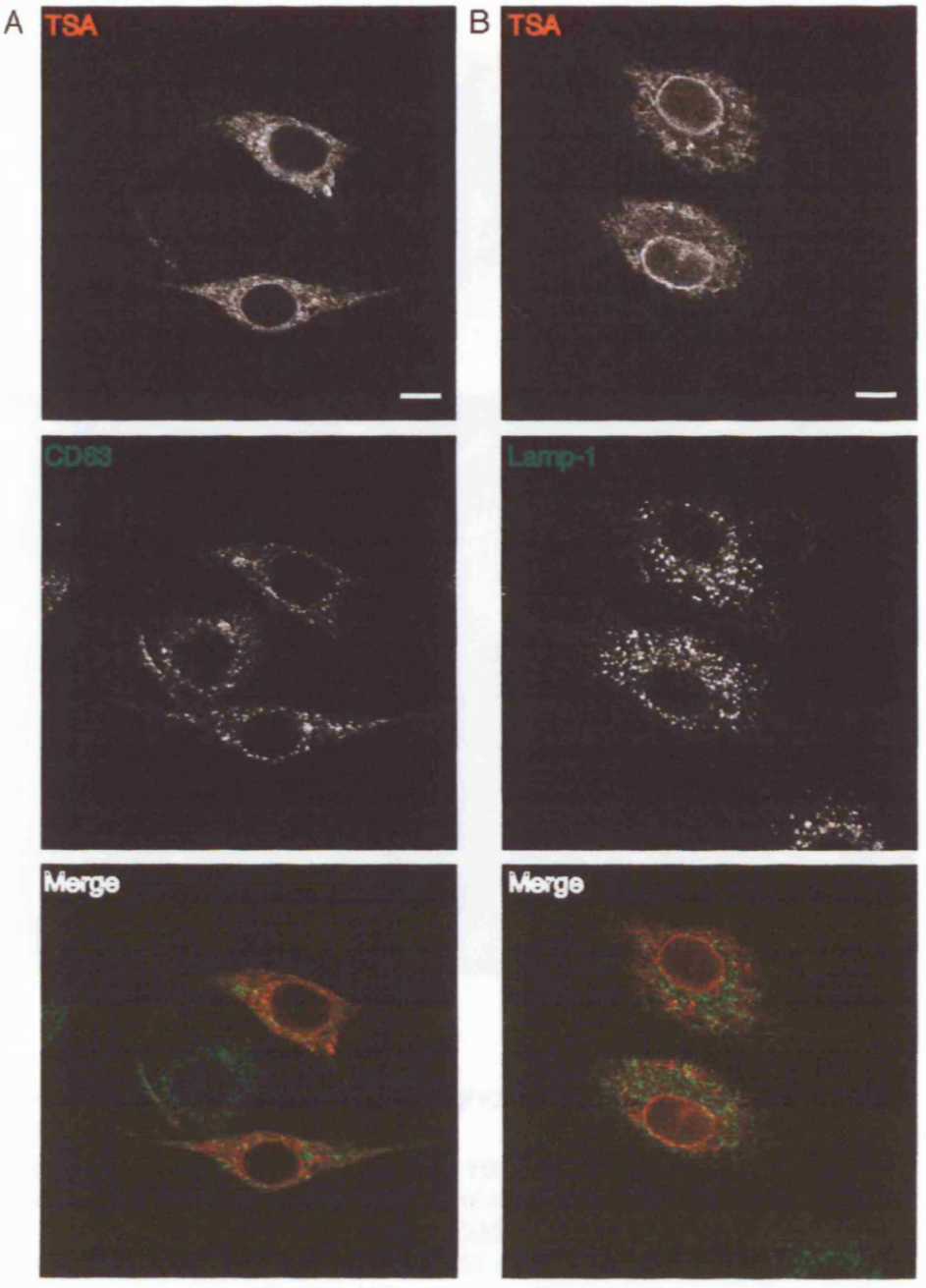

Figure 4.2.3: CLN6-HRP does not co-localise with the late endosomal/lysosomal markers CD63 and Lamp-1

CLN6-HRP was overexpressed in HeLa cells. Coverslips were stained with TSA (red) at 1:50 and (A) anti-CD63 (green) at 1:300 and (B) anti-Lamp-1 (green) at 1:100. Bar, 10 μm.

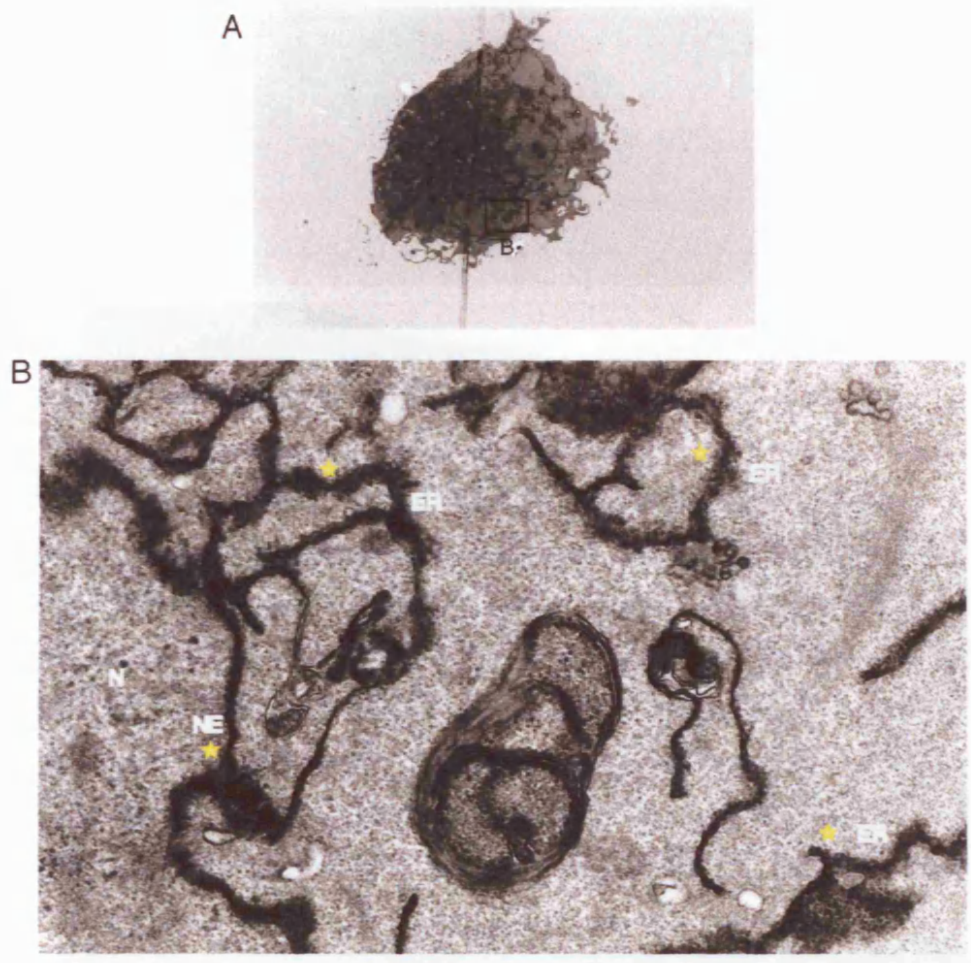

Figure 4.2.4: CLN6-HRP throughout the ER in HEK293 cells - EM cell 1

CLN6-HRP was overexpressed in HEK cells and the DAB reaction performed. Cells were embedded, semi-thin sections cut and images taken by Dr. Lucy Collinson, MRC, LMCB. DAB positive reaction product can be seen throughout the tubules of the ER and around the nuclear envelope. ER = endoplasmic reticulum, N = nucleus, NE = nuclear envelope, yellow star indicates tubules containing DAB reaction product .

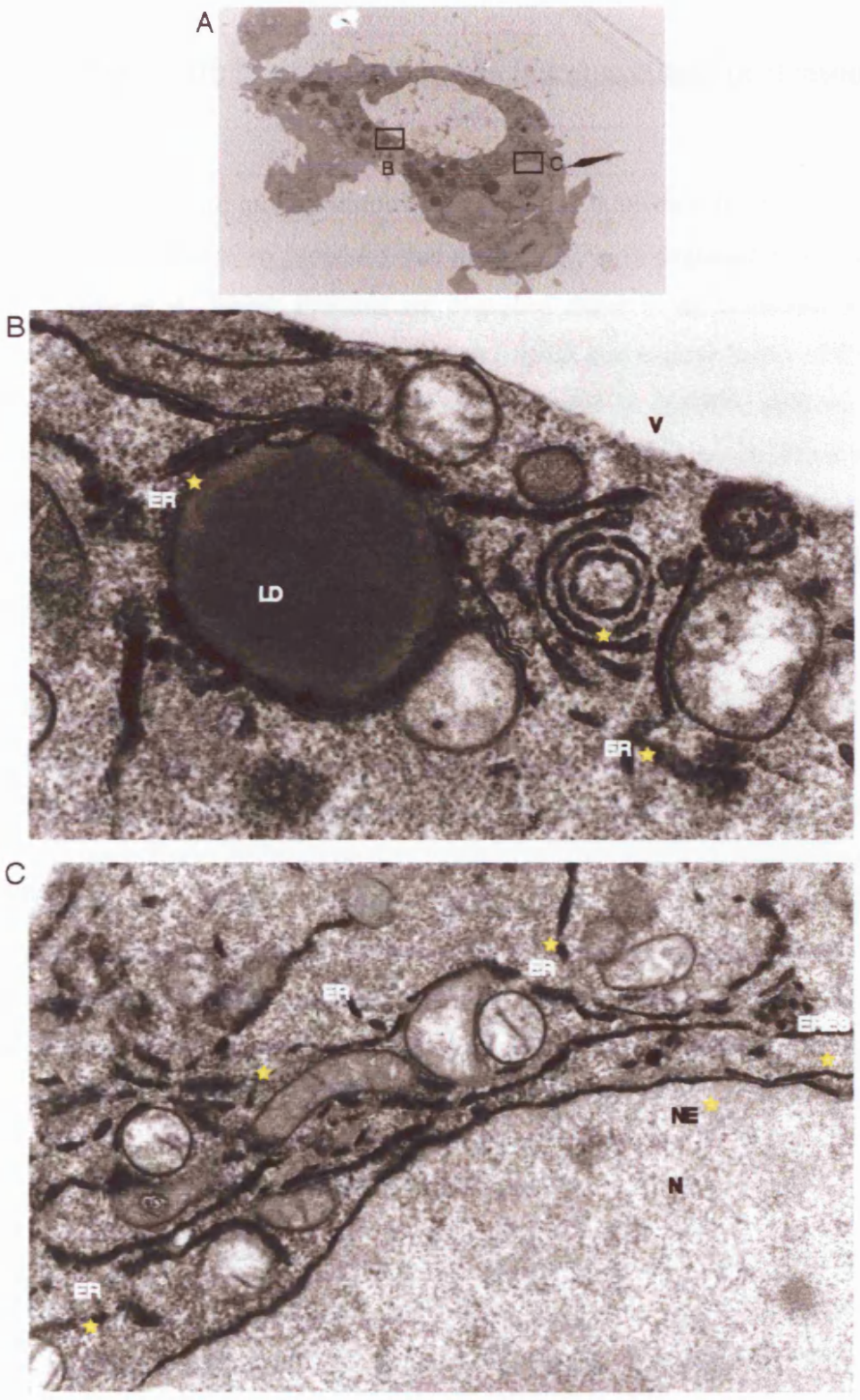

Figure 4.2.5: CLN6-HRP throughout the ER in HEK293 cells - EM cell 2

CLN6-HRP was overexpressed in HEK cells and the DAB reaction performed. Cells were embedded, semi-thin sections cut and images taken by Dr. Lucy Collinson, MRC, LMCB. DAB reaction product can be seen throughout the ER, in the nuclear envelope and in the ERES. ER = endoplasmic reticulum, LD = lipid droplet, N = nucleus, V = vacuole, NE = nuclear envelope, ERES = ER exit site, yellow stars indicate tubules containing DAB reaction product.

4.3 CLN6 trafficking in response to lysosomal and proteasomal inhibitors

Both wild-type and mutant forms of CLN6 have been reported to be located in the ER, and it has been proposed that mutant CLN6 is degraded at an increased rate (Mole et al., 2004). Proteins are degraded either in the lysosome or by the proteasome in the cytosol. It would seem logical that mutant forms of CLN6, at least, are degraded by the ER-associated degradation (ERAD) process. In this process misfolded proteins are retro-translocated into the cytosol, where they are ubiquitinated and degraded by the proteasome complex. If CLN6 is degraded by ERAD, then inhibiting the proteasome complex may stabilise CLN6 within the ER, at sites of retro-translocation or at the proteasome.

Furthermore, as the pathological effect of vLINCL caused by mutations in CLN6 can be observed in lysosomes, it could be that some CLN6 traffics from the ER to the lysosome and performs a specific function there. Although no trafficking motifs have been identified in the sequence of CLN6 to date, non-classical and indeed non-vesicular traffic could allow this protein to be located in more than one organelle. It might be that the majority of CLN6 is located in the ER and small amounts traffic to the lysosome, which would be difficult to detect by immunofluorescence microscopy at steady-state. If this was indeed the case, inhibition of lysosomal hydrolases might stabilise CLN6 and allow its visualisation in the lysosome.

It was therefore decided to use lysosomal or proteasomal inhibitors on endogenous and mutant CLN6. The system chosen for this experiment were fibroblast cell lines from healthy control individuals and from patients with mutations in CLN6 as these provide a naturally occurring disease model. It was proposed that if wild-type and mutant CLN6 were degraded by the proteasome, the use of proteasomal inhibitors should stabilise protein levels. If wild-type or mutant CLN6 did traffic from the ER to the lysosome, then the use of lysosomal inhibitors should stabilise the protein in this organelle. The results could then be visualised using Western blotting and immunofluorescence microscopy.

Three fibroblast cell lines were chosen for this experiment. The healthy control cell line BR3 and the cell lines from CLN6 patients, HF364Pa and HF471Pa. Patient HF364Pa was heterozygous for p.[Ile154del]+[Val277fsX5] and one of these alleles, which was assumed to be non-functional, could be detected by Western blotting. Patient HF471Pa was homozygous for p.[Glu72X] and at steady-state, no protein could be detected.

The lysosomal inhibitors used were leupetin and pepstatin. Leupeptin is a reversible inhibitor of trypsin-like proteases and cystein proteases. Pepstatin is a reversible inhibitor of aspartic proteases such as cathepsin D, pepsin and renin. MG-132 was used to inhibit the proteasome. This is a reversible inhibitor of the degradation of ubiquitin-conjugated proteins by the 26S complex of the proteasome (Calbiochem Product information). Fibroblast cells were grown to approximately 80% conflucency and the inhibitors added every 24 hours (leupeptin, pepstatin) or every 12 hours (MG-132) for 48 hours. At this stage, the cells treated with MG-132 had started to die. The cell bodies were swollen while the peripheral parts of the cells had shrunk to filamentous protrusions. Cell numbers were reduced compared to cells mock treated with DMSO. The experiment was stopped and analysed at this point.

Figure 4.3.1 shows the results from this experiment. Panel A shows a Western blot of cell lysates from the mock- and inhibitor-treated cells. Tubulin was used as a loading control. The intensity of the bands detected by the CLN6 antibody seemed to decrease upon inhibitor treatment in both the control cell line as well as cells from patient HF364Pa. No bands were detected with the CLN6 antibody in the cell line from patient HF471Pa. Densitometric analysis shown in panel B revealed that levels of CLN6 were indeed decreased upon inhibitor treatment. In the control cell line, CLN6 levels were reduced to 66% when treated with lysosomal inhibitors and reduced to 50% when treated with proteasomal inhibitors. In the cell line from patient HF364Pa, levels were reduced to 33% when either inhibitor was used. This data showed that using lysosomal or proteasomal inhibitors did not stabilise the levels of CLN6 in the cell and in fact

resulted in less CLN6 being present. It is however unclear why treatment with inhibitors would lead to such a drastic decrease in protein levels.

The localisation of CLN6 following lysosomal or proteasomal inhibition was evaluated. Panel C of figure 4.3.1 shows immunofluorescence staining of CLN6 in the control cell line BR3 after mock treatment with DMSO and treatment with lysosomal or proteasomal inhibitors. Although the fluorescence intensity appears increased upon treatment with MG-132, this is most likely due to the change in cell shape in response to the inhibitor. Compared to the DMSO treated cells, no change in localisation of CLN6 was observed when either inhibitor was used and the discontinous nuclear ring was still clearly visible.

From this experiment, a number of conclusions were drawn. This experiment did not support the proposed theory that wild-type or mutant CLN6 were degraded by the proteasome. However, the treatment with MG-132 affected the cells quite severely. Less severe treatment using MG-132 or other proteasomal inhibitors would need to be tested before it would be possible to conclusively state that CLN6 was not degraded by ERAD. The proposed theory that CLN6 could traffic to the lysosome could also not be supported by this data as no change in localisation was observed upon lysosomal inhibitor treatment, although protein levels surprisingly were decreased. It was therefore concluded that CLN6 does not exit the ER and traffic to the lysosome.

Future experiments should be conducted using a range of concentrations of lysosomal and proteasomal inhibitors, as well as different time-points. Controls must be included to validate whether the inhibitors worked correctly. These should be ER membrane proteins, which are known to be degraded by either ERAD or in the lysosome. Therefore, the results for CLN6 could then be compared to a stabilisation of these control proteins following inhibitor treatment. It must further be ascertained that proteins are not degraded by other pathways. It is possible that when proteasomal inhibitors are used, misfolded proteins accumulate in the cytosol and are degraded by the autophagic pathway. Therefore, a combination of both lysosomal and proteasomal inhibitors should

also be used. Once optimal conditions are established, it may then be possible to conclude whether CLN6 is degraded by ERAD and/or traffics to the lysosome.

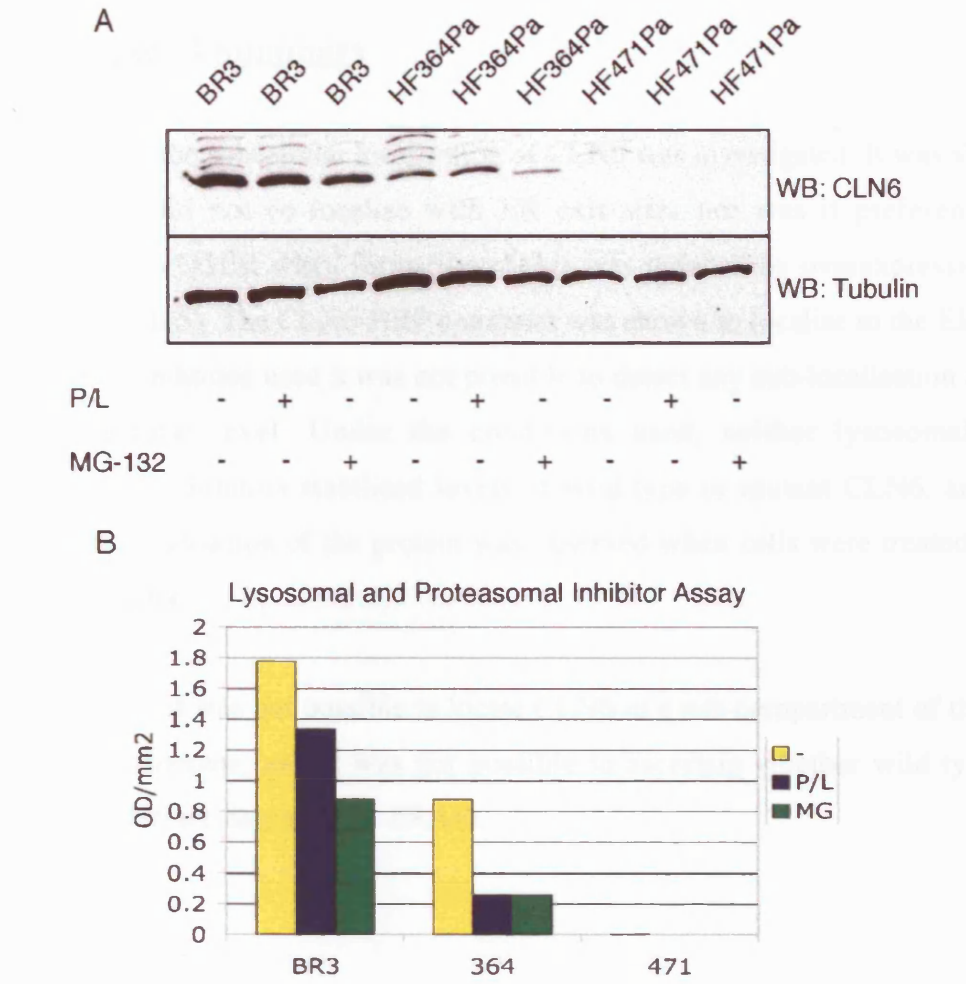

Figure 4.3.1: Lysosomal and proteasomal inhibitor assay
Fibroblast cell lines from healthy controls (BR3) and CLN6 patients (HF364Pa, HF471Pa) were treated with Pepstatin/Leupeptin (P/L) or MG-132 (MG) or with DMSO (-) for 48 hours. (A) Total cell lysates were analysed by Western blotting for CLN6 and the loading control marker tubulin. (B) Western blots were scanned using a Bio-Rad densitometer and the optical density of the bands determined using Quantity One software. CLN6 density values were normalised to tubulin and displayed graphically. (C) Immunofluorescence of CLN6 in control cell line BR3. Bar, 10 µm.

4.4 Chapter 4 Summary

In chapter 4, the subcellular localisation of CLN6 was investigated. It was shown that CLN6 did not co-localise with ER exit sites nor was it preferentially recruited into OSER when formation of this was induced by overexpression of cytochrome b(5). The CLN6-HRP construct was shown to localise to the ER, but under the conditions used it was not possible to detect any sub-localisation at the ultra-structural level. Under the conditions used, neither lysosomal nor proteasomal inhibitors stabilised levels of wild-type or mutant CLN6, and no change in localisation of the protein was observed when cells were treated with either inhibitor.

To conclude, it was not possible to locate CLN6 in a sub-compartment of the ER or in the lysosome, and it was not possible to ascertain whether wild-type or mutant CLN6 are degraded by ERAD.

Chapter 5 – CLN6 interactors

This chapter describes the search for proteins that interact with CLN6. It was proposed that by finding proteins that bind to CLN6 it would be possible to make a prediction about its function and perhaps implicate it in one of the many functions of the ER. Co-immunoprecipitation experiments have in the past been employed successfully to identify interactions between proteins including proteins located in the ER membrane. An example of this is the identification of the Derlin-1/VIMP complex, which binds to the ATPase p97 in the ER membrane and retro-translocates misfolded proteins during ERAD (Lilley and Ploegh, 2004; Ye et al., 2004). The ability to immunoprecipitate endogenous protein is a great advantage as it allows the analysis of a protein in its natural intracellular environment. It was therefore decided to employ this method to search for proteins that co-immunoprecipitate with endogenous CLN6.

Endogenous CLN6 could be immunoprecipitated, as described in chapter 3.2. To identify interacting partners, the following questions were addressed:

Could proteins be co-immunoprecipitated with CLN6?

Could these proteins be identified using mass spectrometry?

Could any of the identified proteins be confirmed as interactors of CLN6?

5.1 Co-immunoprecipitation 1

The initial co-immunoprecipitation experiment was conducted using the same conditions that had been employed while testing the technique. Briefly, cells were lysed in NDLB (non-denaturing lysis buffer) (Roberts et al., 2003).

NDLB
500 mM Tris, pH 7
200 mM NaCl
0.5% Triton-X
0.25% NP-40
7.25 mM EDTA and EGTA

Table 5.1.1: Non-denaturing lysis buffer

Although detection of CLN6 by Western blotting after immunoprecipitation was very successful, a band of the correct molecular weight was much more difficult to detect by coomassie or silver staining when comparable amounts of starting material were used. The experiment was scaled up and successful results obtained when 55 x 15 cm diameter cell culture dishes of confluent HEK293 cells were used. These were immunoprecipitated as described in Materials and Methods, chapter 2.5.2. Briefly, cells were lysed and the lysate cleared by centrifugation. The lysate was then "pre-cleared" by incubation with magnetic beads without antibody. This step was undertaken in order to immunoprecipitate proteins that bound non-specifically to the magnetic beads. The lysate was then incubated with anti-CLN6 antibody conjugated to magnetic beads. Co-immunoprecipitated material was dissociated from the antibody and beads using 20% SDS (Woods et al., 2002). Both eluted sample and material remaining bound to the beads were boiled in sample buffer, run on an SDS-PAGE gel and bands detected by silver staining by Dr. Oliver Kleiner, UCL. The resulting gel is shown in figure 5.1.1. The eluted sample was split between two lanes because the volume was too large to run in a single lane. A few distinct bands were visible that were present in the eluted sample and had not remained bound to the antibody or beads. These were marked and excised by Dr. Kleiner. The band of the molecular weight corresponding to CLN6 (band 7) was excised from the

beads sample as there was more material available for sequencing. The bands were analysed by Maldi-Tof mass spectrometry as described in Materials and Methods, chapter 2.5.7. Table 5.1.2 shows the highest scoring predicted proteins for each band. The raw sequencing data can be found in Appendix B. Predicted proteins that were of a different molecular weight to the estimated molecular weight of the band on the gel were discounted.

Band	Predicted protein	Accession number
2	DEAD box polypeptide 48	gi_7661920
2	Beta-tubulin	gi_18088719
3	Gamma-actin	gi_7441428
5	PPR repeat domain 2	gi_20127634
7	CLN6	gi_8923532

Table 5.1.2: Sequencing results from co-immunoprecipitation 1

In this experiment, it was proposed that CLN6 would co-immunoprecipitate with CLN6, as the protein can dimerise, together with interacting proteins. It was then investigated whether the identified proteins could be detected in a co-immunoprecipitation with CLN6 using specific antibodies and Western blotting.

For technical reasons it was not possible to sequence band 1.

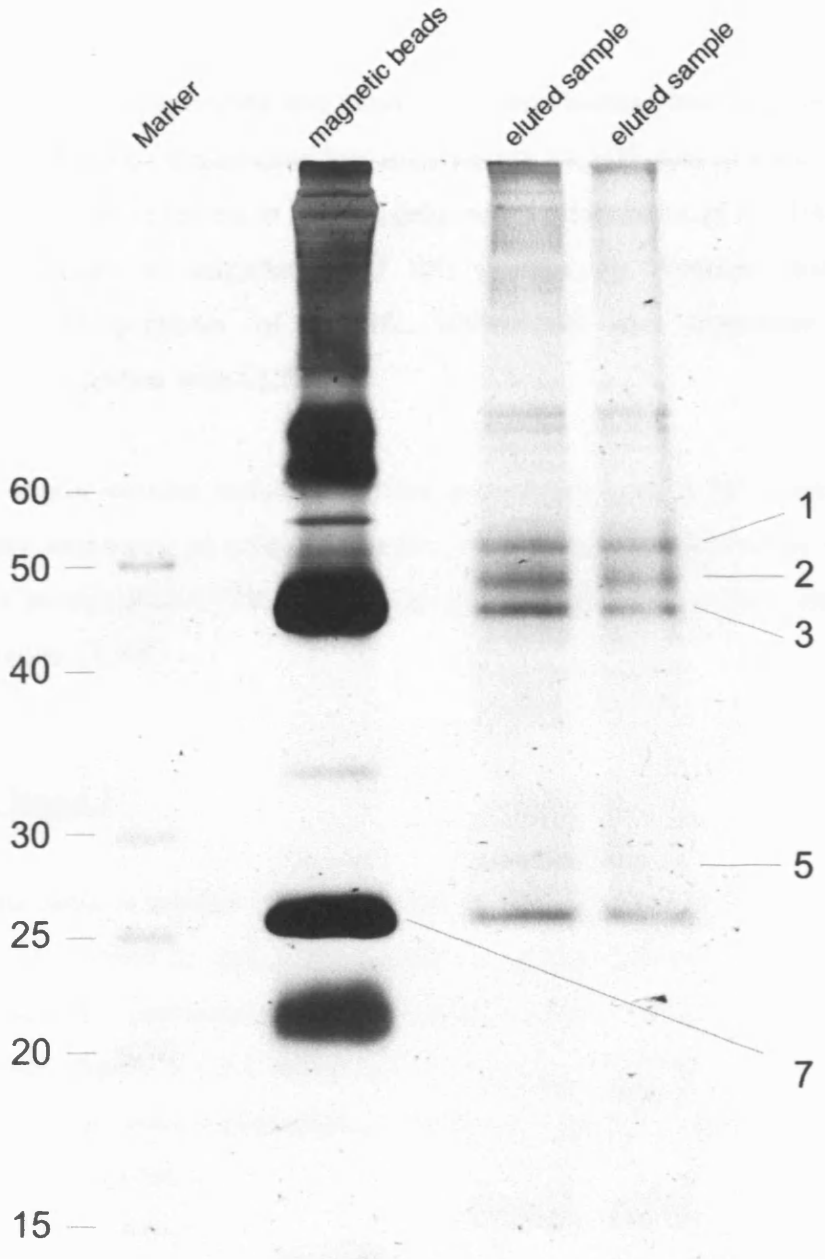

Figure 5.1.1: Silver stain of CLN6 co-immunoprecipitation 1
Gel and silver stain by Dr. Oliver Kleiner, UCL.

5.1.1 Band 2

DEAD-box polypeptide 48 also known as human nuclear matrix protein (hNMP) 265 or Eukaryotic Translation Initiation Factor 4A (eIF-4A) is a nuclear protein proposed to be involved in mRNA processing (Holzmann et al., 2000). Figure 5.1.1.1 shows no enrichment of this protein by Western blotting after immunoprecipitation of CLN6. hNMP265 did therefore not co-immunoprecipitate with CLN6.

Beta-tubulin was the second predicted protein for band 2. In figure 5.1.1.1, a Western blot using an antibody specific for beta-tubulin showed no enrichment of this protein after CLN6 was immunoprecipitated. Beta-tubulin therefore did not bind to CLN6.

5.1.2 Band 3

Gamma-actin is distinct from beta-actin in its residues at the N-terminus. This area was covered by one of the peptides sequenced in this experiment, which increased the confidence that the identification of this band was correct. However, figure 5.1.2.1 shows no enrichment of gamma-actin by Western blotting after immunoprecipiation of CLN6. Therefore, gamma-actin did not interact with CLN6.

5.1.3 Band 5

Pentatricopeptide repeats (PPR) are found in proteins that are involved in RNA processing. Repeats of the PPR α-helical motifs have been proposed to form a superhelix, which has a luminal space into which an RNA molecule can fit. Members of this family are spread extensively throughout the plant kingdom. In plants they are mainly located in chloroplasts but members of this family can also be found in eukaryotes. One particular PPR protein is usually associated with one organelle only, such as the mitochondria or the nucleus (Blatch and

Lassle, 1999). It was not possible to predict which protein containing a PPR motif was identified by mass spectrometry. Therefore, no further steps were undertaken to search for this particular interaction partner. Moreover, as there is no indication that CLN6 may have a role in RNA processing, it seemed unlikely that this was a real candidate.

5.1.4 Band 7

Mass spectrometry confirmed CLN6 to be the band of the correct molecular weight as shown by Western blotting. This confirmed the ability of the antibody to detect CLN6 by Western blotting, and it showed that CLN6 was indeed immunoprecipitated successfully. A small amount of CLN6 was eluted in 20% SDS. This may indicated that endogenous CLN6 dimerises as has been reported for the overexpressed protein (Heine et al., 2004). However, this experiment is not conclusive proof as the protein was not sequenced from a higher molecular weight dimeric complex.

The first attempt to co-immunoprecipitate proteins with CLN6 was unsuccessful. The use of a large amount of starting material in the experiment probably resulted in significant non-specific binding to the antibody and to the magnetic beads. It was subsequently decided to optimise the technique and use chemical cross-linking reagents to identify proteins interacting with CLN6 to allow less starting material to be used.

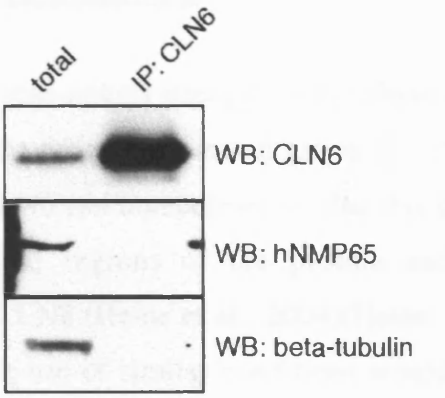

Figure 5.1.1.1: CLN6 does not co-immunoprecipitate hNMP65 or beta-tubulin

HEK293 cells were immunoprecipitated with CLN6 antibody and samples Western blotted with antibodies to CLN6, hNMP65 and beta-tubulin. Left lane: total input material, right lane: material following immunoprecipitation of CLN6.

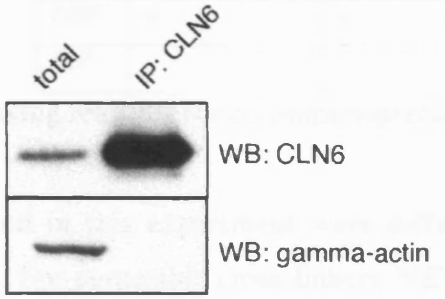

Figure 5.1.2.1: CLN6 does not co-immunoprecipitate gamma-actin

HEK293 cells were immunoprecipitated with CLN6 antibody and samples Western blotted with antibodies to CLN6 and gamma-actin. Left lane: total input material, right lane: material following immunoprecipitation of CLN6.

5.2 Co-immunoprecipitation 2

The use of chemical cross-linkers strengthens the physical bond between proteins that interact. During the time of this investigation, this method was used to show that overexpressed CLN6 can homodimerise, that this dimerisation is facilitated by N- and C-terminal regions of the protein and that CLN6 does not heterodimerise with CLN8 (Heine et al., 2004)(Heine, et al., 2006, *in press*). It was proposed that the use of similar conditions would enhance the binding of interacting proteins to CLN6, making it easier to co-immunoprecipitate them. Three different cross-linking reagents were used for subsequent experiments. These are shown in table 5.2.1. Two were capable of permeating cell membranes and one was cleavable allowing release of protein that bound to and co-immunoprecipitated with CLN6.

Name	Cell-permeable	Cleavable
DSS	+	-
DSP	+	+
BS^3	-	-

Table 5.2.1: Cross-linking reagents for co-immunoprecipitation

The lysis buffers used in this experiment were different to the one used in previous experiments. For permeable cross-linkers, NET buffer was used to lyse the cells as this was more efficient in immunoprecipitating CLN6. For non-permeable cross-linkers cells were lysed in HEPES buffer as suggested by the manufacturer of the cross-linkers, as the presence of Tris quenches their activity. Furthermore, after the pre-clearing step, lysates were incubated only with CLN6 antibody, followed by the addition of the magnetic beads, as opposed to incubation with the antibody conjugated to the beads as previously used. This change was introduced to increase the efficiency of antibody binding to CLN6 and decrease the chance of the antibody-bead complex aggregating. Table 5.2.2 shows the constituents of NET and HEPES lysis buffers:

NET buffer
75 mM Tris-HCl, pH 7
200 mM NaCl
7.5 mM EDTA
1% Triton-X

HEPES lysis buffer
50 mM HEPES, pH 7.6
200 mM NaCl
1% Triton-X

Table 5.2.2: NET and HEPES lysis buffers used in co-immunoprecipitation 2

Control samples included immunoprecipitation without the addition of cross-linkers and without the addition of CLN6 antibody. The immunoprecipitated samples were run on a large 10% SDS-Page gel and stained using the coomassie blue method 2 described in Materials and Methods, chapter 2.5.4. Figure 5.2.1 shows the results of this experiment. Bands were chosen for sequencing according to the following criteria:

- Not present in samples where no primary antibody was used
- Present in sample with non-cleaveable cross-linker but not in sample without cross-linker (cross-linking should shift the molecular weight of a co-immunoprecipitated complex)
- Present in sample without cross-linker but not in sample with non-cleavable cross-linker

Bands were excised as described in Materials and Methods, chapter 2.5.7. Bands were sequenced by Dr. Catherine Lilley, Cambridge. Unfortunately, all of the bands except one were contaminated with keratin. The only band that could be sequenced was band 2. The raw sequencing data can be found in Appendix B. The highest scoring possible protein for this band was mitochondrial heat shock protein 75 (mtHSP75), gi_292059. This is a chaperone protein located in the mitochondrial inner matrix membrane that has been implicated in the folding of nascent nuclear and mitochondrial proteins and is a member of the HSP70 family of proteins (Bhattacharyya et al., 1995; Mizzen et al., 1989; Mizzen et al., 1991). A monoclonal antibody against mtHSP75 can detect this protein by Western blotting. It was also shown to cross-react with other members of the HSP70 family, namely HSC70 and HSP70, in two-dimensional gel electrophoresis (Bhattacharyya et al., 1995). As shown in figure 5.2.2, this antibody against

mtHSP75 does not detect a band after co-immunoprecipitation with CLN6, confirming that this protein does not interact with CLN6.

Co-immunoprecipiation 2 was therefore unsuccessful in identifying interacting partners of CLN6. As it was very unfortunate that most of the bands were contaminated by keratin, it was decided to repeat the experiment and collaborate with a different laboratory to perform the mass spectrometry sequencing.

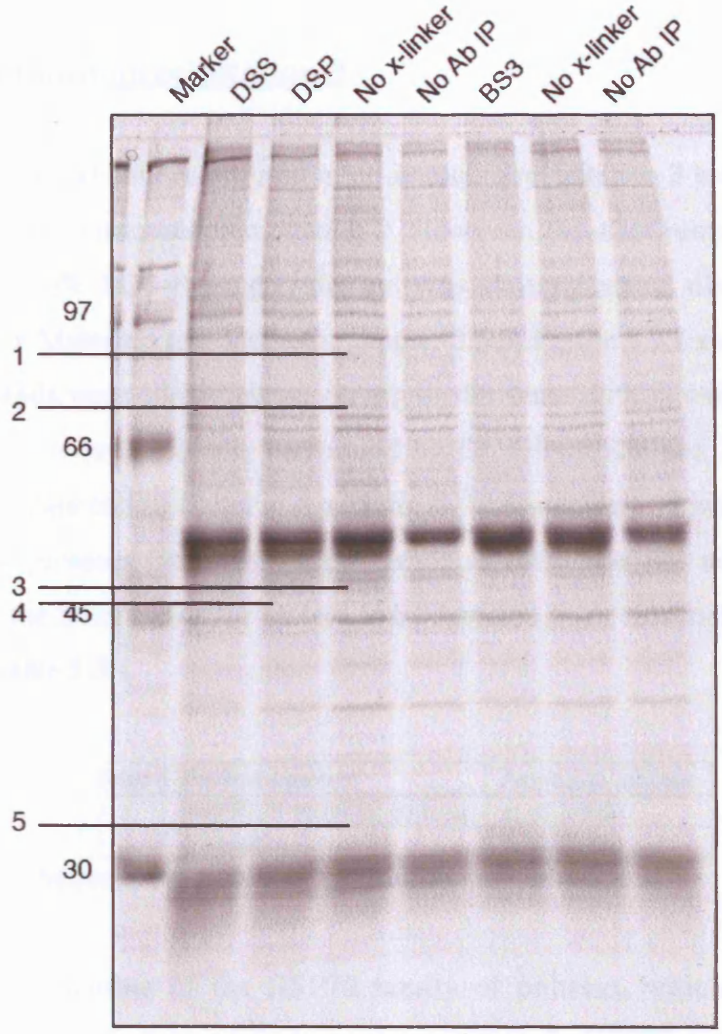

Figure 5.2.1: Coomassie stain of co-immunoprecipiation 2

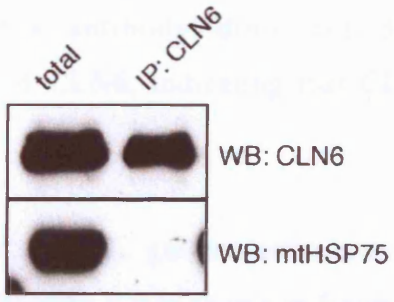

Figure 5.2.2: CLN6 does not co-immunoprecipitate mitochondrial HSP75

HEK293 cells were immunoprecipitated with CLN6 antibody and samples Western blotted with antibodies to CLN6 and mtHSP75. Left lane: total input material, right lane: material following immunoprecipitation of CLN6.

5.3 Co-immunoprecipitation 3

The experimental conditions used in co-immunoprecipitation 3 were the same as those used in co-immunoprecipitation 2. However, the after running the sample on a large 10% SDS-Page gel, the gel was staining using silver staining as described in Materials and Methods, chapter 2.5.5. Figure 5.3.1 shows the results of this. Bands were identified according to the same criteria outlined above in chapter 5.2. Sequencing was performed by Dr. Oliver Kleiner, Eisai. The raw sequencing data can be found in Appendix B. Unfortunately, it was only possible to identify proteins from two of the bands as there was not enough material present in the other bands for protein to be detected using this method. These are shown in table 5.3.1.

Band	Predicted protein	Accession number
3	HSP70, N-terminal domain	gi_6729803
5	Beta-actin	gi_4501885

Table 5.3.1: Sequencing results of co-immunoprecipitation 3

HSP70 is a member of the HSP70 family of proteins, which also contains mtHSP75, identified in co-immunoprecipitation 2. HSP70 is located in the cytoplasm and the nucleus where it assists the folding of nascent polypeptides (Bhattacharyya et al., 1995; Frydman et al., 1994). The antibody recognising mtHSP75 cross-reacts with HSP70 (Bhattacharyya et al., 1995). In figure 5.2.2 it was shown that this antibody does not detect a band after co-immunoprecipitation of CLN6, indicating that CLN6 does not interact with mtHSP75 or HSP70.

In co-immunoprecipitation 1, gamma-actin was identified as a proposed interactor of CLN6, although it was shown in figure 5.1.2.1 that this interaction could not be confirmed. Figure 5.3.2 shows that an antibody against alpha, beta and gamma actin does not detect a band after co-immunoprecipitation of CLN6. The faint doublet of bands that is visible in the co-immunoprecipitation lane when the actin antibody was used for Western blotting is a contamination as the

same bands were visible when the CLN6 antibody was used. Therefore, CLN6 does not interact with alpha, beta or gamma actin.

Co-immunoprecipitation 3 was unsuccessful in identifying interaction partners of CLN6. It was extremely unfortunate that most of the bands identified in this experiment could not be identified due to technical reasons.

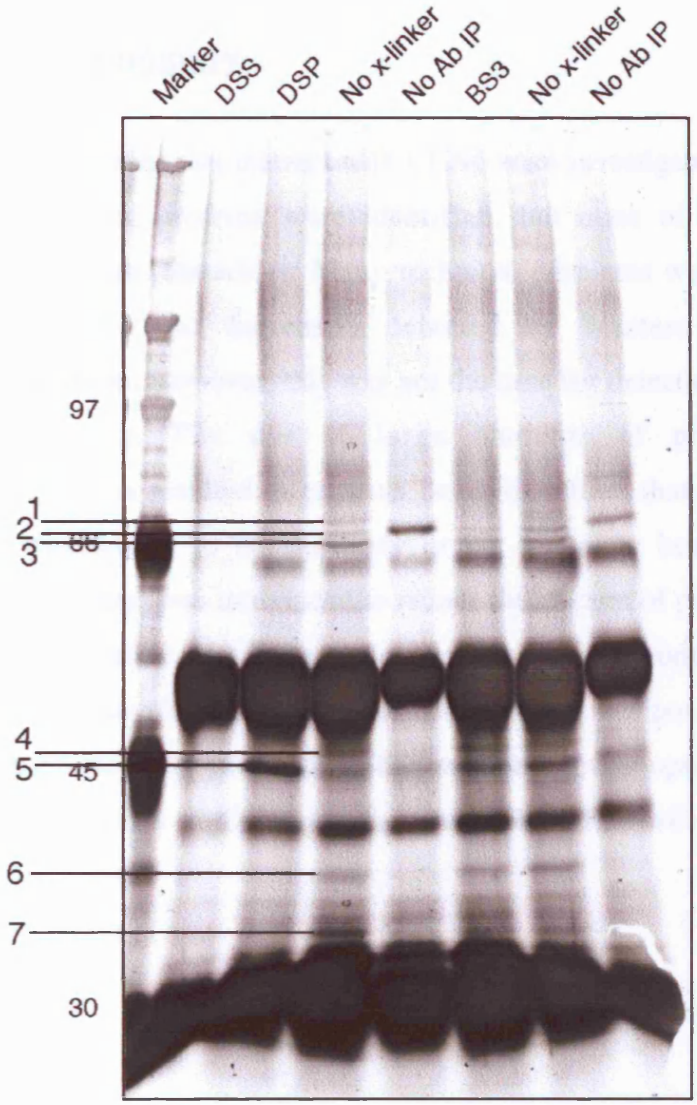

Figure 5.3.2: Silver stain of co-immunoprecipitation 3

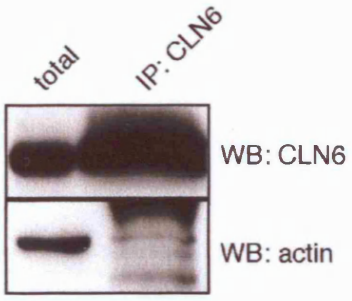

Figure 5.3.3: CLN6 does not co-immunoprecipitate actin
HEK293 cells were immunoprecipitated with CLN6 antibody and samples Western blotted with antibodies to CLN6 and actin (alpha, beta and gamma). Left lane: total input material, right lane: material following immunoprecipitation of CLN6.

5.4 Chapter 5 Summary

In this chapter, proteins that interact with CLN6 were investigated. A number of potential interacting proteins were identified, but none of them could be confirmed to be true interactors. Many technical problems were encountered. Endogenous CLN6 can be easily detected by Western blotting after immunoprecipitation. However, this was not the case for detection by coomassie or silver staining. The use of large amounts of protein for co-immunoprecipitation resulted in proteins being identified that had most likely bound non-specifically to the antibody or the magnetic beads. The use of chemical cross-linkers was introduced to reduce the amount of protein needed for co-immunoprecipitation. However, under the experimental conditions used, this did not prove successful either. In conclusion, it was not possible to identify proteins that interact with CLN6 using this method. Further optimisation will be necessary if interactors of CLN6 are to be identified. This will be addressed in chapter 7.

Chapter 6 – siRNA screen of vLINCL proteins

In order to elucidate the cellular mechanisms underlying NCL pathology, many recent publications have made use of cell lines from NCL patients or animal models. Fibroblast cell lines from CLN6 patients were used to show that the levels of MnSOD were increased in these cells compared to healthy control cells (Heine et al., 2003) and microarray data on fibroblast cell lines has implicated changes in a number of cellular pathways to be involved in CLN6 pathology (Teixeira et al., 2006). In order to investigate cellular changes due to loss of functional proteins in the vLINCL family, it was considered using such a model system. However, it was not possible to obtain fibroblast cell lines from CLN5 patients. Furthermore, as fibroblast cell lines are primary cell lines, they are subject to natural variation between individuals. Moreover, these cell lines can be thought of as having adapted to the mutant vLINCL proteins, as there is no evidence of pathological events in these cells. It was therefore decided to use a simpler, transformed cell system to analyse the immediate cellular events occurring in response to loss of functional vLINCL proteins.

Chapter 6 describes the results of RNA interference experiments of the vLINCL proteins CLN5, CLN6 and CLN8. The aim of this screen was to model and identify early events in response to depletion of functional proteins as well as to investigate whether these events were similar for the different proteins in the vLINCL group.

RNAi targeting of CLN6 was optimised previously and described in chapter 3. RNAi against the two remaining vLINCL proteins CLN5 and CLN8 was designed and tested. A combined screen of RNAi depletion of all three vLINCL proteins was performed. The questions addressed in this chapter therefore were:

Can CLN5 and CLN8 protein levels be successfully reduced using siRNA?

What are the effects of siRNA depletion of the vLINCL proteins CLN5, CLN6 and CLN8?

6.1 siRNA against CLN5 and CLN8

Two siRNAs each were chosen for targeting CLN5 and CLN8. Figure 6.1 panel A depicts a BLAST alignment of the respective mRNAs and siRNAs. No exact matches between the siRNAs and any other human mRNA sequences were found. As there were no antibodies available to endogenous CLN5 and CLN8, quantitative reverse-transcription (Q-) PCR was used to analyse the efficiency of the siRNAs to reduce mRNA levels. Experiments were performed in the same way as described for siRNA against CLN6. Briefly, HeLa cells were nucleofected for two rounds of siRNA treatment, with recovery of 48 hours after each nucleofection. Samples nucleofected without addition of siRNA were used as mock-treated control samples.

Unfortunately, difficulties with Q-PCR of CLN8 mRNA were encountered. Two different primer sets were tested but these did not give any signal under conditions used for Q-PCR of CLN5 and CLN6 mRNA. To trouble-shoot, the following were tested: different annealing temperatures, different concentration of primers and template. The primers did detect an amplicon of the expected size in conventional PCR when the annealing temperature was lowered, however it was not possible to obtain any signal by Q-PCR when the same temperature was used. It was consequently decided to proceed with the siRNA screen nonetheless and use a mixture of both siRNAs to CLN8. However, it cannot be said for certain that CLN8 is indeed depleted successfully in any of the experiments presented below. In the event that better reagents could be obtained and used in the future, RNA was extracted from all samples and stored.

Q-PCR analysis for CLN5 siRNA showed that both siRNAs reduced mRNA levels. It was decided to use a mixture of both in subsequent experiments. Figure 6.1 panel B shows the reduction in mRNA levels to an average of 22% with siRNA targeting CLN5 compared to mock-treated cells. For comparison, the same figure also shows the reduction of CLN6 mRNA to an average of 18.5% in samples treated with siRNA against CLN6 (same data presented in figure 3.5.2).

For all subsequent experiments, mixtures of two siRNAs for each gene were used against CLN5, CLN6 and CLN8.

A

```
CLN5-1 siRNA   1     GGACAGGTCAGTTCATAAA    19
                     ||||||||||||||||||
CLN5 mRNA      1168  GGACAGGTCAGTTCATAAA    1186

CLN5-2 siRNA   1     AACTGCTGTCTGGTAAAAACA  21
                     |||||||||||||||||||||
CLN5 mRNA      544   AACTGCTGTCTGGTAAAAACA  564

CLN8-1 siRNA   1     CAAGGTGTATAGTAACCTA    19
                     ||||||||||||||||||
CLN8 mRNA      3016  CAAGGTGTATAGTAACCTA    3034

CLN8-2 siRNA   1     CGCTAATCATTAATCCATA    19
                     ||||||||||||||||||
CLN8 mRNA      959   CGCTAATCATTAATCCATA    977
```

B

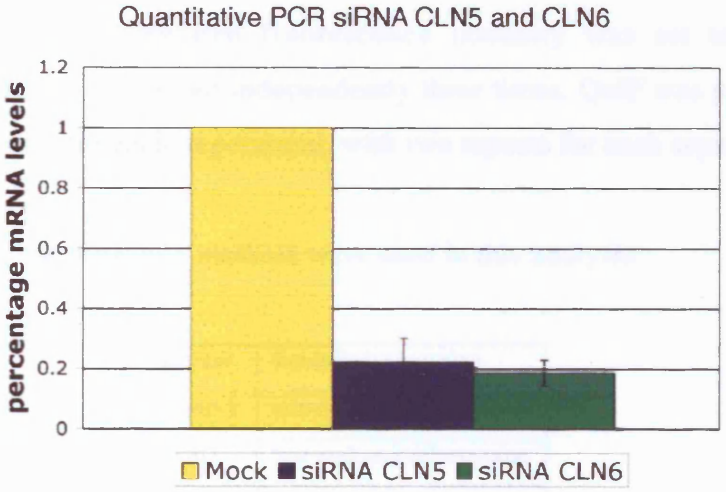

Figure 6.1: siRNA CLN5, CLN6 and CLN8

(A) BLAST alignment of siRNA sequences against CLN5 and CLN8 and their respective mRNAs (CLN5 mRNA gi 5729711, CLN8 mRNA gi 31083052).

(B) CLN5 and CLN6 were depleted in HeLa cells using two rounds of siRNA of a mix of two siRNAs for each protein. Quantitative PCR was performed using the housekeeping gene GAPDH as an internal control. The graph shows a depletion to 22% of mRNA levels for CLN5 and 18.5% mRNA levels for CLN6 compared to mock transfected cells, CLN5 n=2, CLN6 n=4. It was not possible to quantitate depletion of CLN8.

6.2 siRNA against CLN5, CLN6 and CLN8

After two rounds of siRNA treatment, cells were analysed by immunofluorescence to visualise gross changes in organelle morphology. Quantitative immunofluorescence (QuIF) was subsequently used to examine whether the protein levels of any of the organelle markers used were altered. QuIF is described in Materials and Methods, chapter 2.5.8. Briefly, samples were plated into 96-well plates and incubated with organelle markers under the same conditions used for standard immunofluorescence. Secondary antibodies were used at 800 nm wavelength in combination with a DNA stain fluorescing at 700 nm wavelength. Plates were scanned using the Li-Cor Odyssey scanner, which can detect dyes at two different wavelengths. Integrated fluorescence intensity was measured. Samples were normalised to the cell number as counted by DNA stain. Values for siRNA treated samples were displayed in comparison to mock samples whose integrated fluorescence intensity was set to 100%. Each experiment was performed independently three times. QuIF was performed twice independently for each experiment, with two repeats for each separate QuIF.

The following organelle markers were used in this analysis:

Marker	Subcellular location
Lamp-1	late endosome/lysosome
CD63	late endosome/lysosome
EEA-1	early endosome
PDI	endoplasmic reticulum
GM130	*cis*-Golgi

Table 6.1: Organelle markers used in siRNA screen

It was proposed that siRNA targeting of CLN5, CLN6 or CLN8 may have similar effects, as mutations in any of these proteins result in the vLINCL phenotype. It was further hypothesised that there may be an effect on late endocytic/lysosomal compartments when these proteins were depleted, as it is here that the storage material accumulates.

6.2.1 Lamp-1

Immunofluorescence microscopy showed a clear change in the phenotype of Lamp-1-positive structures upon treatment with siRNA to CLN5, CLN6 and CLN8. Lamp-1-positive structures in mock-treated cells were small punctae, which appeared widely dispersed throughout the cells. Cells treated with siRNA to any of the vLINCL proteins showed a variety of changes in the appearance of Lamp-1 positive structures and typical examples of these changes are shown in figure 6.2.1.1. These structures were generally enlarged and appeared ring-shaped with Lamp-1 staining on the perimeter of the compartment as can clearly be seen in the picture of siRNA targeting CLN5, left hand panel. Often the structures appeared brighter, as can be observed in the picture of siRNA to CLN6, left hand panel. Sometimes the compartments were more clustered in the perinuclear region as shown in the picture of siRNA to CLN8, right hand panel. These changes were present to similar degrees in siRNA of all three vLINCL proteins. The changes were also observed when the siRNAs were used individually, indicating that there is a consistent effect due to protein depletion, which is not due to an off-target effect of individual siRNAs.

As the Lamp-1-positive structures often appeared to be brighter in cells treated with siRNA, QuIF was used to test if there was a quantitative change in fluorescence intensity of this marker. Figure 6.2.1.2 shows that there was no statistically significant change in integrated fluorescence intensity after siRNA treatment.

As the immunofluorescence of Lamp-1 in cells treated with siRNA against CLN8 looked very similar to that seen with siRNA against CLN5 and CLN6, confidence was gained that the depletion of CLN8 by siRNA was successful.

To determine whether the phenotype observed by immunofluorescence with Lamp-1 was due to a direct effect on this marker protein when the vLINCL proteins were depleted, another late endosomal/lysosomal marker, CD63, was used.

6.2.2 CD63

Immunofluorescence microscopy showed a similar change in phenotype of CD63-positive structures to the one observed for Lamp-1-containing structures. The results of this are shown in figure 6.2.2 panel A. While CD63-positive structures in mock-treated cells were small, puntate and dispersed throughout the cells, structures in cells treated with siRNA against the vLINCL proteins appeared enlarged and clustered in the perinuclear regions.

QuIF of CD63 did not show any statistically significant changes in integrated fluorescence intensity after siRNA treatment, as shown in figure 6.2.2 panel B.

As CD63 and Lamp-1 are both markers for late endosomal/lysosomal compartments, these data confirmed that the changes observed were most likely due to an effect on the morphology of these compartments occurring as a result of decreased levels of the vLINCL proteins.

Interestingly, similar results for these compartments have been observed by other members of the laboratory in response to siRNA against the JNCL protein CLN3 (C. Kitzmuller, *personal communication*).

6.2.3 EEA1

As shown in figure 6.2.3, no changes were observed in EEA1-positive structures after siRNA treatment. Immunofluorescence microscopy showed small, dispersed early endosomes in mock and siRNA treated cells. QuIF did not show a statistically significant change in integrated fluorescence intensity after siRNA treatment.

6.2.4 PDI

As shown in figure 6.2.4, no changes were observed in PDI staining after siRNA treatment. Immunofluorescence microscopy showed reticular and punctate ER staining with clearly visible nuclear envelopes in mock and siRNA treated cells. QuIF did not show a statistically significant change in integrated fluorescence intensity after siRNA treatment.

6.2.5 GM130

A change in phenotype of GM130-positive structures was observed after treatment with siRNA targeting CLN6 and CLN8 but not with siRNA targeting CLN5. The results of the immunofluorescence microscopy are shown in figure 6.2.5.1 panel A. GM130 staining gave ribbons of varying length in the perinuclear region, some short and some longer. Figure 6.2.5.2 panel A shows typical images of cells that were counted as containing short GM130-postive ribbons (shorter than 5 μm) and cells counted as containing long GM130-positive ribbons (longer than 5 μm). Mock-treated cells tended to have short and long ribbons as did CLN5-depleted cells. However, more cells had long GM130-positive ribbons when they were treated with siRNA against CLN6 and CLN8. An initial attempt was made to quantify this and 3 x 50 cells were counted for each sample. Each cell was counted as containing either short or long ribbons. Figure 6.2.5.2 panel B shows a graph of cells containing predominantly short or long GM130-positive ribbons. While in mock and CLN5-depleted cells around 20% of the cells contained long GM130-positive ribbons, CLN6-depleted cells contained just over 50% and CLN8-depleted cells around 65% of long GM130-positive ribbons. The differences observed upon depletion of CLN6 and CLN8 were statistically significant.

QuIF did not show a statistically significant change in integrated fluorescence intensity after treatment with siRNA, as shown in figure 6.2.5.1.

These results were further investigated by targeting specific cells directly using microinjection. HeLa cells were nucleofected for the first round of siRNA treatment as described previously. Specific cells were then microinjected with water in mock-treated cells and siRNA against CLN5, CLN6 or CLN8. This was performed by Dr. Claudia Kitzmüller. The results of this experiment are shown in figure 6.2.5.3. Microinjected cells are denoted with a star. Twenty microinjected cells were counted for each sample. All cells that were microinjected with water or siRNA against CLN5 showed short *cis*-Golgi ribbons. 50% of cells that were microinjected with siRNA against CLN6 and CLN8 showed long *cis*-Golgi ribbons. These results are consistent with previous results and confirm that cells depleted of CLN6 and CLN8 but not of CLN5 contain more long *cis*-Golgi ribbons.

This data indicates that there is a change in the morphology of the *cis*-Golgi, as shown by GM130 staining when cells were treated with siRNA against CLN6 and CLN8 but not CLN5. GM130 localises to the *cis*-Golgi membrane where it is thought to have a structural role as well as being implicated in facilitating vesicle docking (Barr et al., 1997; Nakamura et al., 1997; Nakamura et al., 1995). There were no previous reports of Golgi abnormalities in vLINCL patients. Therefore, it was unexpected that the morphology of the *cis*-Golgi should change in response to CLN6 or CLN8 depletion. Both CLN6 and CLN8 are located in the ER (Heine et al., 2004; Lonka et al., 2000; Mole et al., 2004), and CLN8 has also been reported in the ER-Golgi intermediate compartment (Lonka et al., 2000). It is possible that depletion of these proteins would have an effect on the *cis*-Golgi as there is a close relationship between the two organelles. It is unclear whether a change in Golgi morphology could be due to a direct effect on the organelle or due to an event in the ER, which could consequently lead to a secondary event affecting the Golgi. As CLN5 is reported to be located in lysosomes (Isosomppi et al., 2002; Vesa et al., 2002), it is consistent that siRNA against this protein would therefore not have an effect on the *cis*-Golgi.

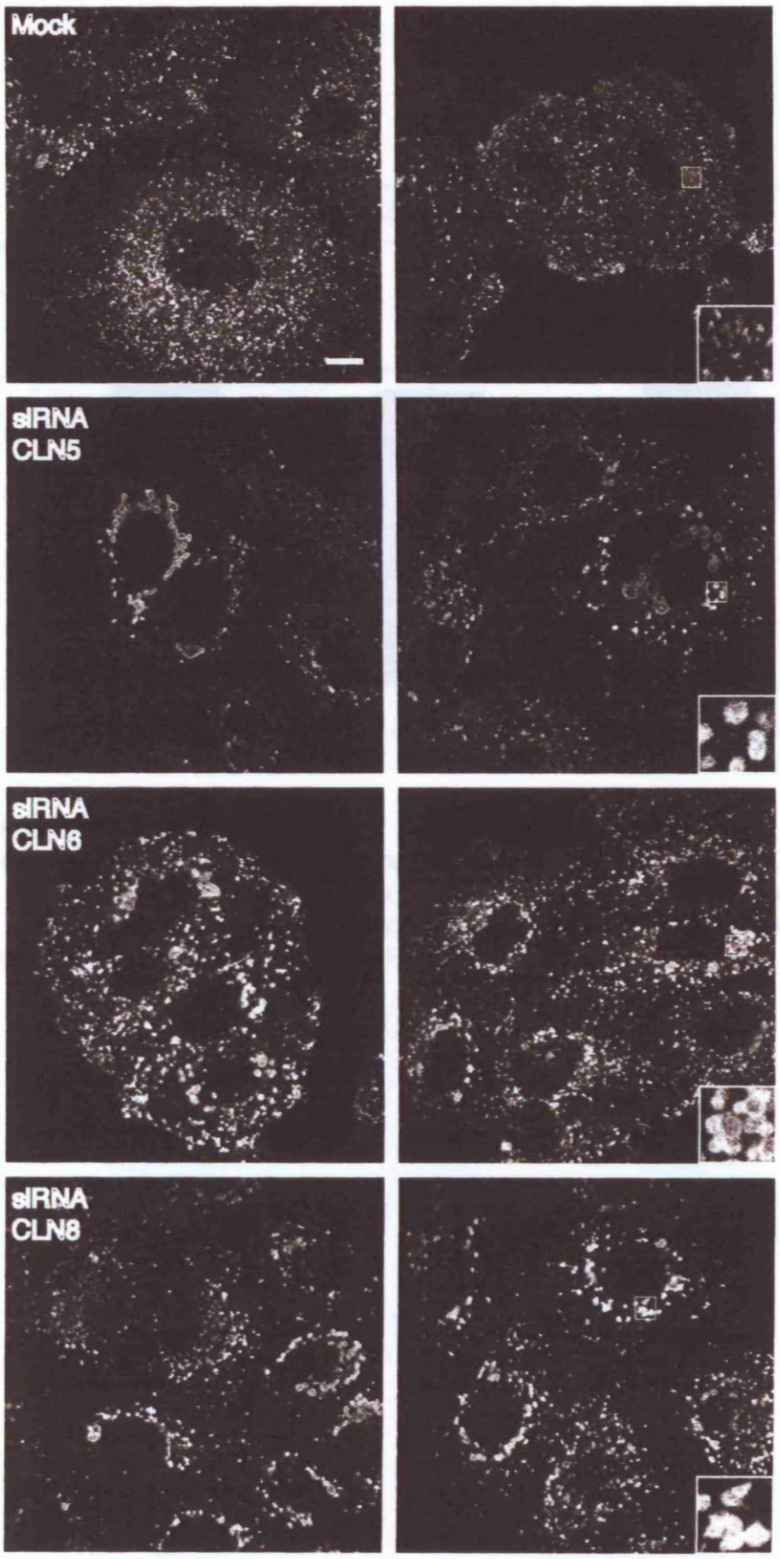

Figure 6.2.1.1: Lamp-1 staining of siRNA treated cells against CLN5, CLN6 and CLN8

HeLa cells were mock transfected and treated with siRNA against CLN5, CLN6 and CLN8. Immunofluorescence of Lamp-1 shows enlarged structures in siRNA treated samples. Bar, 10 µm.

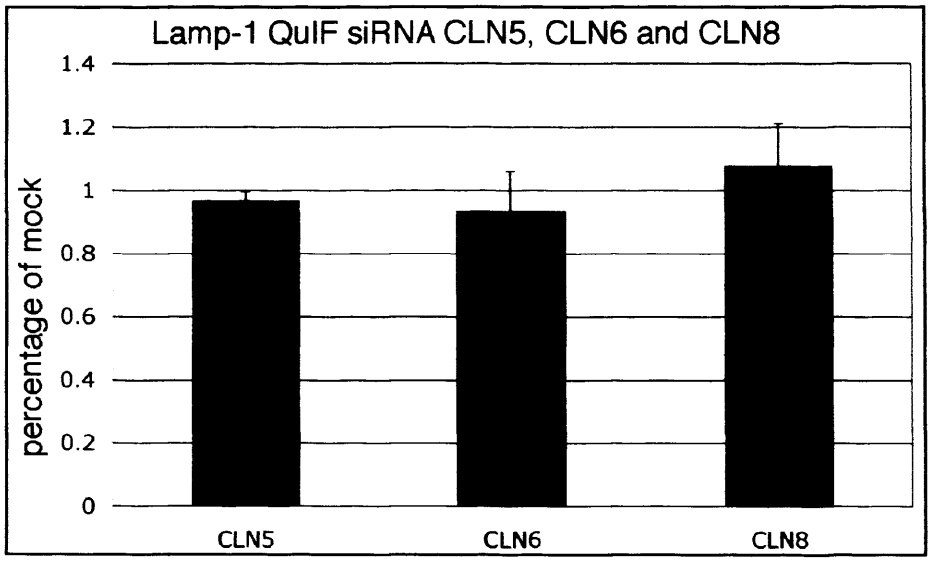

Figure 6.2.1.2: QuIF Lamp-1

HeLa cells were mock transfected and treated with siRNA against CLN5, CLN6 and CLN8. QuIF shows levels of integrated intensity compared to mock. There was no statistically significant change between mock and siRNA samples as determined by two-sample t-test (see appendix A).

A

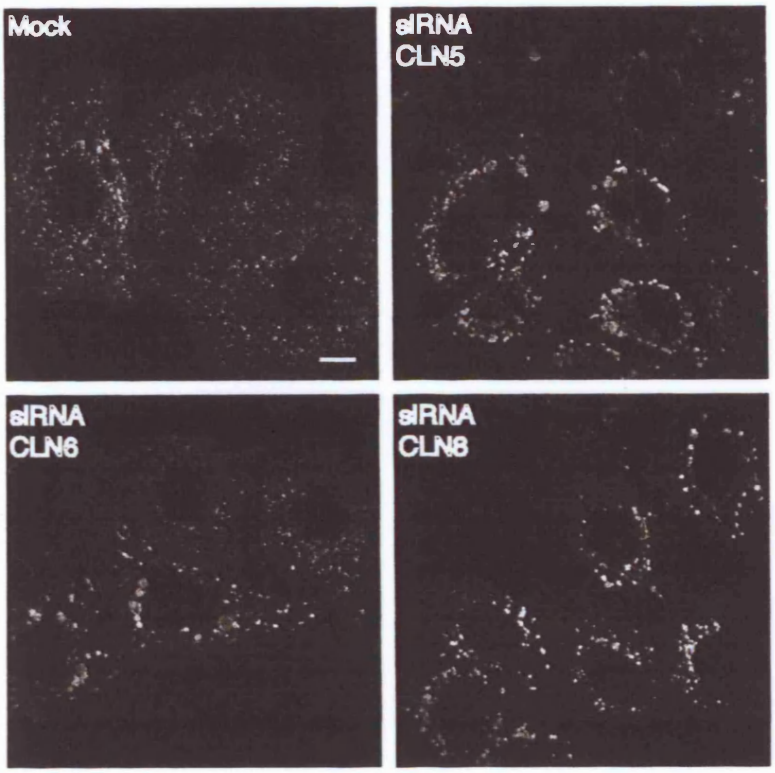

B

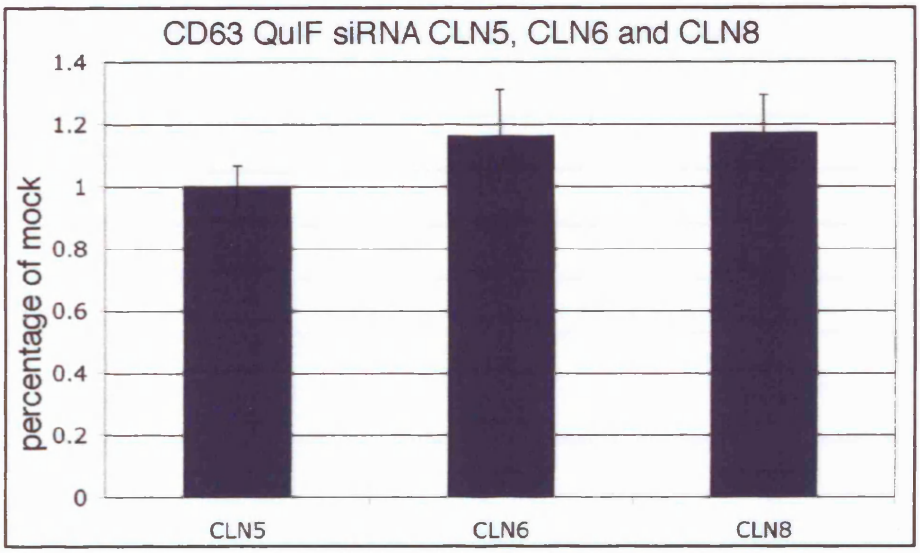

Figure 6.2.2: CD63 staining of siRNA treated cells against CLN5, CLN6 and CLN8

HeLa cells were mock transfected and treated with siRNA against CLN5, CLN6 and CLN8. (A) Immunofluorescence of CD63 shows enlarged structures in siRNA treated samples. Bar, 10 μm. (B) QuIF shows levels of integrated intensity compared to mock. There was no statistically significant change between mock and siRNA treated samples as determined by two-sample t-test (see appendix A).

A

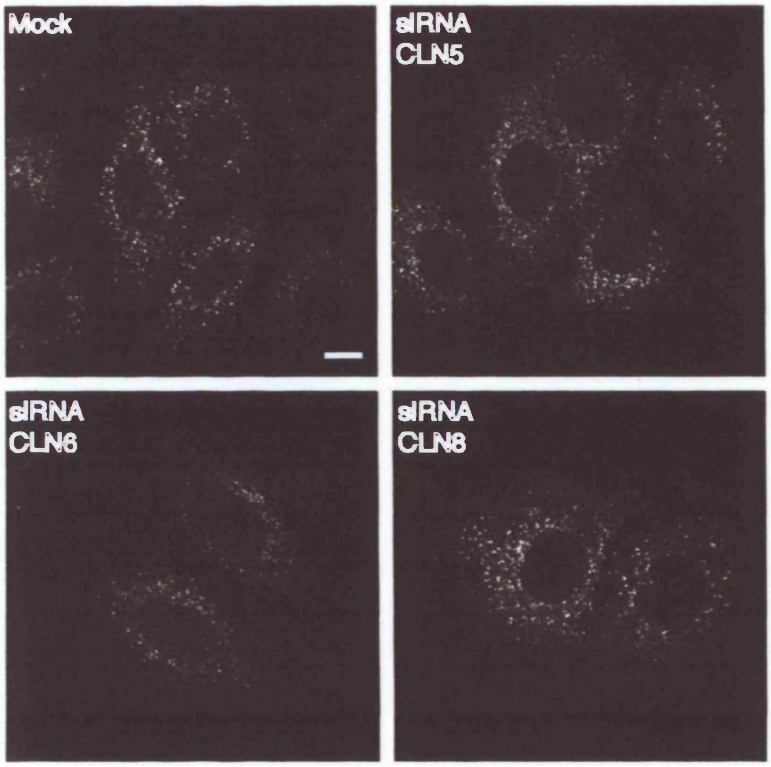

B

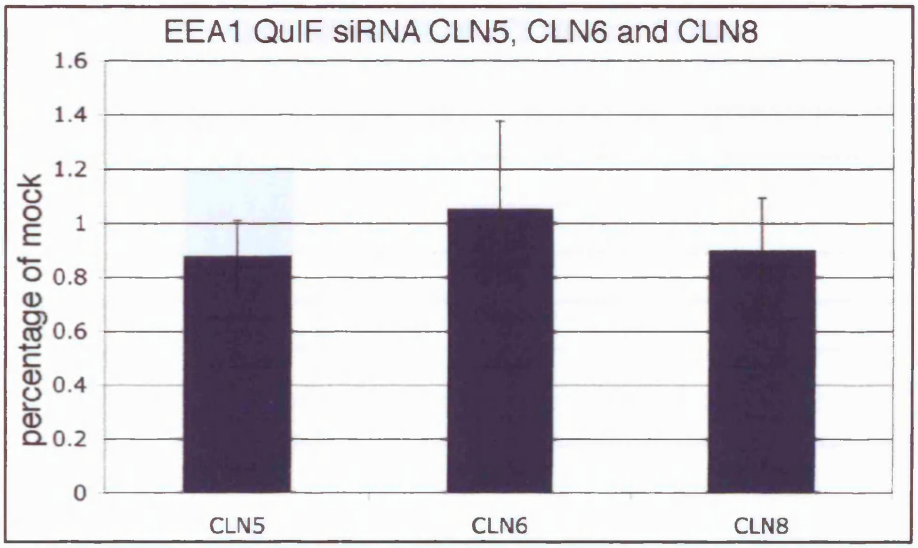

Figure 6.2.3: EEA1 staining of siRNA treated cells against CLN5, CLN6 and CLN8

HeLa cells were mock transfected and treated with siRNA against CLN5, CLN6 and CLN8. (A) Immunofluorescence of EEA1 shows no difference between mock and siRNA treated cells. Bar, 10 μm. (B) QuiF shows levels of integrated intensity compared to mock. There was no statistically significant change between mock and siRNA treated samples as determined by two-sample t-test (see appendix A).

A

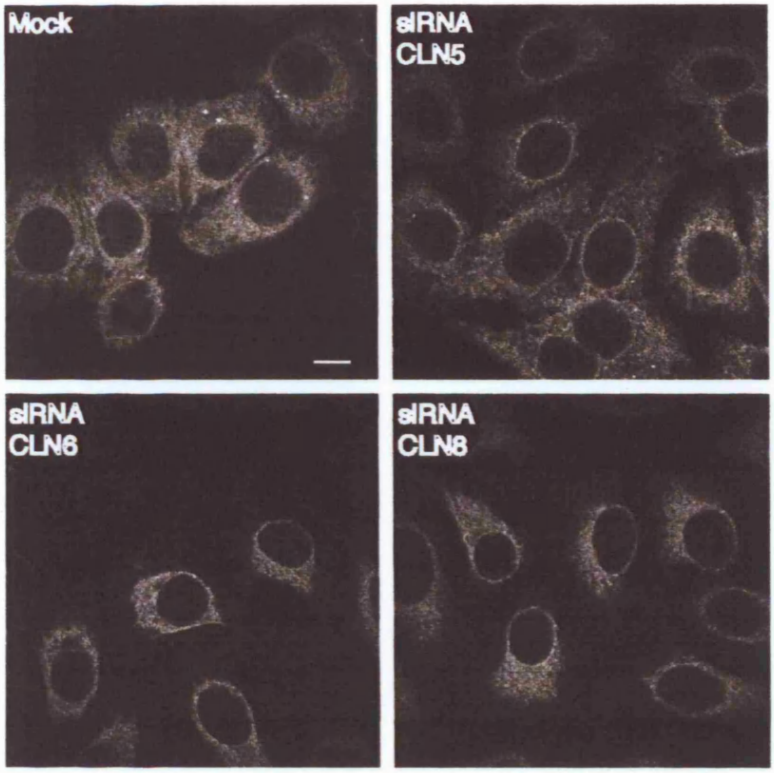

B

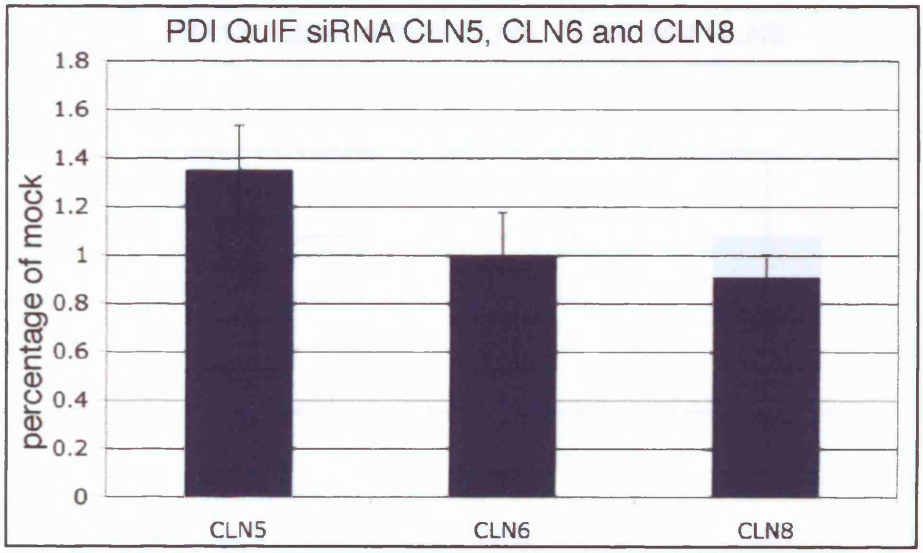

Figure 6.2.4: PDI staining of siRNA treated cells against CLN5, CLN6 and CLN8

HeLa cells were mock transfected and treated with siRNA against CLN5, CLN6 and CLN8. (A) Immunofluorescence of PDI shows no difference between mock and siRNA treated cells. Bar, 10 µm. (B) QuIF shows levels of integrated intensity compared to mock. There was no statistically significant change between mock and siRNA treated cells as determined by two-sample t-test (see appendix A).

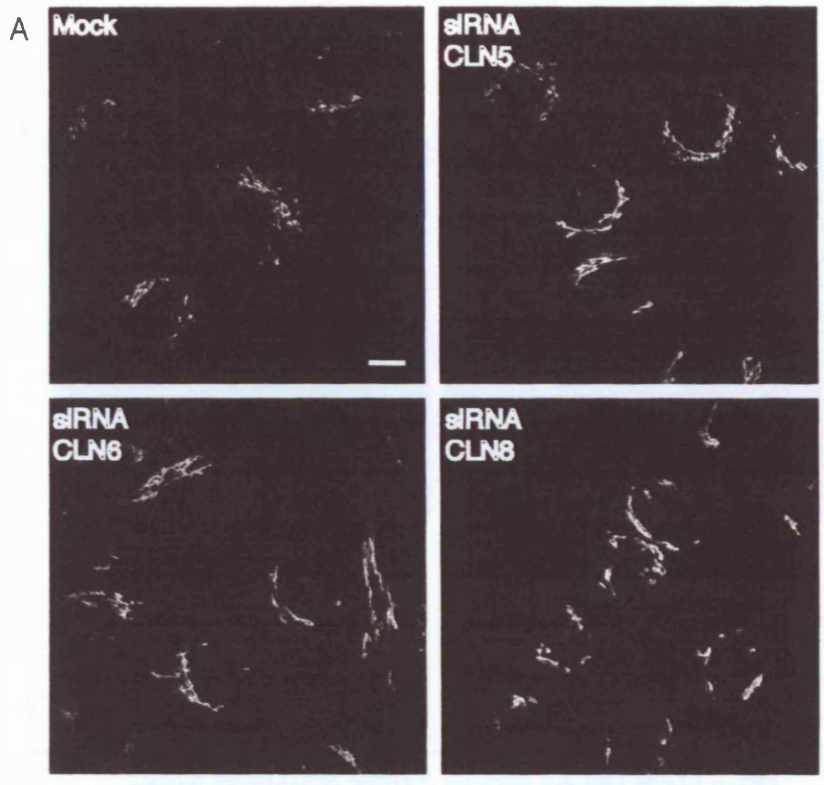

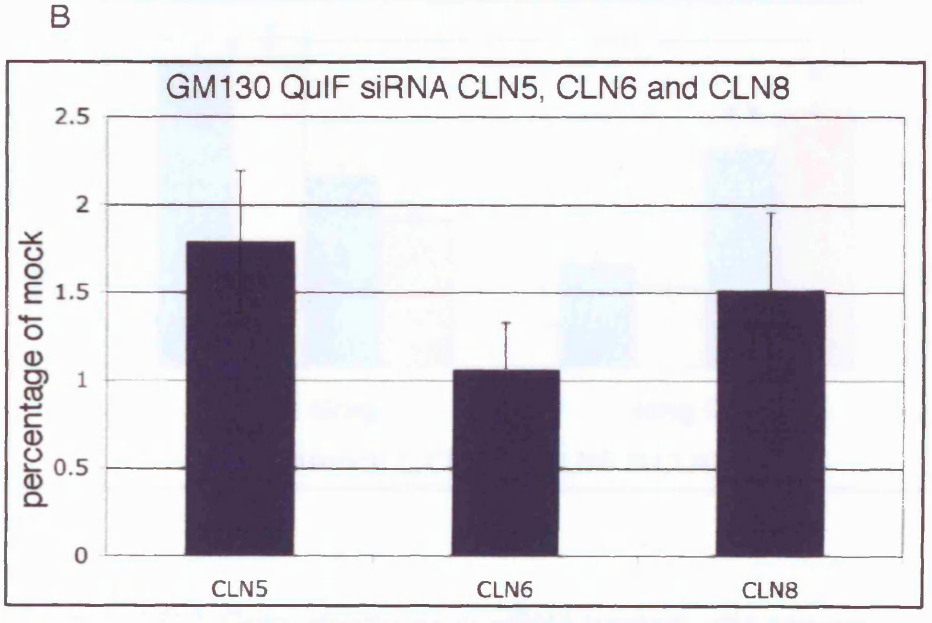

Figure 6.2.5.1: GM130 staining of siRNA treated cells against CLN5, CLN6 and CLN8

HeLa cells were mock transfected and treated with siRNA against CLN5, CLN6 and CLN8. (A) Immunofluorescence of GM130 shows short Golgi ribbons in mock and CLN5 depleted cells and long Golgi ribbons in CLN6 and CLN8 depleted cells. Bar, 10 μm. (B) QuIF shows levels of integrated intensity compared to mock. There was no statistically significant change between mock and siRNA treated samples as determined by two-sample t-test (see appendix A).

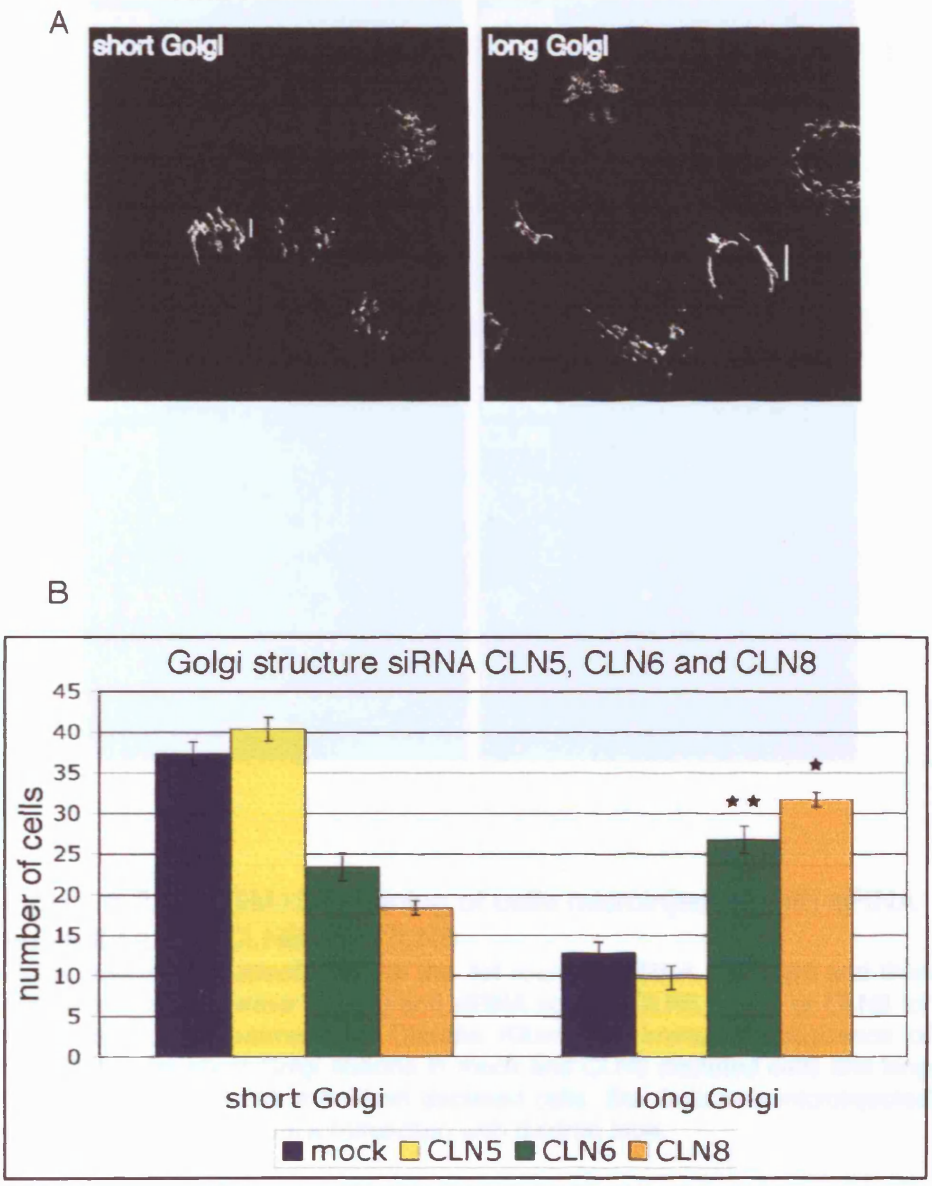

Figure 6.2.5.2: Golgi structures in siRNA treated cells against CLN5, CLN6 and CLN8

(A) Examples of Golgi structures counted as short, bar 5 µm, and long, bar 10 µm. (B) Number of cells containing short and long Golgi ribbons (3 x 50 cells counted per sample).p-values were determined by two-sample t-test compared to mock (see appendix A). One star $p > 0.05$, two stars $p > 0.01$.

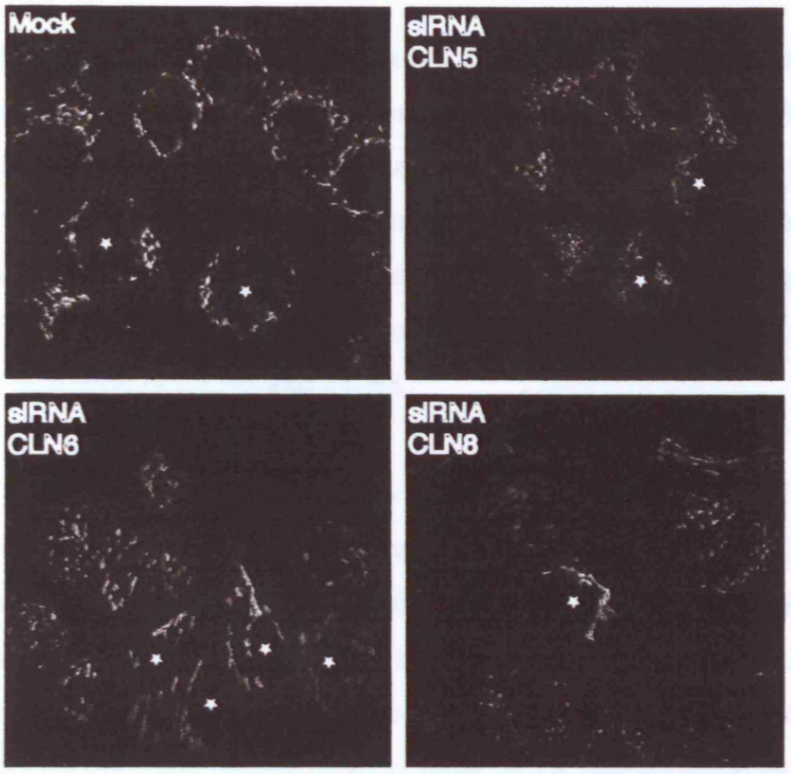

Figure 6.2.5.3: GM130 staining of cells microinjected with siRNA against CLN5, CLN6 and CLN8

HeLa cells were nucleofected for the 1st round of siRNA treatment and then microinjected with water (mock) and siRNA against CLN5, CLN6 or CLN8 for the 2nd round treatment by Claudia Kitzmuller. Immunofluorescence of GM130 shows short Golgi ribbons in mock and CLN5 depleted cells and long Golgi ribbons in CLN6 and CLN8 depleted cells. Star indicates microinjected cells as detected by co-microinjection with dextran blue.

6.3 Chapter 6 Summary

The siRNA screen of CLN5, CLN6 and CLN8 revealed two interesting changes in organelle morphology. There was an effect on the size and distribution of late endosomes and lysosomes in response to siRNA targeting all three proteins. The compartments became enlarged and more clustered in the perinuclear region. In response to siRNA against CLN6 and CLN8 but not CLN5 there appeared to be a specific effect on the structure of the *cis*-Golgi with more ribbons tending to be long on depletion of CLN6 and CLN8.

Future work within the laboratory will ensure the continuation of this project. Future work will focus on establishing more detailed knowledge of the different responses to depletion of CLN5, CLN6 and CLN8. These results will be put into a wider context by comparison with results from experiments of siRNA targeting of other NCL genes. Particular attention will focus on lysosomal morphology, as this may be a common feature of all or most NCLs, and on Golgi morphology, as this may be a mechanism specific to a subset of NCLs.

7. Discussion

7.1 Summary of findings

The aims of this project were to establish the tools and techniques necessary to analyse the CLN6 protein and to utilise these to investigate its subcellular location, to identify proteins that interact with CLN6 and to elucidate the early cellular responses to loss of functional vLINCL proteins, CLN5, CLN6 and CLN8.

It was first shown that a number of different techniques can be utilised to analyse CLN6. The endogenous protein can be detected by Western blotting, indirect immunofluorescence and immunoprecipitation using the purified peptide antibody 1747p. A construct of CLN6 fused to horseradish peroxidase (HRP) was cloned for localisation studies by indirect immunofluorescence and electron microscopy. CLN6 protein and mRNA levels could be successfully depleted using siRNA specific to CLN6 mRNA and this depletion assessed by Western blotting, indirect immunofluorescence and Q-PCR.

The subcellular localisation of CLN6 was investigated. CLN6 has been reported to be localised in the ER (Heine et al., 2004; Mole et al., 2004) and findings in this project were consistent with this. However, CLN6 did not co-localise with markers of ER exit sites or become specifically recruited into organised smooth ER structures when formation of these was induced by overexpression of GFP-cytochrome b(5). Furthermore, it was not possible to detect CLN6 within a sub-domain of the ER by indirect immunofluorescence or electron microscopy using the CLN6-HRP construct. The levels of wild-type or mutant CLN6 were not stabilised using proteasomal or lysosomal inhibitors, and the location of the proteins within the cell did not change under the conditions used. It was therefore not possible to locate CLN6 within a sub-compartment of the ER or in the lysosome and it was also not possible to show that wild-type or mutant CLN6 are degraded by ERAD.

CLN6 has been reported to exist as a dimer using overexpression and chemical cross-linking (Heine et al., 2004). Co-immunoprecipitation of endogenous CLN6

supported this, when a large amount of starting material was used. However, it was not possible to identify and confirm that other proteins bind to CLN6, even when different conditions including chemical cross-linkers were used.

Depletion of CLN5, CLN6 and CLN8 showed changes in the size and distribution of late endocytic compartments, resulting in enlarged structures positive for the late endosomal/lysosomal markers Lamp-1 and CD63, which were clustered in perinuclear regions. A change in the structure of the *cis*-Golgi was also observed in response to siRNA against CLN6 and CLN8 but not CLN5, resulting in an increase in cells with long ribbons positive for the *cis*-Golgi marker GM130. No changes were detected in early endosomal or ER structures in response to siRNA.

7.2 Localisation of CLN6

Proteins that are located within the ER can be involved in one or more of its different functions. A localisation within a specific sub-compartment of the ER may be indicative of these functions. During this project, data became available about the localisation of overexpressed CLN6 in neurons (Heine, et al. 2006, *in press*), which shows CLN6 in PDI-positive as well as in PDI-negative structures. This staining pattern further suggests that CLN6 is located within distinct regions of the ER, as has been previously reported for non-neuronal cells (Mole et al., 2004). It could also indicate a localisation for CLN6 specific to neuronal cells. If this was the case, it might implicate that CLN6 has an additional function in neurons.

7.2.1 Co-localisation study within the endoplasmic reticulum using immunofluorescence microscopy

CLN6 was proposed to be located within specific regions of the ER, as the immunofluorescence pattern of endogenous CLN6 appears less tubular than classic ER staining and co-localisation with ER markers is only partial (Mole et al., 2004). The immunofluorescence pattern of the ER exit site marker Sec24 is very similar to the one observed for CLN6, as it appears as distinct punctae distributed throughout the ER (Shimoi et al., 2005). CLN6 could have a function in recruitment of other NCL proteins to ER exit sites and thus regulate their trafficking through the ER. However, no co-localisation between endogenous CLN6 and overexpressed Sec24 was observed. It therefore seems unlikely that CLN6 is located in ER exit sites and that it has a function in COPII vesicle recruitment or cargo selection.

The immunofluorescence pattern of low overexpression of GFP-cytochrome b(5) closely resembles the immunofluorescence pattern of CLN6 (Snapp et al., 2003). Organised smooth ER (OSER) structures, formation of which can be induced by overexpression of cytochrome b(5), have been implicated in diseases such as Charcot-Marie-Tooth syndrome and early onset torsion dystonia (Dickson et al.,

2002; Hewett et al., 2000). It is possible that similar structural defects of the ER exist in CLN6 patients, however, no data has been published to date. Therefore it was investigated whether CLN6 is preferentially recruited into OSER, since this may suggest a role for CLN6 in the maintenance of ER structure. There was no indication that CLN6 was recruited into OSER structures preferentially to the ER marker PDI, indicating that CLN6 becomes incorporated into OSER by bulk recruitment of ER membrane. This data therefore indicates that CLN6 does not have a role in the formation of OSER. However, it may be possible that it has another function in the maintenance of the structural integrity of the ER.

7.2.2 CLN6-HRP distribution within the endoplasmic reticulum

The experiments using the CLN6-HRP construct by indirect immunofluorescence indicated that the construct localises to the ER but most likely not in the same distribution pattern as endogenous CLN6. At the ultra-structural level, the construct was located throughout the entire ER. It is therefore difficult to directly compare the localisation results of the overexpressed construct to those of the endogenous protein. Modification of the construct will be necessary and suggestions for this were made in chapter 4.2.

7.2.3 CLN6 trafficking in response to lysosomal and proteasomal inhibitors

The use of lysosomal inhibitors did not show a change in the localisation of wild-type or mutant CLN6, suggesting that CLN6 does not exit the ER. This indicates that CLN6 does not have a function in the lysosome but that it most likely has a function in the ER that impacts on lysosome function. This data is consistent with published results about the location of CLN6 in the ER (Heine et al., 2004; Mole et al., 2004).

The use of proteasomal inhibitors did not show a stabilisation of the protein levels of wild-type or mutant CLN6. It was proposed that mutant or misfolded CLN6 at least should be degraded by ERAD as is the case with many misfolded

proteins such as wild-type and mutant forms of the cystic fibrosis transmembrane conductance regulator (CFTR) (Sun et al., 2006; Zhang et al., 2001). However, this data showed that wild-type and mutant CLN6 used in the experiment were not degraded by ERAD. It is of course possible that the mutant protein misfolds and aggregates in the ER. However, no changes in the appearance of the ER, such as increased amounts of OSER, have been observed at the ultra-structural level when these cells were analysed by electron microscopy (data not shown).

There is no data published about the half-life of wild-type CLN6, although siRNA experiments show a reduction in protein levels after two days of treatment with siRNA, suggesting that the protein is actively turned over in this time period. It would therefore be expected that two days of treatment with proteasomal inhibitors should show an increase in protein levels if the protein was degraded by the proteasome. However, as discussed in chapter 4.3, the cells were severely affected by the treatment with the inhibitor. There was also no positive control in this experiment, such as another protein known to be degraded by ERAD, whose protein levels were increased after inhibitor treatment. It would therefore be necessary to optimise the conditions and repeat the experiment in order to elucidate the degradation of wild-type and mutant CLN6, and technical suggestions for this have been described in chapter 4.3.

7.2.4 Future work

The ER is a very versatile organelle and its structure and specialised functions differ between cell types. The following experiments are proposed to further investigate the localisation of endogenous CLN6:

The localisation of endogenous and overexpressed CLN6 could be further investigated using indirect immunofluorescence in different cell types. These experiments should include the use of specialised cell types such as polarised cells, hepatocytes with a large proportion of smooth ER, and neurons or neuroblastoma cell lines. This would help clarify whether there is a differential distribution of CLN6 in different cell types.

Further co-localisation studies could be performed using other markers for different ER functions. This could be done in different cell types to further investigate whether CLN6 has a differential distribution dependent on cell type.

The CLN6-HRP construct should be further improved. Technical suggestions for this were described in chapter 4.2. If the construct could be expressed more efficiently, it may be possible to clarify its location within the ER at the ultra-structural level. This would help to elucidate the location and function of CLN6.

The proteasomal inhibitor treatment of fibroblast cell lines from CLN6 patients should be repeated. The concentration of the inhibitor should be optimised to minimise cell death and positive controls included in the experiment.

7.3 CLN6 binding partners

It was proposed that by identifying proteins that interact with CLN6 it might be possible to elucidate its function. There are different approaches to analyse this, such as yeast-two-hybrid screens, GST-pull down experiments and others. Immunoprecipitation of the endogenous protein was successful. It was therefore decided to use this technique as it captures the protein in its natural intracellular environment. However co-immunoprecipitation of CLN6 with other proteins proved very challenging. Two different approaches were used. The first one used a large amount of starting material, as it was difficult to detect CLN6 by silver staining when less starting material was used. This method successfully identified CLN6 as the protein of the correct molecular weight detected by Western blotting. It further indicated that CLN6 may bind to itself which has been reported for the overexpressed protein (Heine et al., 2004). However, other proteins identified by this method could not be confirmed as interactors of CLN6. The large amount of starting material most likely resulted in non-specific binding of these proteins to the antibody or the magnetic beads. The amount of starting material was reduced and chemical cross-linkers used to strengthen the physical interaction between CLN6 and proteins that bind to it, as this technique had been used to show the dimerisation of overexpressed CLN6 (Heine et al., 2004). Interestingly, a dimer of endogenous CLN6 could never be detected by Western blotting even after cross-linking (data not shown). It is possible that only a small population of endogenous CLN6 dimerises, making it difficult to detect the dimeric complex. It was further reported that regions in both the N- and C-termini of the protein are implicated in dimerisation (Heine, et al., 2006, *in press*). As the antibody recognises the first fifteen amino acids of the N-terminal of the protein, it may be that the ability of the antibody to detect the dimer is greatly reduced due to steric interference.

It was also not possible to identify and confirm interacting proteins when chemical cross-linkers were used. It is possible that the amount of starting material used in the second and third co-immunoprecipitations experiments was too low, which could be further optimised by using increasing amounts of cells.

However, other technical difficulties were encountered. The contamination of most bands in the second co-immunoprecipitation experiment with keratin meant that although interacting proteins may have been present in the bands, they could not be identified. In the third co-immunoprecipitation experiment there was no contamination but only two bands could be identified. However HSP70 has been shown by Western blotting not to be enriched after co-immunoprecipitation of CLN6, as the antibody that recognises mtHSP75 cross-reacts with HSP70. It was further shown that CLN6 does not interact with alpha, beta or gamma actin using an antibody that detects all three isoforms.

From these data it is clear that this technique must be optimised if interactors are to be successfully identified using this method. In this context, the following could be tested:

The amount of starting material used in combination with cross-linkers should be further optimised. Different numbers of cells should be used to find the lowest amount necessary that would allow positive identification of bands while keeping the amount of non-specific binding to a minimum.

Different detergents could be used to test if other interacting proteins can be identified. Some proteins are easily solubilised in one detergent but not in another or require the addition of other reagents to be successfully detected. For example, the ER protein ribophorin I can only be detected when 0.6% SDS is added to the Triton-X lysate (de Virgilio et al., 1998)(C. Kitzmüller, *personal communication*). Furthermore, proteins that are post-translationally modified might be more difficult to detect. For example, proteins that are glycosylated are often seen as a smear of many bands when detected by Western blotting, as is the case for CLN3 (Storch et al., 2004)(C. Kitzmüller, *personal communication*). It might be possible that these smears are more difficult to see than distinct bands when visualised by silver staining. In the case of glycosylated proteins, the co-immunoprecipitated samples could be deglycosylated prior to running them on gels.

If CLN6 interacts with other NCL proteins, it may be very difficult to detect this interaction using endogenous proteins, as some NCL proteins, such as CLN3, are expressed at very low levels (C. Kitzmüller, *personal communication*). Indeed CLN6 and CLN5 are the only human NCL proteins that have been reported to be detected at their endogenous expression levels (Bessa et al., 2006; Mole et al., 2004). Although CLN6 has been reported not to interact with CLN8 (Heine, et al., 2006, *in press*), it is possible that CLN6 could interact with other NCL proteins and perhaps have a function in their transit through the ER. These interactions may be better investigated using overexpressed NCL proteins to facilitate their detection. However, there are disadvantages associated with overexpressing proteins for this purpose. If proteins are expressed at high levels to ease their detection, it is possible that they aggregate or do not integrate into their intracellular environment correctly. This is especially true if proteins are tagged, as the addition of the tag may prevent correct folding or integration into multimeric complexes (Bauer and Kuster, 2003). Thus interactions may be detected which occur as a result of overexpression. It would therefore have to be proven that interactions detected this way are physiologically relevant.

It is also possible that CLN6 does not bind to another protein. It could bind to lipids, which could be tested using a lipid overlay assay. Furthermore it may form a channel and therefore only bind to itself. In this case the properties of dimeric or multimeric CLN6 should be further investigated.

In conclusion, there are many possibilities to optimise the co-immunoprecipitation of endogenous CLN6 with interacting proteins. Future work should certainly focus on this, as elucidation and clarification of proteins that bind to CLN6 would greatly further the understanding of its function.

7.4 siRNA screen of vLINCL proteins

7.4.1 Lamp-1 and CD63

Depletion of the vLINCL proteins showed an increase in the size and a redistribution into perinuclear regions of late endocytic compartments positive for Lamp-1 and CD63. It was postulated that there may be an effect on late endocytic structures in response to reduced protein levels, as this is the site of the accumulation of storage material. It was surprising that this effect was so immediate and so striking as the onset of vLINCL symptoms in patients does not occur until late infancy. From this it can be postulated that a change in the structure and distribution of the lysosome is present throughout the development of vLINCL patients, long before the onset of symptoms. In fact, it was recently reported that in the brains of OCL6 sheep, the South Hampshire sheep model of CLN6, neurodegeneration occurs before the onset of symptoms (Oswald et al., 2005).

The question that then arises is how this change in size and distribution of the late endocytic compartments is caused and how it relates to the accumulation of storage material and the pathological effect on the neurons in patients. It is likely that a change in size and distribution of the lysosomes is accompanied by a defect in function, which could result in an accumulation of undegraded material in the lysosomes. However, as the onset of pathological changes in not immediate and only a sub-set of cell types are affected by this, it can be assumed that most cells can tolerate the structural lysosomal defect. Two different possibilities can be considered to explain the neuropathology:

It can be postulated that the change in size and distribution of the lysosomes and the accumulation of the storage material may not necessarily be the cause of the neurodegeneration, and that neuronal cell death may occur via a cell-type specific effect related to an effect on lysosome function. Indeed glial activation in the South Hampshire OCL6 sheep was observed independently of the storage

material (Oswald et al., 2005). However, it is also possible that neurons are simply more susceptible to metabolic changes and are therefore more affected by the storage accumulation and the effect on lysosome function. It can therefore be postulated that the pathological effect of the storage is first observed in the neurons and that the patients do not live long enough for pathological changes to occur in other cell types.

The following questions could be addressed to further elucidate this:

Is the lysosomal function compromised at the same time as the changes in size and distribution are observed? It has been reported that the activities of cathepsin D, beta-hexosaminidase, arylsulfatase A and TPP-I were normal in fibroblast cell lines from CLN6 patients (Heine et al., 2004; Sohar et al., 1999). It would therefore be expected that the activities of these enzymes would also be unaffected after siRNA treatment. However, in brain samples from CLN3 patients the levels of TPP-I were reported to be increased although it was indicated that some of this was enzymatically inactive. Therefore other lysosomal hydrolases should be tested after depletion of CLN5, CLN6 and CLN8 to clarify this question as a defect in lysosomal hydrolase activity would result in an accumulation of undegraded material as has been reported for many LSDs (Futerman and van Meer, 2004).

Is there a change in pH? Elevated lysosomal pH levels have been reported for fibroblast cell lines from CLN5, CLN6 and CLN8 patients (Holopainen et al., 2001). It could therefore be expected that the pH of lysosomes in cells depleted of the vLINCL proteins should also increase. Changes in cytoplasmic pH have been shown to influence the distribution and size of lysosomes. As the cytoplasmic pH was lowered, lysosomes moved towards the cell periphery and became smaller (Heuser, 1989). It is possible that depleting cells of CLN5, CLN6 or CLN8 results in an increase in intra-lysosomal pH and the change in size and distribution of lysosomes occurs as a secondary event. Therefore, lysosomal pH should be monitored to establish the earliest cellular events that occur after depletion of vLINCL proteins.

Is there an accumulation of autofluorescent material? Autofluorescence was not observed in any of the siRNA experiments conducted. However, it may be that autofluorescent material would accumulate over time. For this an inducible RNAi system where cells are stably transfected with an RNAi vector that can be activated over longer periods of time would be necessary. It could then be possible to follow the accumulation of autofluorescent material over time and correlate this with any other cellular changes that might occur.

Are the effects similar in neurons from the vLINCL mouse models? In order to find out if the changes observed in the siRNA experiments are physiologically relevant, it would be possible to test whether neurons from the *nclf*, the *mnd* and the Cln5-/- mouse models show similar changes in late endocytic structures.

Another important implication can be drawn from the siRNA experiments. The effect on late endocytic structures was the same when siRNA was used against the vLINCL proteins CLN5, CLN6 and CLN8 as well as against CLN3 (C. Kitzmüller, *personal communication*). This may indicate a functional relationship between these and potentially between other NCL proteins on a common pathway. To further investigate this, the following experiment could be performed:

Is there an additive effect when more than one NCL protein is targeted by siRNA? The use of combinations of siRNAs against two or more proteins at the same time could answer this question. It may be postulated that if proteins are involved in the same cellular pathway, then depleting one should have the same effect as depleting more than one, as this pathway would already be disturbed. However, if there was an additive effect, this may indicate an involvement in separate pathways. It would however have to be taken into consideration that NCL proteins could have more than one function, as has been suggested for CLN3 (C. Kitzmüller, R. Haines, S. Mole, *personal communication*). Therefore, additional effects upon protein depletion may still indicate that the proteins are involved in the same cellular pathway but that they also have other functions that are not related.

7.4.2 GM130

In response to depletion of CLN6 and CLN8 but not CLN5, there was a change in the structure of *cis*-Golgi ribbons, resulting in an increase of long GM130-positive structures. This result is interesting because it shows for the first time a difference in cellular phenotype between the ER located vLINCL proteins and the lysosomal vLINCL protein CLN5. There are no reports of abnormal Golgi in vLINCL patients to date, however it is unclear whether this has been investigated in detail. It therefore remains to be determined how this phenomenon contributes to the vLINCL phenotype. The following could be addressed to elucidate this in greater detail:

Is there a change in rate of collapse/reassembly of the *cis*-Golgi when CLN6 and CLN8 are depleted? The Golgi can be formed *de novo* from constituents of the ER. These leave the ER via ER exit sites and mature into ERGIC structures, which then fuse to form the *cis*-Golgi (Altan-Bonnet et al., 2004; Puri and Linstedt, 2003). If CLN6 or CLN8 had a function in Golgi biogenesis or maintenance, there may be changes in the collapse or reassembly of the Golgi when the proteins are depleted. This could be assayed using the drug brefeldin A (BFA), which inhibits Sar1, a key protein involved in the formation of ER exit sites, and relocalises most Golgi proteins to the ER upon drug treatment (Altan-Bonnet et al., 2004; Peyroche et al., 1999). After the drug is removed, the rate of reassembly of Golgi components can then be measured. The dynamics of this could be compared between mock and CLN6- or CLN8-depleted cells. This would help to establish if CLN6 or CLN8 have a function in the formation or maintenance of the Golgi.

Is there a change in actin recruitment at the Golgi? Actin filaments have been implicated in the positioning and morphology of the Golgi complex as well as in retrograde traffic from the Golgi to the ER (Valderrama et al., 1998; Valderrama et al., 2001). The Rho GTPase Cdc42 has been implicated in regulating actin assembly on Golgi membranes and microinjection of a constitutively active Cdc42 mutant resulted in longer *cis*-Golgi ribbons (Matas et al., 2005). These

closely resemble the long ribbons seen upon depletion of CLN6 and CLN8. However, it was shown in chapter 5.3 that CLN6 does not interact directly with alpha, beta or gamma actin. It is possible that CLN6 interacts with a protein that in turn interacts with actin. It is further possible that CLN8 binds to actin. Both beta- and gamma-actin have been reported to localise to Golgi structures and COPI-coated vesicles (Valderrama et al., 2000). It could therefore be postulated that CLN6 and CLN8 are involved in an actin-mediated process of retrograde traffic or maintenance of Golgi structure, a disruption of which could result in the morphological changes observed after depletion of CLN6 and CLN8. To further investigate this, actin dynamics at the Golgi after siRNA treatment could be analysed.

Is there a change in the rate of protein traffic through the Golgi? The structural changes observed after depletion of CLN6 and CLN8 may directly influence the rate at which proteins traffic through the ER. The rate of traffic through the Golgi varies greatly and can be in the range of 1 min to 60 min (Altan-Bonnet et al., 2004). A structural change could have an effect on the rate of traffic of all proteins or perhaps of a subset of proteins. This could be assayed using time-lapse microscopy following the trafficking of tagged overexpressed proteins. This experiment would establish whether depletion of CLN6 or CLN8 have a direct effect on protein trafficking through the Golgi. It would be particularly interesting to follow the trafficking of other NCL proteins to test whether depletion of CLN6 or CLN8 has a direct effect on this. This could further the understanding of the relationship of different NCL proteins to each other.

Is there a change in the rate of lipid traffic through the Golgi? CLN8 has been reported to belong to the TLC family of proteins and has been implicated in lipid metabolism (Winter and Ponting, 2002). It is possible that depletion of CLN8 results in a disturbance of lipid metabolism that leads to a change in Golgi structure. Dilated *trans*-Golgi structures have been reported in Tangier disease (Robenek and Schmitz, 1991). This disorder is caused by mutations in the adenosine triphosphate (ATP)-binding cassette transporter A1 (ABCA1), which is implicated in lipid trafficking, and manifests with the storage of cholesteryl

esters in reticuloendothelial tissues and peripheral neuropathy (Kolovou et al., 2006). These defects are thought to be caused by low plasma levels of high-density lipoprotein cholesterol (HDL-C). It has been reported that ABCA1 plays a role in the trafficking of cholesterol and phospholipids from the Golgi and late endosomes to the plasma membrane (Neufeld et al., 2004; Orso et al., 2000). Interestingly, late endosomes but not lysosomes of fibroblast cell lines from Tangier disease patients have been shown by electron microscopy to be enlarged (Neufeld et al., 2004; Robenek and Schmitz, 1991). Similarly, it may be possible that the depletion of CLN8 may have an effect on lipid trafficking or homeostasis. Abnormalities in sphingo- and phospholipid profiles have been reported in brain tissue from CLN8 patients (Hermansson et al., 2005). This should be further investigated. Fluorescently labelled lipids or lipid analogues could be used to analyse lipid trafficking and intracellular distribution upon depletion of CLN8. Although no involvement of CLN6 in lipid metabolism has been proposed to date, it is possible that CLN6 may have a function in this as depletion of CLN6 shows the same effect on the Golgi as depletion of CLN8, and experiments should therefore be performed on both proteins. It is however possible that CLN6 and CLN8 affect the Golgi through different mechanisms that result in the same phenotype. Elucidation of this would provide an understanding of whether CLN6 and CLN8 are involved in lipid metabolism or trafficking and establish whether this is involved in the vLINCL disease phenotype.

7.5 Possible functions of CLN6

As CLN6 is a protein of unknown function, the processes it is involved in are unknown. Examining the data presented in this thesis, the following mechanism of action for CLN6 can be proposed:

The CLN6 protein has a role in trafficking of other proteins and/or lipids through the ER and/or a role in Golgi to ER or ER to Golgi trafficking

7.5.1 Trafficking of proteins or lipids

CLN6 could be involved in the traffic of other proteins through the ER. This could especially be the case for other NCL proteins, such as CLN3 and CLN5. It is also possible that CLN6 has a function in trafficking certain lipids. If the function of CLN6 is compromised, then these proteins or lipids may traffic more slowly or aberrantly. It is feasible that the functions of CLN6 and CLN8 are interlinked, even if they do not interact directly. Thus, if one is mutated, this might have an effect on the other protein. The result of this could be that the proteins or lipids being trafficked are disturbed in their homeostasis. Abnormalities in lipid profiles have indeed been reported in CLN8 patients (Hermansson et al., 2005). Furthermore if CLN6 and CLN8 affect the trafficking of the lysosomal proteins CLN3 and CLN5 this could explain the lysosomal phenotype observed in vLINCL.

7.5.2 Golgi to ER or ER to Golgi traffic

As there is a change in the structure of the *cis*-Golgi when CLN6 is depleted, it is possible that this protein has a functional link with the Golgi. This could either be through an actin-mediated pathway or through a lipid trafficking pathway. The same can be proposed for CLN8. If these proteins are mutated or depleted, the Golgi could be directly affected. This could then either lead to a secondary effect in the lysosome through a change in the rate of trafficking of lysosomal

components, especially CLN3 and CLN5, or of lipid components. It is also possible that retrograde traffic from the ER to the Golgi is affected when CLN6 is not present. This may lead to disturbances in lipid trafficking and perhaps in an accumulation of proteins in the *cis*-Golgi, unable to be retrieved to the ER. This may explain the increase in long Golgi ribbons observed upon depletion of CLN6 and CLN8. It may also indicate a secondary effect on traffic from the Golgi to the lysosome.

7.6 Summary and Conclusions

As part of the thesis it was investigated whether CLN6 is located within a sub-compartment of the ER, whether CLN6 binds to other proteins and what cellular responses occur when the vLINCL proteins CLN5, CLN6 and CLN8 are depleted. It was not possible to locate CLN6 within a sub-compartment of the ER, however it was shown that CLN6 does not traffic to the lysosome. Wild-type and mutant CLN6 were not found to be degraded by ERAD. It was not possible to identify proteins that bind to endogenous CLN6 in co-immunoprecipitation experiments other than CLN6 itself. After depletion of CLN5, CLN6 and CLN8 a change in the size and distribution of late endocytic compartments was observed, which indicates that these compartments are affected immediately when the vLINCL proteins are absent. Furthermore, in response to depletion of CLN6 and CLN8 but not CLN5, an increase in the number of cells with long *cis*-Golgi ribbons was observed, indicating a difference in the cellular response to depletion of the ER-resident vLINCL proteins CLN6 and CLN8 and the lysosomal vLINCL protein CLN5.

The tools and techniques to analyse the CLN6 protein have been established and will provide a basis for future investigation. Using a derivative of the CLN6-HRP construct, it may be possible to locate CLN6 at the ultra-structural level and draw conclusions about its localisation within the ER. The identification of proteins that bind to CLN6 will provide an insight into the function of the protein, and this should be further investigated applying complementary techniques to these used here, especially with regard to interactions between CLN6 and other NCL proteins. Using RNAi experiments it was successfully shown that loss of the vLINCL proteins has an immediate effect on late endocytic compartments, implicating this as one of the earliest steps that occur in vLINCL pathogenesis and possibly a common phenomenon in NCL. The challenge for future investigations will be to further dissect the mechanism that leads to the effect on late endocytic compartments. It will also be necessary to establish whether there is a functional link between events in the Golgi and in late endocytic compartments when CLN6 or CLN8 are absent. The identification

of the early cellular events that occur in the different types of vLINCL will enhance the understanding of this disease and the mechanisms that causes it.

References

Ahtiainen, L., O.P. Van Diggelen, A. Jalanko, and O. Kopra. 2003. Palmitoyl protein thioesterase 1 is targeted to the axons in neurons. *J Comp Neurol.* 455:368-77.

Altan-Bonnet, N., R. Sougrat, and J. Lippincott-Schwartz. 2004. Molecular basis for Golgi maintenance and biogenesis. *Curr Opin Cell Biol.* 16:364-72.

Anderson, G., V.V. Smith, M. Malone, and N.J. Sebire. 2005. Blood film examination for vacuolated lymphocytes in the diagnosis of metabolic disorders; retrospective experience of more than 2,500 cases from a single centre. *J Clin Pathol.* 58:1305-10.

Antonny, B., and R. Schekman. 2001. ER export: public transportation by the COPII coach. *Curr Opin Cell Biol.* 13:438-43.

Appenzeller, C., H. Andersson, F. Kappeler, and H.P. Hauri. 1999. The lectin ERGIC-53 is a cargo transport receptor for glycoproteins. *Nat Cell Biol.* 1:330-4.

Awano, T., M.L. Katz, P. O'Brien D, I. Sohar, P. Lobel, J.R. Coates, S. Khan, G.C. Johnson, U. Giger, and G.S. Johnson. 2006a. A frame shift mutation in canine TPP1 (the ortholog of human CLN2) in a juvenile Dachshund with neuronal ceroid lipofuscinosis. *Mol Genet Metab.* 89: 254-60

Awano, T., M.L. Katz, D.P. O'Brien, J.F. Taylor, J. Evans, S. Khan, I. Sohar, P. Lobel, and G.S. Johnson. 2006b. A mutation in the cathepsin D gene (CTSD) in American Bulldogs with neuronal ceroid lipofuscinosis. *Mol Genet Metab.* 87:341-8.

Bannykh, S.I., T. Rowe, and W.E. Balch. 1996. The organization of endoplasmic reticulum export complexes. *J Cell Biol.* 135:19-35.

Barlowe, C., L. Orci, T. Yeung, M. Hosobuchi, S. Hamamoto, N. Salama, M.F. Rexach, M. Ravazzola, M. Amherdt, and R. Schekman. 1994. COPII: a membrane coat formed by Sec proteins that drive vesicle budding from the endoplasmic reticulum. *Cell.* 77:895-907.

Barr, F.A., M. Puype, J. Vandekerckhove, and G. Warren. 1997. GRASP65, a protein involved in the stacking of Golgi cisternae. *Cell.* 91:253-62.

Bauer, A., and B. Kuster. 2003. Affinity purification-mass spectrometry. Powerful tools for the characterization of protein complexes. *Eur J Biochem.* 270:570-8.

Bernstein, E., A.A. Caudy, S.M. Hammond, and G.J. Hannon. 2001. Role for a bidentate ribonuclease in the initiation step of RNA interference. *Nature.* 409:363-6.

Bessa, C., C.A. Teixeira, M. Mangas, A. Dias, M.C. Sa Miranda, A. Guimaraes, J.C. Ferreira, N. Canas, P. Cabral, and M.G. Ribeiro. 2006. Two novel CLN5 mutations in a Portuguese patient with vLINCL: Insights into molecular mechanisms of CLN5 deficiency. *Mol Genet Metab.* 89: 245-53

Bhattacharyya, T., A.N. Karnezis, S.P. Murphy, T. Hoang, B.C. Freeman, B. Phillips, and R.I. Morimoto. 1995. Cloning and subcellular localization of human mitochondrial hsp70. *J Biol Chem.* 270:1705-10.

Blatch, G.L., and M. Lassle. 1999. The tetratricopeptide repeat: a structural motif mediating protein-protein interactions. *Bioessays.* 21:932-9.

Bonsignore, M., A. Tessa, G. Di Rosa, F. Piemonte, C. Dionisi-Vici, A. Simonati, F. Calamoneri, G. Tortorella, and F.M. Santorelli. 2006. Novel CLN1 mutation in two Italian sibs with late infantile neuronal ceroid lipofuscinosis. *Eur J Paediatr Neurol.* 10:154-6.

Bronson, R.T., L.R. Donahue, K.R. Johnson, A. Tanner, P.W. Lane, and J.R. Faust. 1998. Neuronal ceroid lipofuscinosis (nclf), a new disorder of the mouse linked to chromosome 9. *Am J Med Genet.* 77:289-97.

Bronson, R.T., B.D. Lake, S. Cook, S. Taylor, and M.T. Davisson. 1993. Motor neuron degeneration of mice is a model of neuronal ceroid lipofuscinosis (Batten's disease). *Ann Neurol.* 33:381-5.

Broom, M.F., C. Zhou, J.E. Broom, K.J. Barwell, R.D. Jolly, and D.F. Hill. 1998. Ovine neuronal ceroid lipofuscinosis: a large animal model syntenic with the human neuronal ceroid lipofuscinosis variant CLN6. *J Med Genet.* 35:717-21.

Broom, M.F., C. Zhou, and D.F. Hill. 1999. Progress toward positional cloning of ovine neuronal ceroid lipofuscinosis, a model of the human late-infantile variant CLN6. *Mol Genet Metab.* 66:373-5.

Camp, L.A., and S.L. Hofmann. 1993. Purification and properties of a palmitoyl-protein thioesterase that cleaves palmitate from H-Ras. *J Biol Chem.* 268:22566-74.

Cannelli, N., D. Cassandrini, E. Bertini, P. Striano, L. Fusco, R. Gaggero, N. Specchio, R. Biancheri, F. Vigevano, C. Bruno, A. Simonati, F. Zara, and F.M. Santorelli. 2006. Novel mutations in CLN8 in Italian variant late infantile neuronal ceroid lipofuscinosis: another genetic hit in the Mediterranean. *Neurogenetics.* 7:111-7.

Cao, Y., J.A. Espinola, E. Fossale, A.C. Massey, A.M. Cuervo, M.E. MacDonald, and S.L. Cotman. 2006. Autophagy is disrupted in a knock-in mouse model of juvenile neuronal ceroid lipofuscinosis. *J Biol Chem.* 281:20483-93.

Caplen, N.J., S. Parrish, F. Imani, A. Fire, and R.A. Morgan. 2001. Specific inhibition of gene expression by small double-stranded RNAs in invertebrate and vertebrate systems. *Proc Natl Acad Sci U S A.* 98:9742-7.

Connolly, C.N., C.E. Futter, A. Gibson, C.R. Hopkins, and D.F. Cutler. 1994. Transport into and out of the Golgi complex studied by transfecting cells with cDNAs encoding horseradish peroxidase. *J Cell Biol.* 127:641-52.

Cook, R.W., R.D. Jolly, D.N. Palmer, I. Tammen, M.F. Broom, and R. McKinnon. 2002. Neuronal ceroid lipofuscinosis in Merino sheep. *Aust Vet J.* 80:292-7.

Cotman, S.L., V. Vrbanac, L.A. Lebel, R.L. Lee, K.A. Johnson, L.R. Donahue, A.M. Teed, K. Antonellis, R.T. Bronson, T.J. Lerner, and M.E. MacDonald. 2002. Cln3(Deltaex7/8) knock-in mice with the common JNCL mutation exhibit progressive neurologic disease that begins before birth. *Hum Mol Genet.* 11:2709-21.

D'Arrigo, A., E. Manera, R. Longhi, and N. Borgese. 1993. The specific subcellular localization of two isoforms of cytochrome b5 suggests novel targeting pathways. *J Biol Chem.* 268:2802-8.

de Duve, C. 2005. The lysosome turns fifty. *Nat Cell Biol.* 7:847-9.

de Duve, C., B.C. Pressman, R. Gianetto, R. Wattiaux, and F. Appelmans. 1955. *Biochem J.* 60:604-617.

de Virgilio, M., H. Weninger, and N.E. Ivessa. 1998. Ubiquitination is required for the retro-translocation of a short-lived luminal endoplasmic reticulum glycoprotein to the cytosol for degradation by the proteasome. *J Biol Chem.* 273:9734-43.

de Voer, G., P. van der Bent, A.J. Rodrigues, G.J. van Ommen, D.J. Peters, and P.E. Taschner. 2005. Deletion of the Caenorhabditis elegans homologues of the CLN3 gene, involved in human juvenile neuronal ceroid lipofuscinosis, causes a mild progeric phenotype. *J Inherit Metab Dis.* 28:1065-80.

Derwort, A., and K. Detering. 1959. [Vacuolated lymphocytes in familial amaurotic idiocy and their diagnostic significance.]. *Nervenarzt.* 30:442-8.

Dickson, K.M., J.J. Bergeron, I. Shames, J. Colby, D.T. Nguyen, E. Chevet, D.Y. Thomas, and G.J. Snipes. 2002. Association of calnexin with mutant peripheral myelin protein-22 ex vivo: a basis for "gain-of-function" ER diseases. *Proc Natl Acad Sci U S A.* 99:9852-7.

Dierks, T., B. Schmidt, L.V. Borissenko, J. Peng, A. Preusser, M. Mariappan, and K. von Figura. 2003. Multiple sulfatase deficiency is caused by mutations in the gene encoding the human C(alpha)-formylglycine generating enzyme. *Cell.* 113:435-44.

Drisdel, R.C., E. Manzana, and W.N. Green. 2004. The role of palmitoylation in functional expression of nicotinic alpha7 receptors. *J Neurosci.* 24:10502-10.

Dunn, W.A., Jr. 1990. Studies on the mechanisms of autophagy: formation of the autophagic vacuole. *J Cell Biol.* 110:1923-33.

Elbashir, S.M., W. Lendeckel, and T. Tuschl. 2001. RNA interference is mediated by 21- and 22-nucleotide RNAs. *Genes Dev.* 15:188-200.

Elleder, M., J. Sokolova, and M. Hrebicek. 1997. Follow-up study of subunit c of mitochondrial ATP synthase (SCMAS) in Batten disease and in unrelated lysosomal disorders. *Acta Neuropathol (Berl).* 93:379-90.

Ellgaard, L., and A. Helenius. 2003. Quality control in the endoplasmic reticulum. *Nat Rev Mol Cell Biol.* 4:181-91.

Eskelinen, E.L., Y. Tanaka, and P. Saftig. 2003. At the acidic edge: emerging functions for lysosomal membrane proteins. *Trends Cell Biol.* 13:137-45.

Ezaki, J., M. Takeda-Ezaki, M. Koike, Y. Ohsawa, H. Taka, R. Mineki, K. Murayama, Y. Uchiyama, T. Ueno, and E. Kominami. 2003. Characterization of Cln3p, the gene product responsible for juvenile neuronal ceroid lipofuscinosis, as a lysosomal integral membrane glycoprotein. *J Neurochem.* 87:1296-308.

Ezaki, J., M. Takeda-Ezaki, and E. Kominami. 2000. Tripeptidyl peptidase I, the late infantile neuronal ceroid lipofuscinosis gene product, initiates the lysosomal degradation of subunit c of ATP synthase. *J Biochem (Tokyo).* 128:509-16.

Ezaki, J., I. Tanida, N. Kanehagi, and E. Kominami. 1999. A lysosomal proteinase, the late infantile neuronal ceroid lipofuscinosis gene (CLN2) product, is essential for degradation of a hydrophobic protein, the subunit c of ATP synthase. *J Neurochem.* 72:2573-82.

Ezaki, J., L.S. Wolfe, K. Ishidoh, and E. Kominami. 1995. Abnormal degradative pathway of mitochondrial ATP synthase subunit c in late infantile neuronal ceroid-lipofuscinosis (Batten disease). *Am J Med Genet.* 57:254-9.

Falcon-Perez, J.M., R. Nazarian, C. Sabatti, and E.C. Dell'Angelica. 2005. Distribution and dynamics of Lamp1-containing endocytic organelles in fibroblasts deficient in BLOC-3. *J Cell Sci.* 118:5243-55.

Fire, A. 1999. RNA-triggered gene silencing. *Trends Genet.* 15:358-63.

Fire, A., S. Xu, M.K. Montgomery, S.A. Kostas, S.E. Driver, and C.C. Mello. 1998. Potent and specific genetic interference by double-stranded RNA in Caenorhabditis elegans. *Nature.* 391:806-11.

Fossale, E., P. Wolf, J.A. Espinola, T. Lubicz-Nawrocka, A.M. Teed, H. Gao, D. Rigamonti, E. Cattaneo, M.E. MacDonald, and S.L. Cotman. 2004. Membrane trafficking and mitochondrial abnormalities precede subunit c deposition in a cerebellar cell model of juvenile neuronal ceroid lipofuscinosis. *BMC Neurosci.* 5:57.

Fraile-Ramos, A., T.N. Kledal, A. Pelchen-Matthews, K. Bowers, T.W. Schwartz, and M. Marsh. 2001. The human cytomegalovirus US28 protein is located in endocytic vesicles and undergoes constitutive endocytosis and recycling. *Mol Biol Cell.* 12:1737-49.

Frydman, J., E. Nimmesgern, K. Ohtsuka, and F.U. Hartl. 1994. Folding of nascent polypeptide chains in a high molecular mass assembly with molecular chaperones. *Nature.* 370:111-7.

Futerman, A.H., and G. van Meer. 2004. The cell biology of lysosomal storage disorders. *Nat Rev Mol Cell Biol.* 5:554-65.

Gachet, Y., S. Codlin, J.S. Hyams, and S.E. Mole. 2005. btn1, the Schizosaccharomyces pombe homologue of the human Batten disease gene CLN3, regulates vacuole homeostasis. *J Cell Sci.* 118:5525-36.

Gao, H., R.M. Boustany, J.A. Espinola, S.L. Cotman, L. Srinidhi, K.A. Antonellis, T. Gillis, X. Qin, S. Liu, L.R. Donahue, R.T. Bronson, J.R. Faust, D. Stout, J.L. Haines, T.J. Lerner, and M.E. MacDonald. 2002. Mutations in a novel CLN6-encoded transmembrane protein cause variant neuronal ceroid lipofuscinosis in man and mouse. *Am J Hum Genet.* 70:324-35.

Garcia, M., D. Derocq, P. Pujol, and H. Rochefort. 1990. Overexpression of transfected cathepsin D in transformed cells increases their malignant phenotype and metastatic potency. *Oncogene.* 5:1809-14.

Goebel, H.H., and K.E. Wisniewski. 2004. Current state of clinical and morphological features in human NCL. *Brain Pathol.* 14:61-9.

Goebel, H.H.M.S.E.L., B.D. (eds). 1999. The Neuronal Ceroid Lipofuscinoses (Batten Disease). IOS Press, Amsterdam. 197 pp.

Golabek, A.A., E. Kida, M. Walus, P. Wujek, P. Mehta, and K.E. Wisniewski. 2003. Biosynthesis, glycosylation, and enzymatic processing in vivo of human tripeptidyl-peptidase I. *J Biol Chem.* 278:7135-45.

Graham, R.C., Jr., and M.J. Karnovsky. 1966. The early stages of absorption of injected horseradish peroxidase in the proximal tubules of mouse kidney: ultrastructural cytochemistry by a new technique. *J Histochem Cytochem.* 14:291-302.

Greene, N.D., D.L. Bernard, P.E. Taschner, B.D. Lake, N. de Vos, M.H. Breuning, R.M. Gardiner, S.E. Mole, R.L. Nussbaum, and H.M. Mitchison. 1999. A murine model for juvenile NCL: gene targeting of mouse Cln3. *Mol Genet Metab.* 66:309-13.

Gupta, P., A.A. Soyombo, A. Atashband, K.E. Wisniewski, J.M. Shelton, J.A. Richardson, R.E. Hammer, and S.L. Hofmann. 2001. Disruption of PPT1 or PPT2 causes neuronal ceroid lipofuscinosis in knockout mice. *Proc Natl Acad Sci U S A.* 98:13566-71.

Haltia, M., J. Rapola, and P. Santavuori. 1973. Infantile type of so-called neuronal ceroid-lipofuscinosis. Histological and electron microscopic studies. *Acta Neuropathol (Berl).* 26:157-70.

Hammond, S.M., E. Bernstein, D. Beach, and G.J. Hannon. 2000. An RNA-directed nuclease mediates post-transcriptional gene silencing in Drosophila cells. *Nature.* 404:293-6.

Hayat, M.A. 1993. Stains and cytochemical methods. Plenum Press, New York.

Hegesh, E., J. Hegesh, and A. Kaftory. 1986. Congenital methemoglobinemia with a deficiency of cytochrome b5. *N Engl J Med.* 314:757-61.

Heine, C., B. Koch, S. Storch, A. Kohlschutter, D.N. Palmer, and T. Braulke. 2004. Defective endoplasmic reticulum-resident membrane protein CLN6 affects lysosomal degradation of endocytosed arylsulfatase A. *J Biol Chem.* 279:22347-52.

Heine, C., J. Tyynela, J.D. Cooper, D.N. Palmer, M. Elleder, A. Kohlschutter, and T. Braulke. 2003. Enhanced expression of manganese-dependent superoxide dismutase in human and sheep CLN6 tissues. *Biochem J.* 376:369-76.

Helenius, A., and M. Aebi. 2001. Intracellular functions of N-linked glycans. *Science.* 291:2364-9.

Helenius, A., E.S. Tombretta, D.N. Hebert, and J.F. Simons. 1997. Calnexin, calreticulin and the folding of glycoproteins. *Trends Cell Biol.* 7:193-200.

Hellsten, E., J. Vesa, V.M. Olkkonen, A. Jalanko, and L. Peltonen. 1996. Human palmitoyl protein thioesterase: evidence for lysosomal targeting of the enzyme and disturbed cellular routing in infantile neuronal ceroid lipofuscinosis. *Embo J.* 15:5240-5.

Hermansson, M., R. Kakela, M. Berghall, A.E. Lehesjoki, P. Somerharju, and U. Lahtinen. 2005. Mass spectrometric analysis reveals changes in phospholipid, neutral sphingolipid and sulfatide molecular species in progressive epilepsy with mental retardation, EPMR, brain: a case study. *J Neurochem.* 95:609-17.

Herrmann, J.M., P. Malkus, and R. Schekman. 1999. Out of the ER--outfitters, escorts and guides. *Trends Cell Biol.* 9:5-7.

Heuser, J. 1989. Changes in lysosome shape and distribution correlated with changes in cytoplasmic pH. *J Cell Biol.* 108:855-64.

Hewett, J., C. Gonzalez-Agosti, D. Slater, P. Ziefer, S. Li, D. Bergeron, D.J. Jacoby, L.J. Ozelius, V. Ramesh, and X.O. Breakefield. 2000. Mutant torsinA, responsible for early-onset torsion dystonia, forms membrane inclusions in cultured neural cells. *Hum Mol Genet.* 9:1403-13.

Hickey, A.J., H.L. Chotkowski, N. Singh, J.G. Ault, C.A. Korey, M.E. MacDonald, and R.L. Glaser. 2006. Palmitoyl-protein thioesterase 1 deficiency in Drosophila melanogaster causes accumulation of abnormal storage material and reduced life span. *Genetics.* 172:2379-90.

Hiller, M.M., A. Finger, M. Schweiger, and D.H. Wolf. 1996. ER degradation of a misfolded luminal protein by the cytosolic ubiquitin-proteasome pathway. *Science.* 273:1725-8.

Hirvasniemi, A., H. Lang, A.E. Lehesjoki, and J. Leisti. 1994. Northern epilepsy syndrome: an inherited childhood onset epilepsy with associated mental deterioration. *J Med Genet.* 31:177-82.

Holmberg, V., A. Jalanko, J. Isosomppi, A.L. Fabritius, L. Peltonen, and O. Kopra. 2004. The mouse ortholog of the neuronal ceroid lipofuscinosis CLN5 gene encodes a soluble lysosomal glycoprotein expressed in the developing brain. *Neurobiol Dis.* 16:29-40.

Holmer, L., and H.J. Worman. 2001. Inner nuclear membrane proteins: functions and targeting. *Cell Mol Life Sci.* 58:1741-7.

Holopainen, J.M., J. Saarikoski, P.K. Kinnunen, and I. Jarvela. 2001. Elevated lysosomal pH in neuronal ceroid lipofuscinoses (NCLs). *Eur J Biochem.* 268:5851-6.

Holthuis, J.C., and T.P. Levine. 2005. Lipid traffic: floppy drives and a superhighway. *Nat Rev Mol Cell Biol.* 6:209-20.

Holzmann, K., C. Gerner, A. Poltl, R. Schafer, P. Obrist, C. Ensinger, R. Grimm, and G. Sauermann. 2000. A human common nuclear matrix protein homologous to eukaryotic translation initiation factor 4A. *Biochem Biophys Res Commun.* 267:339-44.

Hopkins, C.R. 1985. The appearance and internalization of transferrin receptors at the margins of spreading human tumor cells. *Cell.* 40:199-208.

Houweling, P.J., J.A. Cavanagh, D.N. Palmer, T. Frugier, N.L. Mitchell, P.A. Windsor, H.W. Raadsma, and I. Tammen. 2006a. Neuronal ceroid lipofuscinosis in Devon cattle is caused by a single base duplication (c.662dupG) in the bovine CLN5 gene. *Biochim Biophys Acta.*1762: 898-905

Houweling, P.J., J.A. Cavanagh, and I. Tammen. 2006b. Radiation hybrid mapping of three candidate genes for bovine Neuronal Ceroid Lipofuscinosis: CLN3, CLN5 and CLN6. *Cytogenet Genome Res.* 115:5-6.

Isosomppi, J., J. Vesa, A. Jalanko, and L. Peltonen. 2002. Lysosomal localization of the neuronal ceroid lipofuscinosis CLN5 protein. *Hum Mol Genet.* 11:885-91.

Ito, A. 1980. Cytochrome b5-like hemoprotein of outer mitochondrial membrane; OM cytochrome b. I. Purification of OM cytochrome b from rat liver mitochondria and comparison of its molecular properties with those of cytochrome b5. *J Biochem (Tokyo).* 87:63-71.

Jalanko, A., J. Vesa, T. Manninen, C. von Schantz, H. Minye, A.L. Fabritius, T. Salonen, J. Rapola, M. Gentile, O. Kopra, and L. Peltonen. 2005. Mice with Ppt1Deltaex4 mutation replicate the INCL phenotype and show an inflammation-associated loss of interneurons. *Neurobiol Dis.* 18:226-41.

Janes, R.W., P.B. Munroe, H.M. Mitchison, R.M. Gardiner, S.E. Mole, and B.A. Wallace. 1996. A model for Batten disease protein CLN3: functional implications from homology and mutations. *FEBS Lett.* 399:75-7.

Jarplid, B., and M. Haltia. 1993. An animal model of the infantile type of neuronal ceroid-lipofuscinosis. *J Inherit Metab Dis.* 16:274-7.

Jarvela, I., M. Lehtovirta, R. Tikkanen, A. Kyttala, and A. Jalanko. 1999. Defective intracellular transport of CLN3 is the molecular basis of Batten disease (JNCL). *Hum Mol Genet.* 8:1091-8.

Kagedal, K., U. Johansson, and K. Ollinger. 2001. The lysosomal protease cathepsin D mediates apoptosis induced by oxidative stress. *Faseb J.* 15:1592-4.

Katz, M.L., S. Khan, T. Awano, S.A. Shahid, A.N. Siakotos, and G.S. Johnson. 2005. A mutation in the CLN8 gene in English Setter dogs with neuronal ceroid-lipofuscinosis. *Biochem Biophys Res Commun.* 327:541-7.

Kida, E., A.A. Golabek, and K.E. Wisniewski. 2001. Cellular pathology and pathogenic aspects of neuronal ceroid lipofuscinoses. *Adv Genet.* 45:35-68.

Kim, Y., D. Ramirez-Montealegre, and D.A. Pearce. 2003. A role in vacuolar arginine transport for yeast Btn1p and for human CLN3, the protein defective in Batten disease. *Proc Natl Acad Sci U S A.* 100:15458-62.

Kleizen, B., and I. Braakman. 2004. Protein folding and quality control in the endoplasmic reticulum. *Curr Opin Cell Biol.* 16:343-9.

Klionsky, D.J., and S.D. Emr. 2000. Autophagy as a regulated pathway of cellular degradation. *Science.* 290:1717-21.

Koike, M., H. Nakanishi, P. Saftig, J. Ezaki, K. Isahara, Y. Ohsawa, W. Schulz-Schaeffer, T. Watanabe, S. Waguri, S. Kametaka, M. Shibata, K. Yamamoto, E. Kominami, C. Peters, K. von Figura, and Y. Uchiyama. 2000. Cathepsin D deficiency induces lysosomal storage with ceroid lipofuscin in mouse CNS neurons. *J Neurosci.* 20:6898-906.

Kolovou, G.D., D.P. Mikhailidis, K.K. Anagnostopoulou, S.S. Daskalopoulou, and D.V. Cokkinos. 2006. Tangier disease four decades of research: a reflection of the importance of HDL. *Curr Med Chem.* 13:771-82.

Koning, A.J., C.J. Roberts, and R.L. Wright. 1996. Different subcellular localization of Saccharomyces cerevisiae HMG-CoA reductase isozymes at elevated levels corresponds to distinct endoplasmic reticulum membrane proliferations. *Mol Biol Cell.* 7:769-89.

Kopan, S., U. Sivasubramaniam, and M.J. Warburton. 2004. The lysosomal degradation of neuromedin B is dependent on tripeptidyl peptidase-I: evidence for the impairment of neuropeptide degradation in late-infantile

neuronal ceroid lipofuscinosis. *Biochem Biophys Res Commun.* 319:58-65.

Kopra, O., J. Vesa, C. Von Schantz, T. Manninen, H. Minye, A.L. Fabritius, J. Rapola, O.P. Van Diggelen, J. Saarela, A. Jalanko, and L. Peltonen. 2004. A Mouse Model for Finnish Variant Late Infantile Neuronal Ceroid Lipofuscinosis, CLN5, reveals neuropathology associated with early aging. *Hum Mol Genet.* 13: 2893-906

Kornfeld, S., and I. Mellman. 1989. The biogenesis of lysosomes. *Annu Rev Cell Biol.* 5:483-525.

Kremmidiotis, G., I.L. Lensink, R.L. Bilton, E. Woollatt, T.K. Chataway, G.R. Sutherland, and D.F. Callen. 1999. The Batten disease gene product (CLN3p) is a Golgi integral membrane protein. *Hum Mol Genet.* 8:523-31.

Kyttala, A., G. Ihrke, J. Vesa, M.J. Schell, and J.P. Luzio. 2004a. Two motifs target Batten disease protein CLN3 to lysosomes in transfected nonneuronal and neuronal cells. *Mol Biol Cell.* 15:1313-23.

Kyttala, A., K. Yliannala, P. Schu, A. Jalanko, and J.P. Luzio. 2004b. AP-1 and AP-3 facilitate lysosomal targeting of batten disease protein CLN3 via its dileucine motif. *J Biol Chem.* 280: 10277-83

Lake, B.D., and N.A. Hall. 1993. Immunolocalization studies of subunit c in late-infantile and juvenile Batten disease. *J Inherit Metab Dis.* 16:263-6.

Lam, K.K., M. Davey, B. Sun, A.F. Roth, N.G. Davis, and E. Conibear. 2006. Palmitoylation by the DHHC protein Pfa4 regulates the ER exit of Chs3. *J Cell Biol.* 174:19-25.

Landgrebe, J., T. Dierks, B. Schmidt, and K. von Figura. 2003. The human SUMF1 gene, required for posttranslational sulfatase modification, defines a new gene family which is conserved from pro- to eukaryotes. *Gene.* 316:47-56.

Lederer, F., R. Ghrir, B. Guiard, S. Cortial, and A. Ito. 1983. Two homologous cytochromes b5 in a single cell. *Eur J Biochem.* 132:95-102.

Lee, M.C., E.A. Miller, J. Goldberg, L. Orci, and R. Schekman. 2004. Bi-directional protein transport between the ER and Golgi. *Annu Rev Cell Dev Biol.* 20:87-123.

Lehotsky, J., P. Kaplan, E. Babusikova, A. Strapkova, and R. Murin. 2003. Molecular pathways of endoplasmic reticulum dysfunctions: possible cause of cell death in the nervous system. *Physiol Res.* 52:269-74.

Lehtovirta, M., A. Kyttala, E.L. Eskelinen, M. Hess, O. Heinonen, and A. Jalanko. 2001. Palmitoyl protein thioesterase (PPT) localizes into synaptosomes and synaptic vesicles in neurons: implications for infantile neuronal ceroid lipofuscinosis (INCL). *Hum Mol Genet.* 10:69-75.

Lewis, M.J., and H.R. Pelham. 1990. A human homologue of the yeast HDEL receptor. *Nature.* 348:162-3.

Liaudet-Coopman, E., M. Beaujouin, D. Derocq, M. Garcia, M. Glondu-Lassis, V. Laurent-Matha, C. Prebois, H. Rochefort, and F. Vignon. 2006. Cathepsin D: newly discovered functions of a long-standing aspartic protease in cancer and apoptosis. *Cancer Lett.* 237:167-79.

Lilley, B.N., and H.L. Ploegh. 2004. A membrane protein required for dislocation of misfolded proteins from the ER. *Nature.* 429:834-40.

Lin, L., I. Sohar, H. Lackland, and P. Lobel. 2001. The human CLN2 protein/tripeptidyl-peptidase I is a serine protease that autoactivates at acidic pH. *J Biol Chem.* 276:2249-55.

Locke, M., and A.K. Sykes. 1975. The role of the Golgi complex in the isolation and digestion of organelles. *Tissue Cell.* 7:143-58.

Lonka, L., A. Aalto, O. Kopra, M. Kuronen, Z. Kokaia, M. Saarma, and A.E. Lehesjoki. 2005. The neuronal ceroid lipofuscinosis Cln8 gene expression is developmentally regulated in mouse brain and up-regulated in the hippocampal kindling model of epilepsy. *BMC Neurosci.* 6:27.

Lonka, L., A. Kyttala, S. Ranta, A. Jalanko, and A.E. Lehesjoki. 2000. The neuronal ceroid lipofuscinosis CLN8 membrane protein is a resident of the endoplasmic reticulum. *Hum Mol Genet.* 9:1691-7.

Lonka, L., T. Salonen, E. Siintola, O. Kopra, A.E. Lehesjoki, and A. Jalanko. 2004. Localization of wild-type and mutant neuronal ceroid lipofuscinosis CLN8 proteins in non-neuronal and neuronal cells. *J Neurosci Res.* 76:862-71.

Luiro, K., O. Kopra, T. Blom, M. Gentile, H.M. Mitchison, I. Hovatta, K. Tornquist, and A. Jalanko. 2006. Batten disease (JNCL) is linked to disturbances in mitochondrial, cytoskeletal, and synaptic compartments. *J Neurosci Res.* 84:1124-38.

Luiro, K., O. Kopra, M. Lehtovirta, and A. Jalanko. 2001. CLN3 protein is targeted to neuronal synapses but excluded from synaptic vesicles: new clues to Batten disease. *Hum Mol Genet.* 10:2123-31.

Luiro, K., K. Yliannala, L. Ahtiainen, H. Maunu, I. Jarvela, A. Kyttala, and A. Jalanko. 2004. Interconnections of CLN3, Hook1 and Rab proteins link Batten disease to defects in the endocytic pathway. *Hum Mol Genet.* 13: 3017-27

Luzio, J.P., V. Poupon, M.R. Lindsay, B.M. Mullock, R.C. Piper, and P.R. Pryor. 2003. Membrane dynamics and the biogenesis of lysosomes. *Mol Membr Biol.* 20:141-54.

Mao, Q., B.J. Foster, H. Xia, and B.L. Davidson. 2003a. Membrane topology of CLN3, the protein underlying Batten disease. *FEBS Lett.* 541:40-6.

Mao, Q., H. Xia, and B.L. Davidson. 2003b. Intracellular trafficking of CLN3, the protein underlying the childhood neurodegenerative disease, Batten disease. *FEBS Lett.* 555:351-7.

Martinez-Menarguez, J.A., H.J. Geuze, J.W. Slot, and J. Klumperman. 1999. Vesicular tubular clusters between the ER and Golgi mediate concentration of soluble secretory proteins by exclusion from COPI-coated vesicles. *Cell.* 98:81-90.

Matas, O.B., S. Fritz, A. Luna, and G. Egea. 2005. Membrane trafficking at the ER/Golgi interface: functional implications of RhoA and Rac1. *Eur J Cell Biol.* 84:699-707.

Matlack, K.E., B. Misselwitz, K. Plath, and T.A. Rapoport. 1999. BiP acts as a molecular ratchet during posttranslational transport of prepro-alpha factor across the ER membrane. *Cell.* 97:553-64.

Matteoni, R., and T.E. Kreis. 1987. Translocation and clustering of endosomes and lysosomes depends on microtubules. *J Cell Biol.* 105:1253-65.

Matzke, M.A., and J.A. Birchler. 2005. RNAi-mediated pathways in the nucleus. *Nat Rev Genet.* 6:24-35.

Meldolesi, J., and T. Pozzan. 1998. The endoplasmic reticulum Ca2+ store: a view from the lumen. *Trends Biochem Sci.* 23:10-4.

Melville, S.A., C.L. Wilson, C.S. Chiang, V.P. Studdert, F. Lingaas, and A.N. Wilton. 2005. A mutation in canine CLN5 causes neuronal ceroid lipofuscinosis in Border collie dogs. *Genomics.* 86:287-94.

Mitchell, W.A., R.B. Wheeler, J.D. Sharp, S.L. Bate, R.M. Gardiner, U.S. Ranta, L. Lonka, R.E. Williams, A.E. Lehesjoki, and S.E. Mole. 2001. Turkish variant late infantile neuronal ceroid lipofuscinosis (CLN7) may be allelic to CLN8. *Eur J Paediatr Neurol.* 5 Suppl A:21-7.

Mizushima, N., A. Yamamoto, M. Hatano, Y. Kobayashi, Y. Kabeya, K. Suzuki, T. Tokuhisa, Y. Ohsumi, and T. Yoshimori. 2001. Dissection of autophagosome formation using Apg5-deficient mouse embryonic stem cells. *J Cell Biol.* 152:657-68.

Mizzen, L.A., C. Chang, J.I. Garrels, and W.J. Welch. 1989. Identification, characterization, and purification of two mammalian stress proteins present in mitochondria, grp 75, a member of the hsp 70 family and hsp 58, a homolog of the bacterial groEL protein. *J Biol Chem.* 264:20664-75.

Mizzen, L.A., A.N. Kabiling, and W.J. Welch. 1991. The two mammalian mitochondrial stress proteins, grp 75 and hsp 58, transiently interact with newly synthesized mitochondrial proteins. *Cell Regul.* 2:165-79.

Mole, S.E., G. Michaux, S. Codlin, R.B. Wheeler, J.D. Sharp, and D.F. Cutler. 2004. CLN6, which is associated with a lysosomal storage disease, is an endoplasmic reticulum protein. *Exp Cell Res.* 298:399-406.

Mole, S.E., R.E. Williams, and H.H. Goebel. 2005. Correlations between genotype, ultrastructural morphology and clinical phenotype in the neuronal ceroid lipofuscinoses. *Neurogenetics.* 6:107-26.

Montgomery, M.K., and A. Fire. 1998. Double-stranded RNA as a mediator in sequence-specific genetic silencing and co-suppression. *Trends Genet.* 14:255-8.

Mullins, C., and J.S. Bonifacino. 2001. The molecular machinery for lysosome biogenesis. *Bioessays.* 23:333-43.

Munro, S., and H.R. Pelham. 1987. A C-terminal signal prevents secretion of luminal ER proteins. *Cell.* 48:899-907.

Myllykangas, L., J. Tyynela, A. Page-McCaw, G.M. Rubin, M.J. Haltia, and M.B. Feany. 2005. Cathepsin D-deficient Drosophila recapitulate the key features of neuronal ceroid lipofuscinoses. *Neurobiol Dis.* 19:194-9.

Nakamura, N., M. Lowe, T.P. Levine, C. Rabouille, and G. Warren. 1997. The vesicle docking protein p115 binds GM130, a cis-Golgi matrix protein, in a mitotically regulated manner. *Cell.* 89:445-55.

Nakamura, N., C. Rabouille, R. Watson, T. Nilsson, N. Hui, P. Slusarewicz, T.E. Kreis, and G. Warren. 1995. Characterization of a cis-Golgi matrix protein, GM130. *J Cell Biol.* 131:1715-26.

Neufeld, E.B., J.A. Stonik, S.J. Demosky, Jr., C.L. Knapper, C.A. Combs, A. Cooney, M. Comly, N. Dwyer, J. Blanchette-Mackie, A.T. Remaley, S.

Santamarina-Fojo, and H.B. Brewer, Jr. 2004. The ABCA1 transporter modulates late endocytic trafficking: insights from the correction of the genetic defect in Tangier disease. *J Biol Chem.* 279:15571-8.

Nykanen, A., B. Haley, and P.D. Zamore. 2001. ATP requirements and small interfering RNA structure in the RNA interference pathway. *Cell.* 107:309-21.

Orci, L., D.J. Palmer, M. Ravazzola, A. Perrelet, M. Amherdt, and J.E. Rothman. 1993. Budding from Golgi membranes requires the coatomer complex of non-clathrin coat proteins. *Nature.* 362:648-52.

Orso, E., C. Broccardo, W.E. Kaminski, A. Bottcher, G. Liebisch, W. Drobnik, A. Gotz, O. Chambenoit, W. Diederich, T. Langmann, T. Spruss, M.F. Luciani, G. Rothe, K.J. Lackner, G. Chimini, and G. Schmitz. 2000. Transport of lipids from golgi to plasma membrane is defective in tangier disease patients and Abc1-deficient mice. *Nat Genet.* 24:192-6.

Osborne, A.R., T.A. Rapoport, and B. van den Berg. 2005. Protein translocation by the Sec61/SecY channel. *Annu Rev Cell Dev Biol.* 21:529-50.

Oswald, M.J., D.N. Palmer, G.W. Kay, S.J. Shemilt, P. Rezaie, and J.D. Cooper. 2005. Glial activation spreads from specific cerebral foci and precedes neurodegeneration in presymptomatic ovine neuronal ceroid lipofuscinosis (CLN6). *Neurobiol Dis.* 20:49-63.

Palade, G. 1975. Intracellular aspects of the process of protein synthesis. *Science.* 189:347-58.

Palmer, D.N., G. Barns, D.R. Husbands, and R.D. Jolly. 1986a. Ceroid lipofuscinosis in sheep. II. The major component of the lipopigment in liver, kidney, pancreas, and brain is low molecular weight protein. *J Biol Chem.* 261:1773-7.

Palmer, D.N., I.M. Fearnley, S.M. Medd, J.E. Walker, R.D. Martinus, S.L. Bayliss, N.A. Hall, B.D. Lake, L.S. Wolfe, and R.D. Jolly. 1989. Lysosomal storage of the DCCD reactive proteolipid subunit of mitochondrial ATP synthase in human and ovine ceroid lipofuscinoses. *Adv Exp Med Biol.* 266:211-22; discussion 223.

Palmer, D.N., D.R. Husbands, P.J. Winter, J.W. Blunt, and R.D. Jolly. 1986b. Ceroid lipofuscinosis in sheep. I. Bis(monoacylglycero)phosphate, dolichol, ubiquinone, phospholipids, fatty acids, and fluorescence in liver lipopigment lipids. *J Biol Chem.* 261:1766-72.

Paschen, W. 2001. Dependence of vital cell function on endoplasmic reticulum calcium levels: implications for the mechanisms underlying neuronal cell injury in different pathological states. *Cell Calcium.* 29:1-11.

Pearce, D.A., T. Ferea, S.A. Nosel, B. Das, and F. Sherman. 1999. Action of BTN1, the yeast orthologue of the gene mutated in Batten disease. *Nat Genet.* 22:55-8.

Pearce, D.A., and F. Sherman. 1998. A yeast model for the study of Batten disease. *Proc Natl Acad Sci U S A.* 95:6915-8.

Pedrazzini, E., A. Villa, R. Longhi, A. Bulbarelli, and N. Borgese. 2000. Mechanism of residence of cytochrome b(5), a tail-anchored protein, in the endoplasmic reticulum. *J Cell Biol.* 148:899-914.

Persaud-Sawin, D.A., J.O. McNamara, 2nd, S. Rylova, A. Vandongen, and R.M. Boustany. 2004. A galactosylceramide binding domain is involved in trafficking of CLN3 from golgi to rafts via recycling endosomes. *Pediatr Res.* 56:449-63.

Peyroche, A., B. Antonny, S. Robineau, J. Acker, J. Cherfils, and C.L. Jackson. 1999. Brefeldin A acts to stabilize an abortive ARF-GDP-Sec7 domain protein complex: involvement of specific residues of the Sec7 domain. *Mol Cell.* 3:275-85.

Puri, S., and A.D. Linstedt. 2003. Capacity of the golgi apparatus for biogenesis from the endoplasmic reticulum. *Mol Biol Cell.* 14:5011-8.

Rakheja, D., S.B. Narayan, J.V. Pastor, and M.J. Bennett. 2004. CLN3P, the Batten disease protein, localizes to membrane lipid rafts (detergent-resistant membranes). *Biochem Biophys Res Commun.* 317:988-91.

Ranta, S., M. Topcu, S. Tegelberg, H. Tan, A. Ustubutun, I. Saatci, A. Dufke, H. Enders, K. Pohl, Y. Alembik, W.A. Mitchell, S.E. Mole, and A.E. Lehesjoki. 2004. Variant late infantile neuronal ceroid lipofuscinosis in a subset of Turkish patients is allelic to Northern epilepsy. *Hum Mutat.* 23:300-5.

Ranta, S., Y. Zhang, B. Ross, L. Lonka, E. Takkunen, A. Messer, J. Sharp, R. Wheeler, K. Kusumi, S. Mole, W. Liu, M.B. Soares, M.F. Bonaldo, A. Hirvasniemi, A. de la Chapelle, T.C. Gilliam, and A.E. Lehesjoki. 1999. The neuronal ceroid lipofuscinoses in human EPMR and mnd mutant mice are associated with mutations in CLN8. *Nat Genet.* 23:233-6.

Robenek, H., and G. Schmitz. 1991. Abnormal processing of Golgi elements and lysosomes in Tangier disease. *Arterioscler Thromb.* 11:1007-20.

Roberts, M.S., A.J. Woods, P.E. Shaw, and J.C. Norman. 2003. ERK1 associates with alpha(v)beta 3 integrin and regulates cell spreading on vitronectin. *J Biol Chem.* 278:1975-85.

Romisch, K. 2005. Endoplasmic reticulum-associated degradation. *Annu Rev Cell Dev Biol.* 21:435-56.

Saftig, P., M. Hetman, W. Schmahl, K. Weber, L. Heine, H. Mossmann, A. Koster, B. Hess, M. Evers, K. von Figura, and et al. 1995. Mice deficient for the lysosomal proteinase cathepsin D exhibit progressive atrophy of the intestinal mucosa and profound destruction of lymphoid cells. *Embo J.* 14:3599-608.

Santavuori, P., M. Haltia, and J. Rapola. 1974. Infantile type of so-called neuronal ceroid-lipofuscinosis. *Dev Med Child Neurol.* 16:644-53.

Savukoski, M., T. Klockars, V. Holmberg, P. Santavuori, E.S. Lander, and L. Peltonen. 1998. CLN5, a novel gene encoding a putative transmembrane protein mutated in Finnish variant late infantile neuronal ceroid lipofuscinosis. *Nat Genet.* 19:286-8.

Schenkman, J.B., and I. Jansson. 2003. The many roles of cytochrome b5. *Pharmacol Ther.* 97:139-52.

Schmidt, B., T. Selmer, A. Ingendoh, and K. von Figura. 1995. A novel amino acid modification in sulfatases that is defective in multiple sulfatase deficiency. *Cell.* 82:271-8.

Sharp, J.D., R.B. Wheeler, B.D. Lake, M. Fox, R.M. Gardiner, and R.E. Williams. 1999. Genetic and physical mapping of the CLN6 gene on chromosome 15q21-23. *Mol Genet Metab.* 66:329-31.

Sharp, J.D., R.B. Wheeler, B.D. Lake, M. Savukoski, I.E. Jarvela, L. Peltonen, R.M. Gardiner, and R.E. Williams. 1997. Loci for classical and a variant late infantile neuronal ceroid lipofuscinosis map to chromosomes 11p15 and 15q21-23. *Hum Mol Genet.* 6:591-5.

Sharp, J.D., R.B. Wheeler, K.A. Parker, R.M. Gardiner, R.E. Williams, and S.E. Mole. 2003. Spectrum of CLN6 mutations in variant late infantile neuronal ceroid lipofuscinosis. *Hum Mutat.* 22:35-42.

Shibata, Y., G.K. Voeltz, and T.A. Rapoport. 2006. Rough sheets and smooth tubules. *Cell.* 126:435-9.

Shimoi, W., I. Ezawa, K. Nakamoto, S. Uesaki, G. Gabreski, M. Aridor, A. Yamamoto, M. Nagahama, M. Tagaya, and K. Tani. 2005. p125 is

localized in endoplasmic reticulum exit sites and involved in their organization. *J Biol Chem.* 280:10141-8.

Siintola, E., A.E. Lehesjoki, and S.E. Mole. 2006a. Molecular genetics of the NCLs - status and perspectives. *Biochim Biophys Acta.* 1762: 857-64

Siintola, E., S. Partanen, P. Stromme, A. Haapanen, M. Haltia, J. Maehlen, A.E. Lehesjoki, and J. Tyynela. 2006b. Cathepsin D deficiency underlies congenital human neuronal ceroid-lipofuscinosis. *Brain.* 129:1438-45.

Siintola, E., M. Topcu, A. Kohlschutter, T. Salonen, T. Joensuu, A.K. Anttonen, and A.E. Lehesjoki. 2005. Two novel CLN6 mutations in variant late-infantile neuronal ceroid lipofuscinosis patients of Turkish origin. *Clin Genet.* 68:167-73.

Sleat, D.E., R.J. Donnelly, H. Lackland, C.G. Liu, I. Sohar, R.K. Pullarkat, and P. Lobel. 1997. Association of mutations in a lysosomal protein with classical late-infantile neuronal ceroid lipofuscinosis. *Science.* 277:1802-5.

Sleat, D.E., R.M. Gin, I. Sohar, K. Wisniewski, S. Sklower-Brooks, R.K. Pullarkat, D.N. Palmer, T.J. Lerner, R.M. Boustany, P. Uldall, A.N. Siakotos, R.J. Donnelly, and P. Lobel. 1999. Mutational analysis of the defective protease in classic late-infantile neuronal ceroid lipofuscinosis, a neurodegenerative lysosomal storage disorder. *Am J Hum Genet.* 64:1511-23.

Sleat, D.E., I. Sohar, P.S. Pullarkat, P. Lobel, and R.K. Pullarkat. 1998. Specific alterations in levels of mannose 6-phosphorylated glycoproteins in different neuronal ceroid lipofuscinoses. *Biochem J.* 334 (Pt 3):547-51.

Sleat, D.E., J.A. Wiseman, M. El-Banna, K.H. Kim, Q. Mao, S. Price, S.L. Macauley, R.L. Sidman, M.M. Shen, Q. Zhao, M.A. Passini, B.L. Davidson, G.R. Stewart, and P. Lobel. 2004. A mouse model of classical late-infantile neuronal ceroid lipofuscinosis based on targeted disruption of the CLN2 gene results in a loss of tripeptidyl-peptidase I activity and progressive neurodegeneration. *J Neurosci.* 24:9117-26.

Snapp, E.L., R.S. Hegde, M. Francolini, F. Lombardo, S. Colombo, E. Pedrazzini, N. Borgese, and J. Lippincott-Schwartz. 2003. Formation of stacked ER cisternae by low affinity protein interactions. *J Cell Biol.* 163:257-69.

Sohar, I., D.E. Sleat, M. Jadot, and P. Lobel. 1999. Biochemical characterization of a lysosomal protease deficient in classical late infantile neuronal ceroid lipofuscinosis (LINCL) and development of an enzyme-based assay for

diagnosis and exclusion of LINCL in human specimens and animal models. *J Neurochem.* 73:700-11.

Stahmann, M.A. 1977. Cross-linking of protein by peroxidase. *Adv Exp Med Biol.* 86B:285-98.

Steinfeld, R., K. Reinhardt, K. Schreiber, M. Hillebrand, R. Kraetzner, W. Bruck, P. Saftig, and J. Gartner. 2006. Cathepsin D deficiency is associated with a human neurodegenerative disorder. *Am J Hum Genet.* 78:988-98.

Steinfeld, R., H.B. Steinke, D. Isbrandt, A. Kohlschutter, and J. Gartner. 2004. Mutations in classical late infantile neuronal ceroid lipofuscinosis disrupt transport of tripeptidyl-peptidase I to lysosomes. *Hum Mol Genet.* 13:2483-91.

Stengel, C. 1826. Beretning om et maerkeligt Sygdomstilfoelde hos fire sodskende i Naerheden af Rorass. *Eyr et medicinska Tidskrift.* 1.

Stengel, C. 1982. Account of a singular illness among four siblings in the vicinity of Roraas. *In* Ceroid-Lipofuscinosis (Batten Disease). D. Armstrong, editor. Elsevier Biomedical Press, Amsterdam. 17-19.

Stephens, D.J. 2003. De novo formation, fusion and fission of mammalian COPII-coated endoplasmic reticulum exit sites. *EMBO Rep.* 4:210-7.

Stephens, D.J., N. Lin-Marq, A. Pagano, R. Pepperkok, and J.P. Paccaud. 2000. COPI-coated ER-to-Golgi transport complexes segregate from COPII in close proximity to ER exit sites. *J Cell Sci.* 113 (Pt 12):2177-85.

Storch, S., S. Pohl, and T. Braulke. 2004. A dileucine motif and a cluster of acidic amino acids in the second cytoplasmic domain of the batten disease-related CLN3 Protein are required for efficient lysosomal targeting. *J Biol Chem.* 279: 53625-34

Sun, F., R. Zhang, X. Gong, X. Geng, P.F. Drain, and R.A. Frizzell. 2006. Derlin-1 promotes the efficient degradation of CFTR and CFTR folding mutants. *J Biol Chem.* 281: 36856-63

Tammen, I., R.W. Cook, F.W. Nicholas, and H.W. Raadsma. 2001. Neuronal ceroid lipofuscinosis in Australian Merino sheep: a new animal model. *Eur J Paediatr Neurol.* 5 Suppl A:37-41.

Tammen, I., P.J. Houweling, T. Frugier, N.L. Mitchell, G.W. Kay, J.A. Cavanagh, R.W. Cook, H.W. Raadsma, and D.N. Palmer. 2006. A missense mutation (c.184C>T) in ovine CLN6 causes neuronal ceroid

lipofuscinosis in Merino sheep whereas affected South Hampshire sheep have reduced levels of CLN6 mRNA. *Biochim Biophys Acta.* 1762: 898-905

Tange, T.O., T. Shibuya, M.S. Jurica, and M.J. Moore. 2005. Biochemical analysis of the EJC reveals two new factors and a stable tetrameric protein core. *Rna.* 11:1869-83.

Teixeira, C.A., J. Espinola, L. Huo, J. Kohlschutter, D.A. Persaud Sawin, B. Minassian, C.J. Bessa, A. Guimaraes, D.A. Stephan, M.C. Sa Miranda, M.E. MacDonald, M.G. Ribeiro, and R.M. Boustany. 2003. Novel mutations in the CLN6 gene causing a variant late infantile neuronal ceroid lipofuscinosis. *Hum Mutat.* 21:502-8.

Teixeira, C.A., S. Lin, M. Mangas, R. Quinta, C.J. Bessa, C. Ferreira, M.C. Sa Miranda, R.M. Boustany, and M.G. Ribeiro. 2006. Gene expression profiling in vLINCL CLN6-deficient fibroblasts: Insights into pathobiology. *Biochim Biophys Acta.* 1762:637-646.

Tsai, B., Y. Ye, and T.A. Rapoport. 2002. Retro-translocation of proteins from the endoplasmic reticulum into the cytosol. *Nat Rev Mol Cell Biol.* 3:246-55.

Tsiakas, K., R. Steinfeld, S. Storch, J. Ezaki, Z. Lukacs, E. Kominami, A. Kohlschutter, K. Ullrich, and T. Braulke. 2004. Mutation of the glycosylated asparagine residue 286 in human CLN2 protein results in loss of enzymatic activity. *Glycobiology.* 14:1C-5C.

Tyynela, J., M. Baumann, M. Henseler, K. Sandhoff, and M. Haltia. 1995. Sphingolipid activator proteins (SAPs) are stored together with glycosphingolipids in the infantile neuronal ceroid-lipofuscinosis (INCL). *Am J Med Genet.* 57:294-7.

Tyynela, J., D.N. Palmer, M. Baumann, and M. Haltia. 1993. Storage of saposins A and D in infantile neuronal ceroid-lipofuscinosis. *FEBS Lett.* 330:8-12.

Tyynela, J., I. Sohar, D.E. Sleat, R.M. Gin, R.J. Donnelly, M. Baumann, M. Haltia, and P. Lobel. 2000. A mutation in the ovine cathepsin D gene causes a congenital lysosomal storage disease with profound neurodegeneration. *Embo J.* 19:2786-92.

Uchiyama, Y. 2001. Autophagic cell death and its execution by lysosomal cathepsins. *Arch Histol Cytol.* 64:233-46.

Valderrama, F., T. Babia, I. Ayala, J.W. Kok, J. Renau-Piqueras, and G. Egea. 1998. Actin microfilaments are essential for the cytological positioning and morphology of the Golgi complex. *Eur J Cell Biol.* 76:9-17.

Valderrama, F., J.M. Duran, T. Babia, H. Barth, J. Renau-Piqueras, and G. Egea. 2001. Actin microfilaments facilitate the retrograde transport from the Golgi complex to the endoplasmic reticulum in mammalian cells. *Traffic.* 2:717-26.

Valderrama, F., A. Luna, T. Babia, J.A. Martinez-Menarguez, J. Ballesta, H. Barth, C. Chaponnier, J. Renau-Piqueras, and G. Egea. 2000. The golgi-associated COPI-coated buds and vesicles contain beta/gamma -actin. *Proc Natl Acad Sci U S A.* 97:1560-5.

van Diggelen, O.P., S. Thobois, C. Tilikete, M.T. Zabot, J.L. Keulemans, P.A. van Bunderen, P.E. Taschner, M. Losekoot, and Y.V. Voznyi. 2001. Adult neuronal ceroid lipofuscinosis with palmitoyl-protein thioesterase deficiency: first adult-onset patients of a childhood disease. *Ann Neurol.* 50:269-72.

Vance, J.E., S.J. Stone, and J.R. Faust. 1997. Abnormalities in mitochondria-associated membranes and phospholipid biosynthetic enzymes in the mnd/mnd mouse model of neuronal ceroid lipofuscinosis. *Biochim Biophys Acta.* 1344:286-99.

Vellodi, A. 2005. Lysosomal storage disorders. *Br J Haematol.* 128:413-31.

Vergeres, G., T.S. Yen, J. Aggeler, J. Lausier, and L. Waskell. 1993. A model system for studying membrane biogenesis. Overexpression of cytochrome b5 in yeast results in marked proliferation of the intracellular membrane. *J Cell Sci.* 106 (Pt 1):249-59.

Verkruyse, L.A., and S.L. Hofmann. 1996. Lysosomal targeting of palmitoyl-protein thioesterase. *J Biol Chem.* 271:15831-6.

Vesa, J., M.H. Chin, K. Oelgeschlager, J. Isosomppi, E.C. DellAngelica, A. Jalanko, and L. Peltonen. 2002. Neuronal ceroid lipofuscinoses are connected at molecular level: interaction of CLN5 protein with CLN2 and CLN3. *Mol Biol Cell.* 13:2410-20.

Vigneswaran, N., W. Zhao, A. Dassanayake, S. Muller, D.M. Miller, and W. Zacharias. 2000. Variable expression of cathepsin B and D correlates with highly invasive and metastatic phenotype of oral cancer. *Hum Pathol.* 31:931-7.

Vines, D.J., and M.J. Warburton. 1999. Classical late infantile neuronal ceroid lipofuscinosis fibroblasts are deficient in lysosomal tripeptidyl peptidase I. *FEBS Lett.* 443:131-5.

Virmani, T., P. Gupta, X. Liu, E.T. Kavalali, and S.L. Hofmann. 2005. Progressively reduced synaptic vesicle pool size in cultured neurons

derived from neuronal ceroid lipofuscinosis-1 knockout mice. *Neurobiol Dis.* 20:314-23.

Voeltz, G.K., W.A. Prinz, Y. Shibata, J.M. Rist, and T.A. Rapoport. 2006. A class of membrane proteins shaping the tubular endoplasmic reticulum. *Cell.* 124:573-86.

Voeltz, G.K., M.M. Rolls, and T.A. Rapoport. 2002. Structural organization of the endoplasmic reticulum. *EMBO Rep.* 3:944-50.

Walter, P., and G. Blobel. 1980. Purification of a membrane-associated protein complex required for protein translocation across the endoplasmic reticulum. *Proc Natl Acad Sci U S A.* 77:7112-6.

Walter, P., and G. Blobel. 1981a. Translocation of proteins across the endoplasmic reticulum III. Signal recognition protein (SRP) causes signal sequence-dependent and site-specific arrest of chain elongation that is released by microsomal membranes. *J Cell Biol.* 91:557-61.

Walter, P., and G. Blobel. 1981b. Translocation of proteins across the endoplasmic reticulum. II. Signal recognition protein (SRP) mediates the selective binding to microsomal membranes of in-vitro-assembled polysomes synthesizing secretory protein. *J Cell Biol.* 91:551-6.

Walter, P., I. Ibrahimi, and G. Blobel. 1981. Translocation of proteins across the endoplasmic reticulum. I. Signal recognition protein (SRP) binds to in-vitro-assembled polysomes synthesizing secretory protein. *J Cell Biol.* 91:545-50.

Wang, H.J., G. Guay, L. Pogan, R. Sauve, and I.R. Nabi. 2000. Calcium regulates the association between mitochondria and a smooth subdomain of the endoplasmic reticulum. *J Cell Biol.* 150:1489-98.

Warburton, M.J., and F. Bernardini. 2000. Tripeptidyl-peptidase I deficiency in classical late-infantile neuronal ceroid lipofuscinosis brain tissue. Evidence for defective peptidase rather than proteinase activity. *J Inherit Metab Dis.* 23:145-54.

Wheeler, R.B., J.D. Sharp, R.A. Schultz, J.M. Joslin, R.E. Williams, and S.E. Mole. 2002. The gene mutated in variant late-infantile neuronal ceroid lipofuscinosis (CLN6) and in nclf mutant mice encodes a novel predicted transmembrane protein. *Am J Hum Genet.* 70:537-42.

Winchester, B., A. Vellodi, and E. Young. 2000. The molecular basis of lysosomal storage diseases and their treatment. *Biochem Soc Trans.* 28:150-4.

Winter, E., and C.P. Ponting. 2002. TRAM, LAG1 and CLN8: members of a novel family of lipid-sensing domains? *Trends Biochem Sci.* 27:381-3.

Wisniewski, K.E., E. Kida, A.A. Golabek, W. Kaczmarski, F. Connell, and N. Zhong. 2001. Neuronal ceroid lipofuscinoses: classification and diagnosis. *Adv Genet.* 45:1-34.

Wisniewski, K.E., E. Kida, W. Gordon-Majszak, and T. Saitoh. 1990. Altered amyloid beta-protein precursor processing in brains of patients with neuronal ceroid lipofuscinosis. *Neurosci Lett.* 120:94-6.

Woods, A.J., M.S. Roberts, J. Choudhary, S.T. Barry, Y. Mazaki, H. Sabe, S.J. Morley, D.R. Critchley, and J.C. Norman. 2002. Paxillin associates with poly(A)-binding protein 1 at the dense endoplasmic reticulum and the leading edge of migrating cells. *J Biol Chem.* 277:6428-37.

Yamamoto, A., R. Masaki, and Y. Tashiro. 1990. Characterization of the isolation membranes and the limiting membranes of autophagosomes in rat hepatocytes by lectin cytochemistry. *J Histochem Cytochem.* 38:573-80.

Ye, Y., Y. Shibata, C. Yun, D. Ron, and T.A. Rapoport. 2004. A membrane protein complex mediates retro-translocation from the ER lumen into the cytosol. *Nature.* 429:841-7.

Yorimitsu, T., U. Nair, Z. Yang, and D.J. Klionsky. 2006. ER stress triggers autophagy. *J Biol Chem.* 281: 30299-304

Young, A.R., E.Y. Chan, X.W. Hu, R. Kochl, S.G. Crawshaw, S. High, D.W. Hailey, J. Lippincott-Schwartz, and S.A. Tooze. 2006. Starvation and ULK1-dependent cycling of mammalian Atg9 between the TGN and endosomes. *J Cell Sci.* 119:3888-900.

Zeman, W., and P. Dyken. 1969. Neuronal ceroid-lipofuscinosis (Batten's disease): relationship to amaurotic family idiocy? *Pediatrics.* 44:570-83.

Zhang, Y., G. Nijbroek, M.L. Sullivan, A.A. McCracken, S.C. Watkins, S. Michaelis, and J.L. Brodsky. 2001. Hsp70 molecular chaperone facilitates endoplasmic reticulum-associated protein degradation of cystic fibrosis transmembrane conductance regulator in yeast. *Mol Biol Cell.* 12:1303-14.

Appendix

Appendix A

Table 9.1: t-tests (paired student's t-test, two-tail)

6.2.1.2 LAMP-1

	mock	*cln5*	*mock*	*cln6*	*mock*	*cln8*
Mean	3.284246	3.105688	3.284246	2.975449	3.284246	3.798384
Variance	2.663816	1.887616	2.663816	1.547451	2.663816	7.471355
Observations	6	6	6	6	6	6
Pearson Correlation	0.989937		0.782007		0.92782	
Hypothesized Mean Difference	0		0		0	
df	5		5		5	
t Stat	1.30804		0.74319		-0.92422	
P(T<=t) one-tail	0.123882		0.245395		0.198892	
t Critical one-tail	2.015048		2.015048		2.015048	
P(T<=t) two-tail	**0.247764**		**0.490789**		**0.397783**	
t Critical two-tail	2.570582		2.570582		2.570582	

6.2.2 CD63

	mock	*cln5*	*mock*	*cln6*	*mock*	*cln8*
Mean	2.727395	2.701549	2.727395	3.20645	2.727395	3.320224
Variance	0.981188	0.860395	0.981188	2.161642	0.981188	2.563173
Observations	6	6	6	6	6	6
Pearson Correlation	0.871649		0.827399		0.945039	
Hypothesized Mean Difference	0		0		0	
df	5		5		5	
t Stat	0.129277		-1.37073		-1.96348	
P(T<=t) one-tail	0.451089		0.114395		0.053406	
t Critical one-tail	2.015048		2.015048		2.015048	
P(T<=t) two-tail	**0.902178**		**0.22879**		**0.106811**	
t Critical two-tail	2.570582		2.570582		2.570582	

6.2.3 EEA-1

	mock	*cln5*	*mock*	*cln6*	*mock*	*cln8*
Mean	0.475347	0.416073	0.475347	0.494079	0.475347	0.431482
Variance	0.008999	0.02833	0.008999	0.129084	0.008999	0.055198
Observations	6	6	6	6	6	6
Pearson Correlation	0.477169		0.136497		0.45804	
Hypothesized Mean Difference	0		0		0	
df	5		5		5	
t Stat	0.976859		-0.12786		0.513509	
P(T<=t) one-tail	0.186751		0.451621		0.314737	
t Critical one-tail	2.015048		2.015048		2.015048	
P(T<=t) two-tail	**0.373503**		**0.903242**		**0.629473**	
t Critical two-tail	2.570582		2.570582		2.570582	

6.2.4 PDI

	mock	*cln5*	*mock*	*cln6*	*mock*	*cln8*
Mean	6.559477	7.960006	6.559477	6.12629	6.559477	5.650781
Variance	25.97112	24.50633	25.97112	23.8874	25.97112	19.33915
Observations	6	6	6	6	6	6
Pearson Correlation	0.929626		0.831113		0.905317	
Hypothesized Mean Difference	0		0		0	
df	5		5		5	
t Stat	-1.81513		0.364881		1.02324	
P(T<=t) one-tail	0.064608		0.365063		0.176562	
t Critical one-tail	2.015048		2.015048		2.015048	
P(T<=t) two-tail	**0.129217**		**0.730125**		**0.353125**	
t Critical two-tail	2.570582		2.570582		2.570582	

6.2.5.1 GM130

	mock	*cln5*	*mock*	*cln6*	*mock*	*cln8*
Mean	0.156731	0.227194	0.156731	0.124116	0.156731	0.195906
Variance	0.007134	0.003088	0.007134	0.000939	0.007134	0.012461
Observations	6	6	6	6	6	6
Pearson Correlation	0.366052		-0.4708		0.210006	
Hypothesized Mean Difference	0		0		0	
df	5		5		5	
t Stat	-2.09523		0.779325		-0.76742	
P(T<=t) one-tail	0.045149		0.235523		0.238744	
t Critical one-tail	2.015048		2.015048		2.015048	
P(T<=t) two-tail	**0.090298**		**0.471047**		**0.477488**	
t Critical two-tail	2.570582		2.570582		2.570582	

6.2.5.2 GM130 ribbons short and long

	mock	*CLN5*	*mock*	*CLN8*	*mock*	*CLN6*
Mean	37.33333	40.33333	37.33333	18.33333	37.33333	23.33333
Variance	6.333333	6.333333	6.333333	2.333333	6.333333	8.333333
Observations	3	3	3	3	3	3
Pearson Correlation	0.684211		-0.56362		0.802955	
Hypothesized Mean Difference	0		0		0	
df	2		2		2	
t Stat	-2.59808		9.127305		14	
P(T<=t) one-tail	0.060845		0.005896		0.002532	
t Critical one-tail	2.919986		2.919986		2.919986	
P(T<=t) two-tail	**0.12169**		**0.011792**		**0.005063**	
t Critical two-tail	4.302653		4.302653		4.302653	

Appendix B – Co-immunoprecipitation sequencing data

Table 9.2 : Co-immunoprecipitation 1 raw data

Band	Predicted protein	Accession number	Peptides matched	Probability
2	DEAD box polypeptide 48	gi_7661920	10	1.0e+000
2	Beta-tubulin	gi_18088719	4	8.5e-008
3	Gamma-actin	gi_7441428	5	5.7e-001
5	PPR repeat domain 2	gi_20127634	5	7.7e-001
7	CLN6	gi_8923532	3	1.0e-002

Data analysed in ProFound by Dr. Oliver Kleiner, UCL. Probability was computed as the normalised probability that a protein in a database is the protein being analysed.

Table 9.3: Co-immunoprecipitation 2 raw data

Band	Predicted protein	Accession number	Peptides matched	Probability score
2	mtHSP75	gi_292059	2	91

Data analysed in Mascot by Dr. Catherine Lilley, Cambridge. Score is –10xLog(P), where P is the probability that the observed match is a random event. Protein scores greater than 67 are significant ($p < 0.05$).

Table 9.4: Co-immunoprecipitation 3 raw data

Band	Predicted protein	Accession number	Peptides matched	Probability score
3	chain A, HSP70 42 kDa ATPase N-terminal domain	gi_6729803	9	81
5	beta-actin	gi_4501885	7	74

Data analysed in Mascot by Dr. Oliver Kleiner, Eisai. Score is –10xLog(P), where P is the probability that the observed match is a random event. Protein scores greater than 67 are significant ($p < 0.05$).

Acknowledgements

I would like to thank my supervisors Sara Mole and Dan Cutler for their help and guidance during this project. I am grateful to all members of the Mole and Cutler groups, past and present, especially Morwenna Porter, whose excellent thesis I have consulted many times, and Claudia Kitzmüller, Dan Metcalf, Helen Zenner, Kim Harrison-Lavoie, Rebecca Haines, Tim Pullen, Tom Nightingale and Winnie Lui-Roberts for all their help and moral support.

This work was made possible by funding from the Batten Disease Support and Research Association (BDSRA) and the European Commission (503051).

I would like to thank my friends, especially Christina, Jeremy, Liz and Olga, and all members of City and Moorgate Jitsu. Finally I am forever grateful to my parents, my brother and Paul for their immense support.